UNIVERSITÀ DEGLI STUDI DI MODENA E REGGIO EMILIA

PhD course in

Models and Methods for Material and Environmental Sciences

Cycle XXXII

INTEGRATED BIOSTRATIGRAPHY WITH LARGER BENTHIC FORAMINIFERA AND CALCAREOUS PLANKTON OF THE LOWER PALEOGENE

Candidate: Beatrice Fornaciari

Tutor: Dr. Cesare Andrea Papazzoni, Università degli Studi di Modena e Reggio Emilia

Co-tutor: Prof. Eliana Fornaciari, Università di Padova

PhD course coordinator: Prof. Maria Giovanna Vezzalini

2016 - 2019

Ai miei genitori

INDEX

ABSTRACT

The early Paleogene represented an important time for the larger foraminiferal evolution. In the aftermath of the Cretaceous/Paleogene (K/Pg) mass extinction there was a recovery period in which the benthic foraminifera, rare and small, with a simple test, shortly developed bigger and complex-test taxa, progressively increasing in number. Several genera appeared in the Paleocene later broadly diversified at the specific level, acquiring a great importance from the biostratigraphic point of view, especially in the Eocene.

The presence of larger foraminifera (LF) marker species is the criteria on which the main biozonal reference system for shallow-water environments of the Paleocene and the Eocene of the Tethys, the Shallow Benthic (SB) zones, is based. It is currently retained that the beginning of the larger foraminiferal adaptive radiation after the K/Pg boundary corresponds to the base of the SB2 Zone. However, the exact position of the SB1/SB2 boundary has not yet been firmly established. This problem affects the evolutionary studies of the group and the understanding of the effects of the paleoenvironmental and paleoclimatic events on its diversity. The correlation of the SB zones with other biozonational schemes is essential in order to achieve a reliable system of biochronozones in a standard chronostratigraphic scale and to better understand the evolution of the LF.

In the present thesis three Paleocene sections in Northern Italy (Tabiago and Monte Giglio sections in the Lombardian Basin and Ardo section in the Belluno Basin) have been analyzed to obtain an integrated LF and calcareous nannofossils biostratigraphy from the Danian to the Thanetian (SB1 – lower SB4 and CNP1 – CNP11). All these sections are composed of hemipelagites intercalated by turbidites from shallow water environments.

The results indicate that the SB1/SB2 boundary is in the lowermost CNP4. Consequently, the LF radiation after the K/Pg boundary started about 2 Ma earlier than previously asserted.

Among the most important groups which radiated in the lower Paleogene, there are the families Rotaliidae, Miscellaneidae, Discocyclinidae and Orbitoclypeidae.

The obtained integrated biostratigraphy allows to better define the biostratigraphic distributions of the taxa, turning out that the ranges of some Paleocene rotaliids and miscellaneids are different than the ones reported by Hottinger in 2014. However, the first appearance of the orthophragminids (=Discocyclinidae+Orbitoclypeidae) seems to represent the best biostratigraphic event to mark the base of SB3. Furthermore, it should be noticed that this bio-horizon, even if close to the environmental perturbation known as Early Late Paleocene Event (ELPE), seems not correlated with the same, being slightly earlier than it.

The correlation between calcareous nannofossil zones and SB zones has been applied to the family Alveolinidae as well. In particular, as consequence of ongoing researches in the Bolca *Fossil-Lagerstätten* (belonging to the shallow-water Lessini Shelf) in Northern Italy, it has been possible to

identify and describe a new species, *Alveolina postalensis*, from the upper Ypresian SB11 of the Monte Postale and the Pesciara. The biometric investigations allow to distinguish this species from the related *A. croatica*, *A. levantina* and *A. hottingeri* and to hypothesize that *A. postalensis* could be the ancestor of *A. croatica* and form a phylethic line parallel line to *A. levantina-A. hottingeri*.

This thesis therefore contributes to the knowledge of the larger foraminiferal associations of the lower Paleogene and to the development of a new integrated biostratigraphic scheme for the Western Neotethys.

RIASSUNTO

Il Paleogene inferiore rappresentò un importante intervallo per l'evoluzione dei macroforaminiferi. L'estinzione di massa del Cretaceo/Paleogene (K/Pg) ebbe come conseguenza un periodo di recupero in cui i foraminiferi bentonici, da rari e piccoli con guscio semplice, in poco tempo svilupparono taxa dai gusci progressivamente di dimensioni maggiori e complessi, che divennero sempre più numerosi. Successivamente, molti dei generi apparsi nel Paleocene si diversificarono a livello specifico, diventando molto importanti per la biostratigrafia, soprattutto nell'Eocene.

La presenza di specie marker di macroforaminiferi è il criterio su cui è basato il principale sistema di biozonazione di riferimento per gli ambienti di acqua-bassa del Paleocene e dell'Eocene della Tetide, le Shallow Benthic (SB) zones. Attualmente si ritiene che l'inizio della radiazione adattativa dei macroforaminiferi dopo il limite K/Pg coincida con la base della Zona SB2. Tuttavia, l'esatta posizione del limite SB1/SB2 non è ancora stata stabilita con certezza. Questa incertezza influisce sugli studi relativi all'evoluzione del gruppo e sulla comprensione degli effetti degli eventi paleoambientali e paleoclimatici. La correlazione delle zone SB con altri schemi biozonali è fondamentale per acquisire un sistema di biocronozone affidabile in una scala cronostratigrafica standard e per meglio comprendere l'evoluzione dei macroforaminiferi.

Nella presente tesi, tre sezioni paleoceniche del Nord Italia (Tabiago e Monte Giglio, nel Bacino Lombardo, e Ardo, nel Bacino di Belluno) sono state analizzate per ottenere una biostratigrafia integrata a macroforaminiferi e nannofossili calcarei dal Daniano al Thanetiano (SB1 – SB4 inferiore e CNP1 – CNP11). Tutte queste sezioni sono composte da emipelagiti intercalate a torbiditi provenienti da ambienti di acqua poco profonda.

I risultati provenienti dalle analisi di queste sezioni indicano che il limite SB1/SB2 è correlato con la parte più bassa della CNP4: ciò significa che la radiazione dei macroforaminiferi dopo il limite K/Pg iniziò circa 2 Ma prima di quanto affermato finora.

Tra i gruppi più importanti di questa radiazione nel Paleogene inferiore, ci sono le famiglie Rotaliidae, Miscellaneidae, Discocyclinidae e Orbitoclypeidae.

La biostratigrafia integrata ottenuta chiarisce le distribuzioni biostratigrafiche dei taxa, consentendo di stabilire che i range biostratigrafici di alcuni rotaliidi e miscellaneidi del Paleocene sono diversi rispetto a quanto riportato da Hottinger nel 2014. Al contrario, la prima comparsa degli ortofragminidi (=Discocyclinidae+Orbitoclypeidae) sembra essere un ottimo marker per riconoscere la base della zona SB3. Inoltre, si segnala che questo bio-orizzonte non sembra essere correlato alla perturbazione ambientale nota come Early Late Paleocene Event (ELPE) poiché, seppur di poco, la precede.

La correlazione tra zone a nannofossili calcarei e zone SB è stata applicata anche alla famiglia Alveolinidae. In particolare, come conseguenza di ricerche in corso nei *Fossil-Lagerstätten* di Bolca (Piattaforma dei Lessini, Italia settentrionale), è stato possibile identificare e descrivere una nuova specie, *Alveolina postalensis*, dall'Ypresiano superiore del Monte Postale e della Pesciara e assegnarla alla zona SB11. I dati biometrici consentono di distinguere questa specie dalle affini *A. croatica*, *A. levantina* e *A. hottingeri* e di ipotizzare che *A. postalensis* sia l'antenato di *A. croatica* e formi una linea filetica parallela a quella di *A. levantina-A. hottingeri*.

La tesi contribuisce pertanto alla conoscenza delle associazioni a macroforaminiferi del Paleogene inferiore e allo sviluppo di un nuovo schema biostratigrafico integrato per la Neotetide occidentale.

ACKNOWLEDGEMENTS

I wish to thank you all the people who contributed to this work but, above all, who transmitted me important knowledges in biostratigraphy and approaches to the scientific research during my PhD course.

First, I am deeply grateful to my tutor Dr. Cesare Andrea Papazzoni, of the University of Modena and Reggio Emilia (Italy). I owe him the scientific knowledge and method he tried to transmit to me in every way, his helpfulness and continuous support with insightful discussions and his patience. All this was fundamental in my academic *iter* and helped me a lot in all the time of research and writing. The attention with which he reviewed everyone of my manuscripts surely improved the quality of my productions very much.

I gratefully acknowledge also my co-tutor Prof. Eliana Fornaciari, of the University of Padova (Italy), not only for having performed the calcareous nannofossils analyses, but also and most especially for the interesting discussions shared on the biostratigraphy and for her continuous availability and support. Funny moments were also shared for the synonymy of our surnames.

I am sincerely grateful also to Prof. Luca Giusberti, of the University of Padova (Italy), for having given me his efficient practical help and his precious scientific contribution during the sharing of all sampling, research and publication activities.

Furthermore, during the training periods outside my university, I've had the occasion to meet other people who have been important scientific guides for me and also nice friends.

I specially thank Dr. Katica Drobne for having hosted me in the Research Centre of the Slovenian Academy of Sciences and Arts of Ljubljana (Slovenia) and for the enthusiasm with which she made me discover alveolinids and the cultural life of Ljubljana. Her warmth and passion are indescribable in a few lines, as well as her knowledge about alveolinas.

My deep and sincere thanks also goes to Prof. Johannes Pignatti for the dedication and the attention with which he welcomed me in La Sapienza University of Rome (Italy), in spite of his several tasks. During the conversation shared, he tried to transmit me as more as possible of his deep scientific knowledge.

I'd like to express a big thank also to Prof. Antonino Briguglio, who greeted me in the University of Genova (Italy) and introduce to me to the modern larger foraminifera of the Indian and the Pacific Oceans. I am very grateful to him for his continuous support.

I also thank Stefania Bianco, Martina Lando, Sara Marconato, Massimo Plessi and Michela Simonato who helped me and Prof. E. Fornaciari in sampling and acquiring data from the analysed sections in their bachelor's and master's thesis.

Last but not least, I would like to address my deepest and warmest thanks to my parents and my partner who supported and encouraged me with their continuous careful presence and love.

1. INTRODUCTION

The biozonation reference system for the shallow water environments is constituted by the Shallow Benthic zones, referring to Serra-Kiel et al. (1998) for the basal Paleocene (Danian) – late Eocene (Priabonian) of the Tethys and to Cahuzac and Poignant (1997) for the early Oligocene (Rupelian) – late Miocene (Tortonian) of the European basins.

The Shallow Benthic zones have been indicated with two different acronyms since the beginning: SB in Cahuzac and Poignant (1997) and SBZ in Serra-Kiel et al. (1998). Even if in literature the use of the acronym SBZ prevailed, in this thesis the acronym SB is preferred, considered more correct for different reasons: a) the SB zones were created on the model of the planktonic and of the calcareous nannofossils zones, which do not use the word "Zone" in their acronym as the concept expressed by this word is implied in their nature of biozones; b) the work (Cahuzac and Poignant 1997) that first established the SB zones used this acronym; c) the use of the acronym SBZ would create repetition ("SBZ Zones") when speaking about the biozones.

The system of the SB zones is largely Oppelian, as each zone is defined by the stratigraphic distribution of several taxa forming a characteristic assemblage. This implies that the boundaries of the biozones are affected by subjectivity (Pignatti and Papazzoni 2017).

The evolution of the biostratigraphy aims at constraining the boundaries of the SB zones by detecting LF bio-horizons and correlating them with those of different organisms belonging to other biozonation systems. Therefore, the calibration of the SB zones with other biozonation schemes and with the magnetostratigraphy is fundamental in order to achieve a reliable system of biochronozones in a standard chronostratigraphic scale (e.g. Gradstein et al. 2012). The SB zones have been correlated by Serra-Kiel et al. (1998) with the magnetochrons and with the planktonic foraminifera and the calcareous nannofossil zones but, as the authors themselves specified, these correlations were susceptible to be modified according to the future advances of biostratigraphic knowledge. Recently, some updates to the correlation scheme for the Paleocene and the Eocene were proposed by Papazzoni et al. (2017a). However, the uncertainties in positioning some SB zones boundaries still persist, especially because of the scarcity of direct correlations between shallow-water and deep-water environments.

Moreover, achieving a reliable biostratigraphic scheme for the SB zones is the pre-requisite to correctly interpret the influence of the climatic perturbations on the shallow water organisms.

The attention of this thesis is focused on the early Paleogene, as it represents a crucial time both for LF and for the Earth's climate evolution.

The LF, after the K/Pg mass extinction which had wiped out almost all of them (e.g., Consorti and Rashidi 2018), recovered during the Paleocene. This time interval brought to the rise of K-strategist organisms in different phases. The Paleocene represents the first phase of the Global

Community Maturation Cycle (GCM) as described by Hottinger (2001). The LF started the generic diversification since the SB2 and the specific one since the SB3 Zone (Hottinger 2001), originating groups that later became the most successful in the shallow water environments of the Paleogene.

In the meantime, the Earth underwent progressive warming punctuated by transient events of climatic and environmental perturbations whose triggers are still object of strong debate. For instance, immediately before the Selandian/Thanetian boundary, the Early Late Paleocene Event (ELPE; also known as MPBE, see subchapter 2.3.2) represents a remarkable biotic event associated with important evolutionary changes of calcareous nannoplankton assemblages (e.g., the appearances of the genera *Heliolithus* and *Discoasteroides*; Bralower et al. 2006, Agnini et al. 2007). Near this event, several larger foraminiferal genera appeared as *Alveolina* (*Glomalveolina*), *Nummulites*, *Ranikothalia*, *Discocyclina*, *Orbitoclypeus* (see Serra-Kiel et al. 1998) and many of these later radiated in the Eocene. However, the relation between their evolution and the climatic events is not clear because of the uncertainties in the exact timing of the first appearances of many taxa, due to the poorly constrained boundaries between SB zones in the Paleocene (dotted boundaries in Serra-Kiel et al. 1998). As regards the LF of the central-western Neotethys, the available data for the Paleocene are scarce because the shallow water facies are quite rare, whereas the pelagic and hemipelagic successions are more widespread. The best documented and worldwide known are the classical sequences of the Umbria-Marche Basin (e.g., Coccioni et al. 2016), but expanded ones occur in the Southern Alps of northern Italy as well.

For this study, three Paleocene deep-sea sections were investigated: the Tabiago section (Lecco Province) and the Monte Giglio section (Bergamo Province), both in the Lombardian Basin; the Ardo section (Belluno Province) in the Belluno Basin. These sections, containing calcareous turbidites derived from shallow water environments, offer the rare chance to directly correlate LF with calcareous nannofossils bioevents, allowing to integrate the two different biozonation schemes (Fornaciari et al., *in prep*.)

The integrated biostratigraphic approach has been extended to a different time and a different sedimentary paleoenvironment, with the analysis of the shallow-water deposits of the early Eocene Monte Postale section near Bolca. Here the limestone containing the famous fossil fishes were recently ascribed to the SB11 (late Ypresian) by Papazzoni et al. (2017b). During the work on the material from this area, a new species was recorded and described by Fornaciari et al. (2019) as *Alveolina postalensis*. The new species could be distinguished from the related *A. croatica*, *A. levantina,* and *A. hottingeri* according to its biometrical features. The distribution of *A. postalensis* in Bolca is limited to the SB11 zone.

2. THE EARLY PALEOGENE

2.1. THE EARLY PALEOGENE STRATIGRAPHY: historical and current stratigraphical subdivisions

The Paleogene System/Period has been formally divided into three Series/Epochs (Paleocene, Eocene, and Oligocene) and into nine stages/ages (Danian, Selandian, Thanetian, Ypresian, Lutetian, Bartonian, Priabonian, Rupelian, Chattian) by the International Subcommission on Paleogene Stratigraphy (**Fig.1**; **Fig. 2**) (Cohen et al. 2013; Vandenberghe et al. 2012). This thesis is focused on the lower Paleogene and in particular on material from the Danian, Selandian, Thanetian and upper Ypresian.

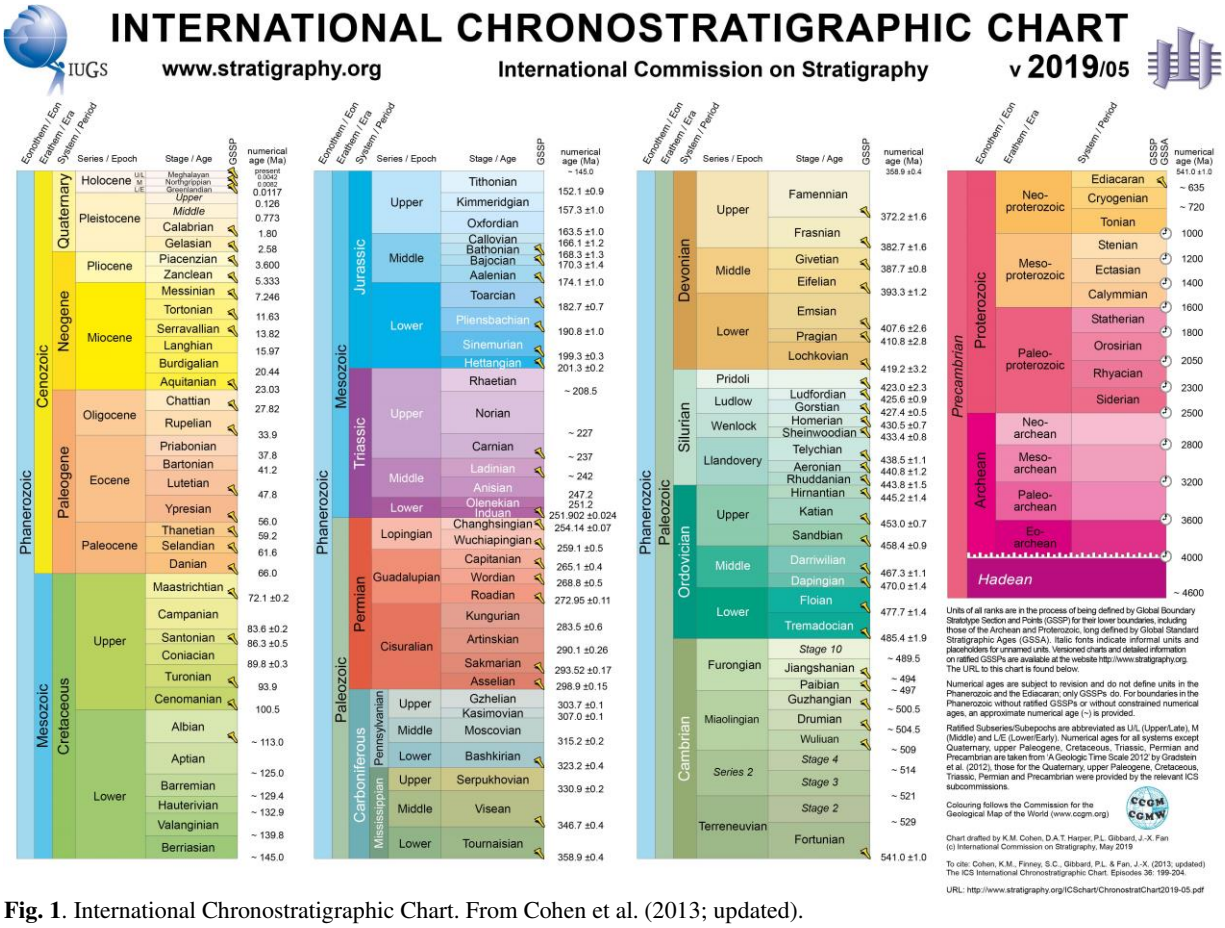

Fig. 1. International Chronostratigraphic Chart. From Cohen et al. (2013; updated).

The investigated stages are introduced in the following chapters.

2.1.1. The Danian Stage

The Danian Stage is named after Denmark, its type area, where it corresponds to the interval between the top of the Maastrichtian Chalk and the base of the Selandian conglomerate. The name was used for the first time by Desor (1847) to indicate these strata, that he attributed to the uppermost/latest Cretaceous. Therefore, Dewalque (1868) introduced a younger stage, the Montian (after Mons, Belgium), for the strata above these, believing they were the base of the Paleocene. Later on, the Montian turned out to represent only the later part of the Danian (in its current meaning) and it lost its significance (De Geyter 2006).

The Danian was formally recognized as the first stage of the Paleocene only after the International Geological Congress (IGC) in 1989 (Jenkins and Luterbacher 1992) and the GSSP for its base was ratified by the IUGS in 1991 in the section of Oued Djerfane, near El-Kef, Tunisia. The base of the Danian here is at the base of a 50 cm-thick clay level in the upper Maastrichtian-Paleocene El Haria Formation, overlaying the upper Campanian-lower Maastrichtian Abiod Formation (Molina et al. 2006).

The clay level corresponding to the K/Pg boundary is now badly preserved in El Kef section but it has been studied in many auxiliary sections located in Italy (Gubbio), Spain (Caravaca, Zumaia), southwest France (Bidart) and Mexico (Bochil and Mulato). It is characterized by an iridium anomaly, microtektites, Ni-rich spinel crystals, shocked quartz grains and a 2-3‰ negative carbon isotope excursion in calcite and organic matter formed in surface waters (Vandenberghe et al. 2012). This level is isochronous all over the world. All these features suggest the hypothesis that an asteroid collided with the Earth and determined catastrophic environmental conditions (extended darkness, global cooling and acid rain) responsible of an abrupt mass extinction. According to Alvarez et al. (1980) and Schulte et al. (2010), evidences of such an impact have been found at Chicxulub, in Mexico. However, different hypothesis have also been formulated, linked to multi-impacts or to the Deccan flood basalt volcanism. The K/Pg boundary was dated to ~65.95 Ma by Kuiper et al. (2008), using a combination of $^{40}Ar/^{39}Ar$ and astronomical ages at the classical Zumaia section.

The Danian spans the Zone SB1 (*sensu* Serra-Kiel et al. 1998), the planktonic foraminiferal Zones P0–P3 *pro parte* (Wade et al. 2011), the calcareous nannofossil Zones NP1–NP4 (Martini et al. 1971), CNP1–CNP7 *pro parte* (Agnini et al. 2014) and the magnetic Chrons C29r–C26r *pro parte* (Westerhold et al. 2008).

2.1.2. The Selandian stage

The Selandian stage was established by Rosenkrantz (1924) in Seland, Denmark, in correspondence of a succession composed of conglomerates, greensand, glauconitic marls and clays, unconformably overlying Danian chalk and overlaid by earliest Eocene deposits (Vandenberghe et al.

2012). The lower Thanetian is included in this succession and before the formal division of the Paleocene into three stages (at the 1989 IGC in Washington; Jenkins and Luterbacher 1992), the Selandian was often considered as being the lower Thanetian (Harland et al. 1990).

The GSSP for the Selandian was ratified by the IUGS in 2008 in the section of Itzurun beach, at Zumaia, Spain, where its base corresponds to the red marls of the Itzurun Formation, overlying the upper part of the Aitzgorri Limestone Formation (Schmitz et al. 2008).

The Selandian spans the Zones SB2 and SB3 *pro parte* (Serra-Kiel et al. 1998), P3 *pro parte*–P4 *pro parte* (Wade et al. 2011), NP4 *pro parte*–NP6 *pro parte* (Martini et al. 1971), the CNP7 *pro parte*–CNP8 *pro parte* (Agnini et al. 2014), the Chron C26r *pro parte* and it is 32 precession cycles above the top of the magnetochron C27n (Dinarès-Turell et al. 2010).

2.1.3. The Thanetian stage

Established by Renevier (1873) for the Thanet Sand on the Isle of Thanet and the Woolwich and Reading Beds in the London Basin, the Thanetian stage was then restricted by Dollfus (1880) only to the first sediments.

The GSSP for the Thanetian was established by the IUGS in 2008 in the same section as the GSSP for the Selandian, at Itzurun beach, in Zumaia, Spain. The base of the Thanetian is a distinct 1 m thick clay level with a reduced carbonate content and an increased magnetic susceptibility in the Itzurun Formation.

The Zumaia section shows a distinct clay horizon characterized by a marked change in the foraminifera and calcareous nannofossil content and corresponding to the Mid-Paleocene Biotic Event (MPBE) or Early-Late Paleocene Event (ELPE). It is located 4.5 m above the first occurrence of *Heliolithus kleinpelli*, whose first appearance corresponds to the base of the NP6 and within the P4 (Bernaola et al. 2007, Petrizzo 2005).

The Thanetian spans the Zones SB3 *pro parte*–SB4 (Serra-Kiel et al. 1998), P4 *pro parte*–P5 *pro parte* (Wade et al. 2011), the NP6 *pro parte*–NP9 (Martini et al. 1971), the CNP8 *pro parte*–CNP11 (Agnini et al. 2014) and the Chrons C26n–C24r *pro parte* (Ali and Jolley 1996).

2.1.4. The Ypresian stage

The Ypresian stage derives its name from the town of Ypres (in French) or Ieper (in Dutch), in Belgium, near where Dumont (1849) described with this term the clayey-sandy strata between the terrestrial to marginal marine Landenian and the marine Brusselian, two stages in the past approximately equivalent to the Thanetian and to the Lutetian, respectively. The Ypresian was traditionally divided by the LF-specialists into two regional stages: the Ilerdian, the lower part, and the Cuisian, the upper one. The latter was defined in the Paris Basin, while the former was introduced as a

regional Mediterranean stage corresponding to an important phase, not represented elsewhere, for the LF evolution. In the Ilerdian, indeed, the genera *Alveolina*, *Assilina*, *Nummulites*, *Orbitolites* and the group of the orthophragminids broadly diversified, becoming the most successful LF group of the lower Paleogene (Hottinger and Schaub 1960, Hottinger 2001).

For years, the scientific community was divided on the position of the Paleocene/Eocene boundary: at the top of the Ilerdian, according to the definition which placed it above the Sparnacian flora in the Lignites du Soissonnais by Schimper (1874) and Hottinger and Schaub (1960), or at the base of the Ilerdian, according to the opinion of most of the participant to a session of the Société Geologique de France in 1974, organized in common with a group working on the Paleogene stratigraphy.

The GSSP for the Ypresian was ratified by the IUGS in 2003 in the Dababiya section, near Luxor, Egypt (Dupuis et al. 2003, Aubry et al. 2007) at the base of a dark grey clay-level in the Esna Shale Formation. The Paleocene/Eocene boundary is marked by a pronounced negative carbon isotope excursion (CIE) considered the geochemical signal of the Paleocene/Eocene thermal maximum (PETM), which was probably triggered by the release of methane from seafloor clathrates. This hyperthermal event coincides with major changes in the global marine biota (see subchapter 2.3.1) and in the terrestrial mammals dispersal in North America.

The Ypresian spans the Zones SB5–SB12 (Serra-Kiel et al. 1998), P5 *pro parte*–P9 *pro parte* (Wade et al. 2011), NP10–NP14 *pro parte* (Martini 1971), CNE1–CNE7 (Agnini et al. 2014), and the Chrons C24r *pro parte*–C21r *pro parte* (Westerhold et al. 2008).

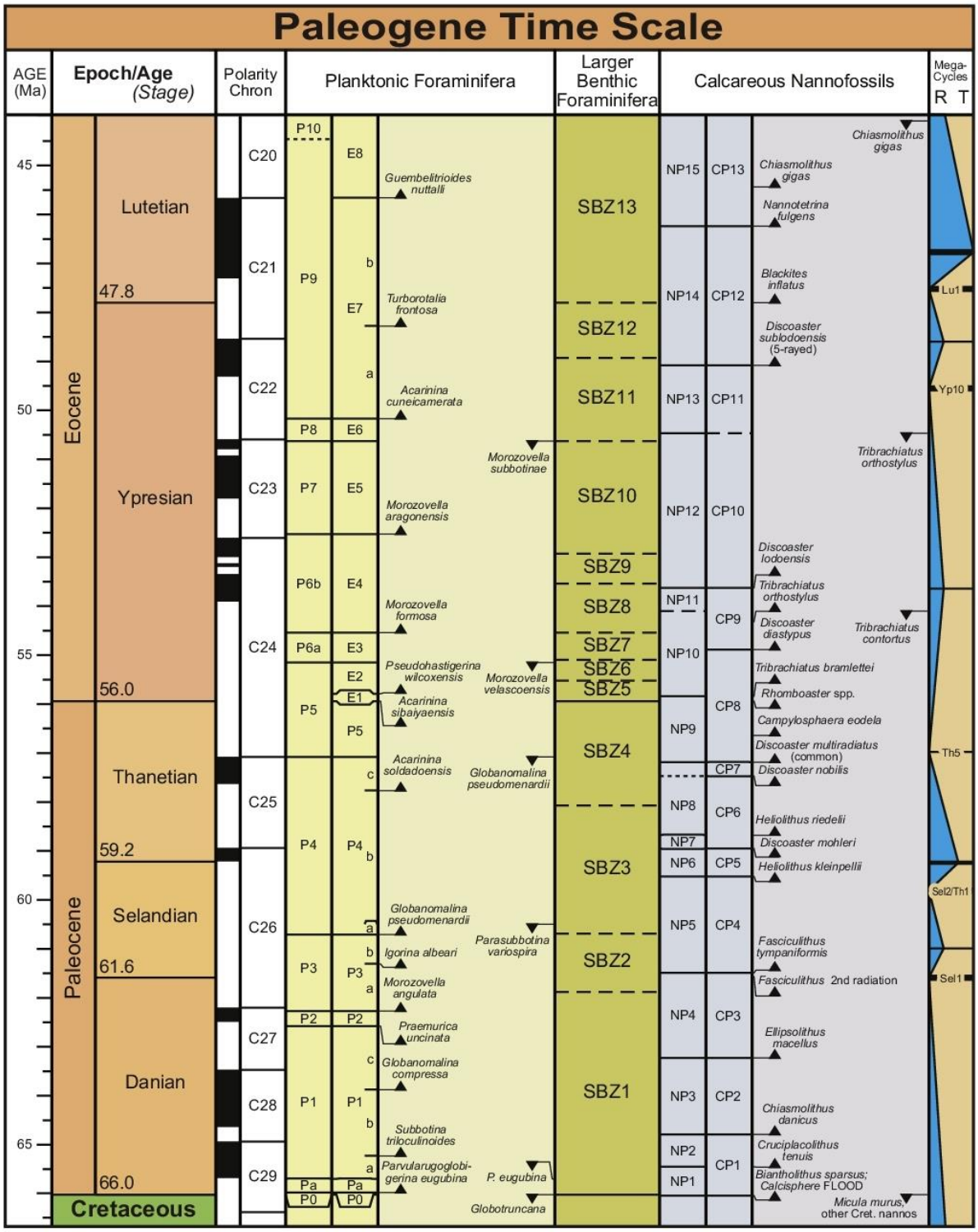

Fig. 2. Paleogene stratigraphic subdivisions, geomagnetic polarity scale, zonations of planktonic foraminifera, larger benthic foraminifera and calcareous nannofossils, and main trends in eustatic sea level from Vandenberghe et al. (2012). Planktonic foraminiferal stratigraphy modified from Wade et al. (2011), Tethyan zonation of larger benthic foraminifera modified from Serra-Kiel et al. (1998), and calcareous nannofossil stratigraphy modified from Pälike et al. (2010). The main Paleogene transgressive-regressive trends are modified from Hardenbol et al. (1998).

2.2. THE EARLY PALEOGENE BIOSTRATIGRAPHY: overview on the larger foraminifera biozonational schemes and problems

2.2.1. The importance of the larger foraminifera of the early Paleogene

The early Paleogene represented an important time for the larger foraminiferal evolution. After the Cretaceous/Paleogene (K/Pg) mass extinction had wiped out almost all larger foraminifera, the Danian was a recovery period in which the benthic foraminiferal assemblages were composed of rare and small taxa. The warm and CO_2-rich shallows seas at the low latitudes of the early Paleogene, in absence of other reef-building and high-temperature tolerating organisms, enabled benthic foraminifera to occupy vacant niches and evolve developing progressively larger and more complex taxa (Scheibner et al. 2005).

According to Hottinger (2001), the diversification started from the Selandian, first at the genus level and then, in the Thanetian, at the species level, following the mode of the Global Community Maturation (GCM).

A GCM is an interval of continuous, gradual biotic change in between two ecological disruptions in the evolutionary history, which is punctuated by repeated GCMs in each taxon. Each GCM produces similar K-strategist (constant growth) foraminifera (as the tests are produced by several analogues steps of growth), often with similar appearances and sizes but with a different architecture which can represent lower or higher grade of organization. Hottinger (2001) observed that after the K/Pg mass extinction, the K-strategist LF disappeared for some million years, namely the whole SB1 Zone. During the time span corresponding to the SB2 Zone, several genera appeared; within the SB3 and SB4 Zones we can observe that

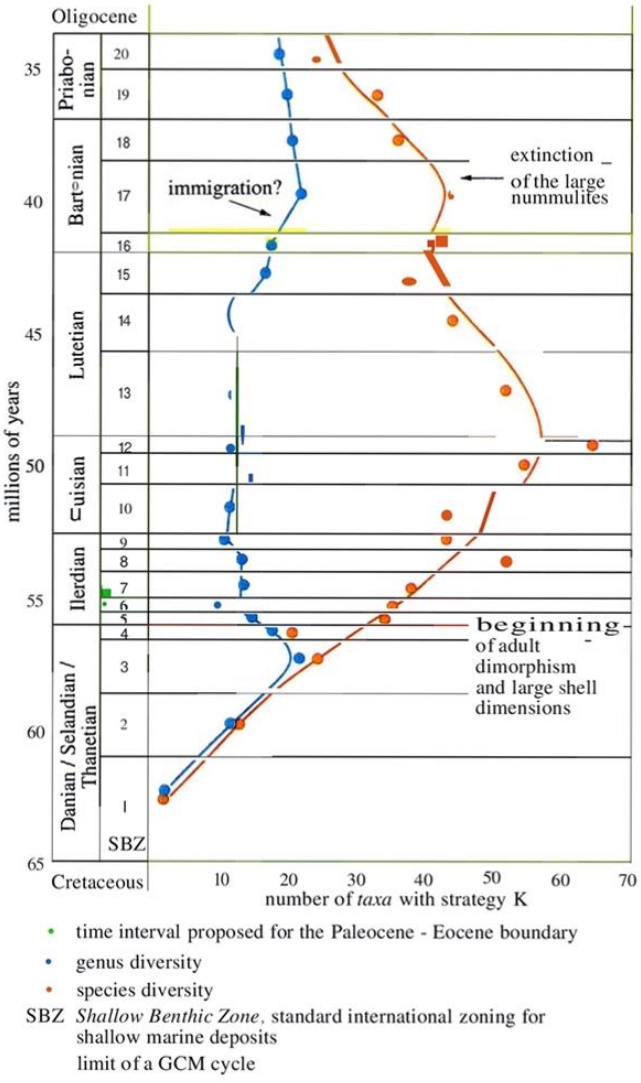

Fig. 3. Generic and specific diversity per biozone (from 1 to 20) during two successive GCM cycles for K strategist tethyan foraminifera during the Paleocene and the Eocene. From Hottinger (2001).

some groups started to dominate by abundance and size (**Fig. 3**). These successful groups developed parallel lineages of species adapted to different ecological niches. During this time span, the development of the adults' dimorphism reflects the progressive differentiation of life strategies within the same species.

The adaptive radiation of the Paleogene LF brought to the success of a few genera which, in the Eocene, underwent a rapid evolution resulting into several short-living species thriving in all the carbonatic shallow-water environments of the Neotethys.

The high rate in the species turnover, the abundance and the wide geographical distribution made the LF important index fossils for the shallow marine environments, where other time-diagnostic methods are scarcely applicable (due to the diagenetic bias in the geochemical signals, the weak magnetic remanence and the scarcity or absence of planktonic organisms).

2.2.2. The history of the larger foraminifera biostratigraphy

The first attempts of biozonation with the LF date back to the middle of the XIX century and are owed to d'Archiac (1850) and d'Archiac and Haime (1853), who established the first biozonational schemes based on Nummulitidae from the Eocene and the Oligocene of India. Later, regional biostratigraphic scales were proposed by de la Harpe (1883), Prever (1905), Boussac (1911), and Douvillé (1920), referring to LF (mostly nummulitids) along with macrofossils from the Eocene and the Oligocene of France, Italy and Egypt. However, these schemes were not conceived in the modern sense as they associate together key species from different regions and they were often affected by the non-recognition of reworking. A refined biozonational approach was developed only with the advancements in the systematics and the phylogeny of the LF and with studies based on more detailed samplings, especially linked to the oil industry. A modern larger foraminiferal zonation, called "The Letter Classification", was proposed by van der Vlerk and Umbgrove (1927) for the East Indian Tertiary.

In the same years, the biometric investigation of larger foraminifera lineages was developed for systematic and biostratigraphy by Hok (1932), who was the first to introduce biometry-based phylozones, and by Van der Vlerk (1955).

Schwager (1883) had described some alveolinids from the Eocene of Egypt and Libya, figuring them in oriented sections and introducing the main parameters on which the study of the alveolinas is still based, but his work was rapidly forgotten. Hottinger (1960) was the first to recognize the importance of this group in biostratigraphy for comparing successions of different regions of the Neotethys. The abundance of the material coming from areas spanning from the Pyrenees to the Egypt allowed him to study the different assemblages, describe several new species, and to introduce biozones based on them (**Fig. 4**).

Drobne (1977), referring to the systematics and the biozonation by Hottinger (1960), studied more alveolinid assemblages in detail and increased the knowledge of this group. In 1981 Schaub observed that the biozones by Hottinger (1960) could be correlated with biozones based on nummulites and assilinas which he introduced (**Fig. 5**). He named his zones after representative nummulitid species and for each biozone he also indicated the corresponding alveolinas biozone and the nannoplankton zone according to Kapellos and Schaub (1975) and Cavelier (1975). The boundaries of the LF zones by Hottinger (1960) and Schaub (1981) were practically the same, because they were both building the scheme on Oppelzones, characterized by specific assemblages and with fuzzy-defined boundaries (see Pignatti and Papazzoni 2017).

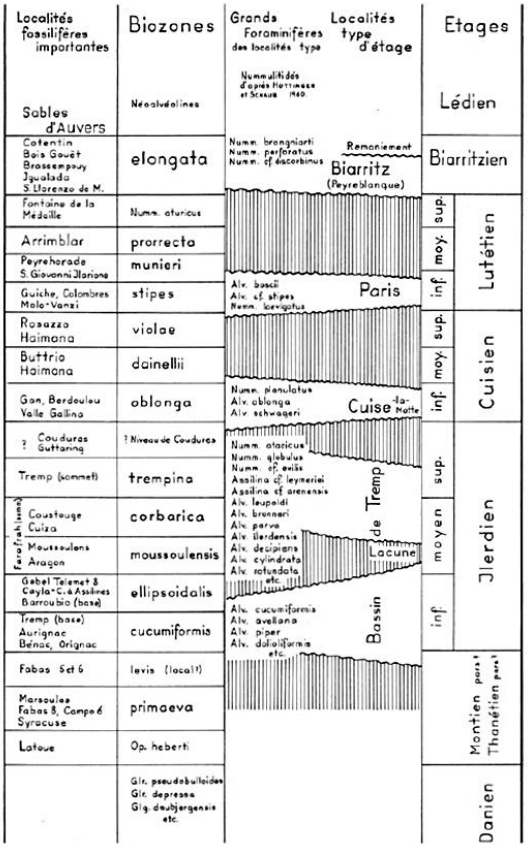

Fig. 4. The biozonation scheme by Hottinger (1960).

SERIES		ETAGES		BIOZONES					
				Nummulites			Assilina	Alveolina	Nannoplancton
				Groupe de N. brongniarti	Groupe de N. perforatus	autres			
OLIGOCENE		inférieur				fichteli			Er. subdisticha
EOCENE	supérieur	Priabonien				fabianii		(Neoalveolina)	I. pseudoradians I. recurvus
	moyen	Biarritzien		brongniarti	perforatus	ptukhiani		elongata	Ch. oamaruensis
		Lutétien	supérieur	herbi	aturicus	bullatus	gigantea		Disc. tani nodifer
			moyen 2	sordensis	crassus		planospira	prorrecta	
			moyen 1	gratus	beneharnensis		spira spira	munieri	Chiphr. alatus
			inférieur 2	laevigatus	obesus gallensis		spira abrardi	stipes	
			inf.1 =basal						
	inférieur	Cuisien	supérieur	manfredi	campesinus	formosus	maior	violae	Disc. sublodoensis
			moyen	praelaevigatus	burd. cantabricus	nitidus	laxispira	dainellii	Disc. lodoensis
			inférieur 2	planulatus	burdigalensis burdigalensis	aff. laxus	plana	oblonga	
			inf.1 =basal						Marth. tribrachiatus
PALEOCENE	supérieur (1)	Ilerdien	supérieur	involutus	pernotus	laxus	adrianensis	trempina	
			moyen 2	exilis		globulus	leymeriei	corbarica	Disc. binodosus
			moyen 1	robustiformis		carcasonensis	aff. arenensis	moussoulensis	Marth. contortus
	(2)		inférieur 2	fraasi	solitarius	minervensis	arenensis	ellipsoidalis	
			inférieur 1			deserti	prisca	cucumiformis	Disc. multiradiatus
	moyen (1)	Thanétien	supérieur				yvettae	levis	
	supérieur (2)		inférieur					primaeva	Hel. riedeli Disc. gemmeus Hel. kleinpelli Fasc. tympaniformis
	inférieur	Danien							Ell. macellus Chiasm. danicus Crucipl. tenuis Markal. inversus

Fig. 5. The biozonation scheme by Schaub (1981). The stages correspond to biozones based on species of the genus *Nummulites* and to biozones base on the genus *Assilina*. These biozones are correlated *Alveolina* biozones from Hottinger, (1960) and to nannoplankton biozones from Kapellos and Schaub (1975), integrated with Cavelier (1975). From Schaub (1981).

An integrated parallel scale of nummulitid and alveolinid biozones for the western Neotethys was obtained and presented at the Colloquium on the Palaeogene in Bordeaux in 1962 (Hottinger et al. 1964). These biozones present superposed key localities, key assemblages and vicariant taxa and represent a discrete biozonation according to the Oppel criteria (Pignatti and Papazzoni 2017).

Alfred Oppel (1831-1865) was one of the founders of the biostratigraphy or zonal stratigraphy, which he applied to the ammonites of the Jurassic. Unfortunately, he gave no definition of what he intended as a zone and therefore later the so called Oppelzones have been considered a particular kind of biostratigraphic unit, chronostratigraphic unit, or even just a time interval (**Fig. 6**). According to Pignatti and Papazzoni (2017), the Oppelzones have a chronostratigraphic character, representing rocks deposited during a certain time interval, but they are at the same time biostratigraphical units, because they refer to the fossil content of the rocks. In any case, they constitute a discrete zonation as their boundaries are undefined (the biozones are separated by interval of unknown length); they are discrete, not overlapping concurrent-range zones; if index taxa are absent in a region, they may include correlative vicariant taxa of other regions. Therefore, the Oppelzones are defined by their characteristic assemblages and not by their lower and upper limits. Even if this makes them less precise than continuous zonation, required for high-resolution stratigraphy, they have been at the base of most of the shallow-water zonations because in these environments, where the sea level changes strongly affect the sedimentary processes, the sedimentary record is inherently discontinuous.

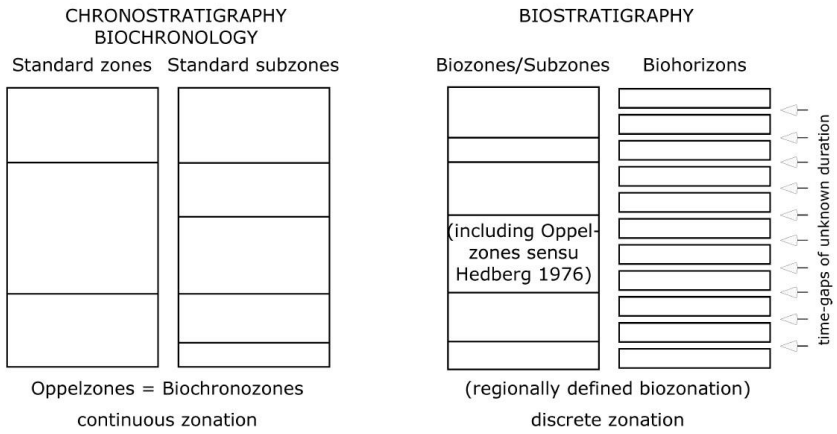

Fig. 6. Oppelzones intended as biochronozones or as biozones. Modified from Pignatti and Papazzoni (2017).

After Hottinger (1960), Drobne (1977) and Schaub (1981), the biostratigraphic data were significant enough to erect biozones based on different taxa of LF of the Tethys, the Shallow-Benthic (SB) zones (see subchapter 2.2.3).

In the meantime, also the knowledge of the systematic of the orthophragmines (=Discocyclinidae+Orbitoclypeidae) was improved and a biozonational approach different from the former ones was developed by Less (1987). After realizing that most of the previous morphological

descriptions of the orthophragmines (Discocyclinidae + Asterocyclinidae in Less, 1987) were based only on the external morphology, he was the first to study their inner structure in detail, defining species and subspecies biometrically and building their phylogenetic scheme. Having analyzed a large amount of material coming from different areas, he perceived their biostratigraphic potential and he later established the Orthophragmine Zones (OZ), a continuous biozonation scale made of phylozones, where the boundaries are defined biometrically (Less 1998). The biometrical approach was then further developed on different taxonomic groups of LF by Less et al. (2008), who applied it to the nummulitid *Heterostegina*, identifying chronospecies which may be used for a further subdivision into subzones of some existing SB zones. Less and Özcan (2008) described two chronospecies of *Spiroclypeus* and considered them as new zonal markers.

2.2.3. The Shallow Benthic (SB) zones

The Shallow Benthic Zones are the reference biozonation system currently in use for the shallow-water environments of the Neotethys from the lower Paleocene (Danian) to the upper Miocene (Tortonian) (Cahuzac & Poignant 1997; Serra-Kiel et al. 1998). Unfortunately, the resolution of the SB zones is very low starting from the middle Miocene, and we have no SB zones after the Tortonian due to the global cooling trend and to the Messinian salinity crisis in the Mediterranean.

The SB zones were defined by Serra-Kiel et al. (1998) for the Paleocene and the Eocene, from SB1 to SB20 (**Fig. 7**), and by Cahuzac and Poignant (1997) for the Oligocene to Miocene, from SB21 to SB26 (**Fig. 8**), for a total of 26 zones, covering an interval of ~58 Ma, which means that the mean duration of one zone is 2.23 Ma (1.76 Ma for the Paleogene). The SB zonation combines the biostratigraphic zonations based on alveolinids (Hottinger 1960), *Nummulites* and *Assilina* (Schaub 1981), orthophragmines (Less 1987, 1998), *Heterostegina*, lepidocyclinids, *Cycloclypeus* and miogypsinids (Drooger 1993), and other taxonomic groups. The SB zones therefore contain non-Oppelian lepidocyclinid and miogypsinid zones and the partly-Oppelian orthophragmine zones, but they rely on the concurrent occurrence of several index taxa and they can be considered as substantially Oppelian, which makes the recognition of their boundaries rather subjective (Pignatti and Papazzoni 2017).

In the scheme by Serra-Kiel et al. (1998), the SB zones are correlated directly with the magnetostratigraphy of sedimentary sequences in the Pyrenees which are in turn correlated with the planktonic foraminifera zones by Berggren and Miller (1988) and Berggren et al. (1995) and the calcareous nannoplankton zones by Martini (1971) and Bukry (1973, 1975). Cahuzac and Poignant (1997) correlated the SB zones with the planktonic foraminiferal zones by Blow (1969) and with the calcareous nannoplankton zones by Martini (1971) which, however, do not appear in their scheme.

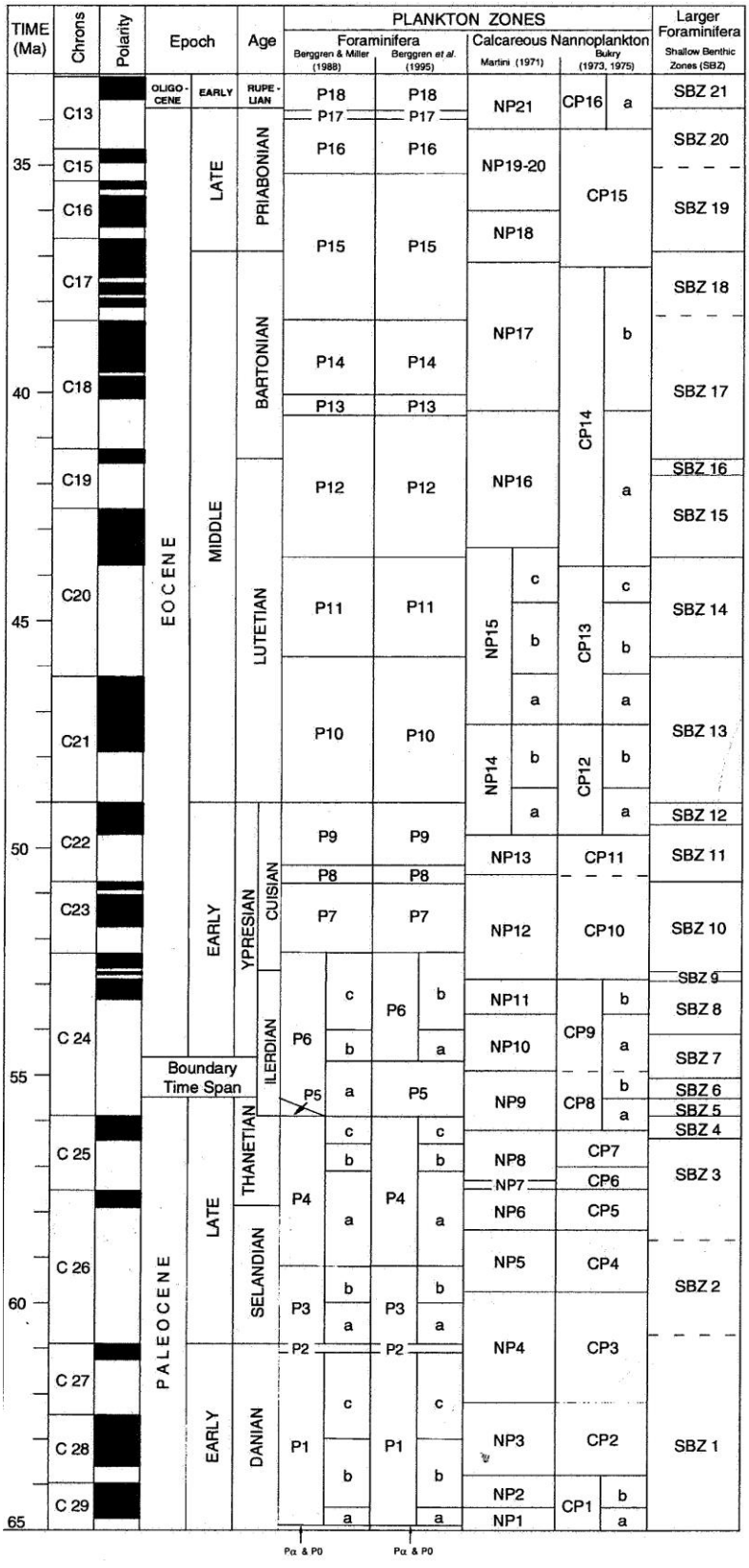

Fig. 7. The biostratigraphic scheme of the Shallow Benthic zones of the Paleocene and the Eocene by Serra-Kiel et al. (1998). The SB zones are correlated with the Time Scale by Berggren et al. (1995).

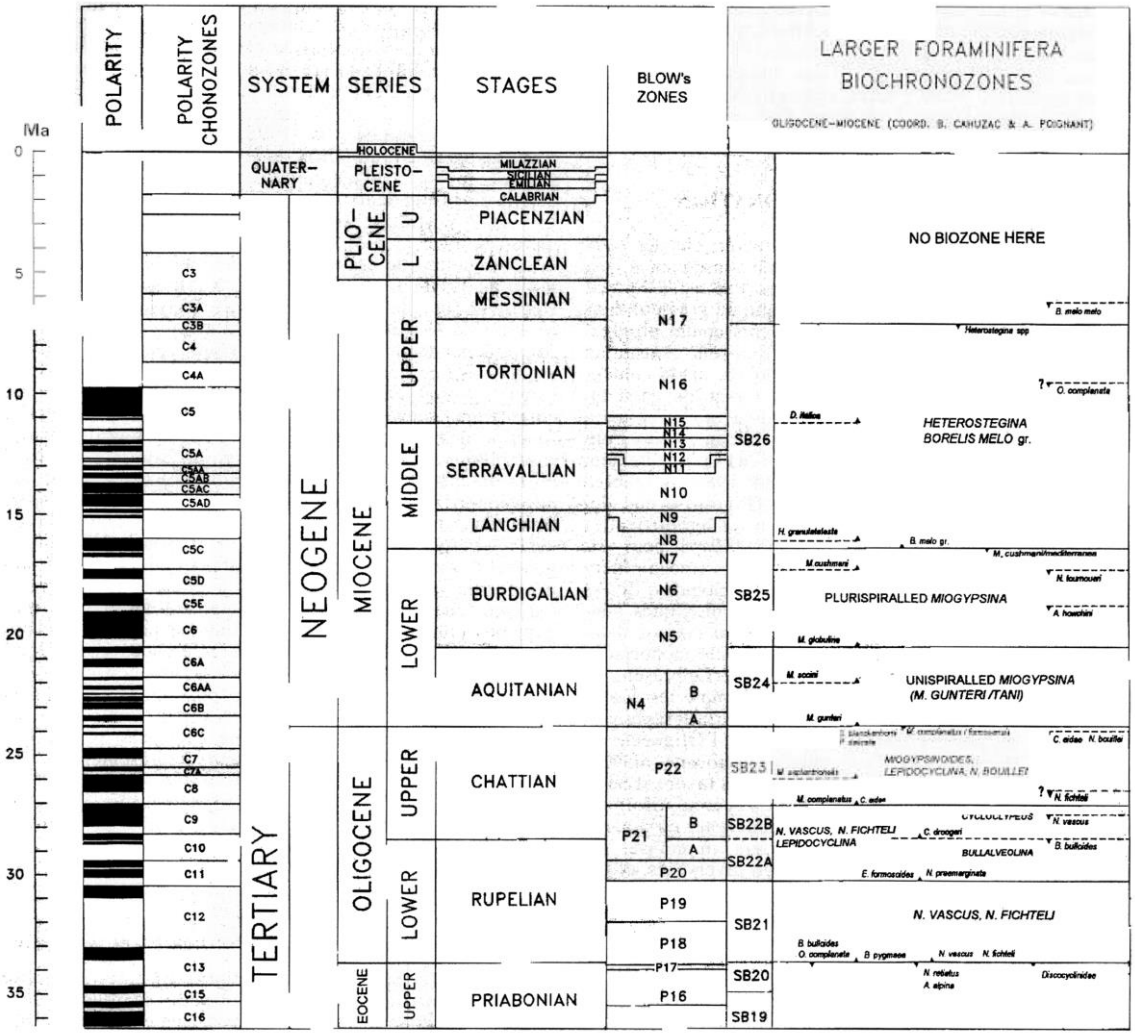

Fig. 8. The biostratigraphic scheme of the Shallow Benthic zones of the Oligocene and the Miocene by Cahuzac and Poignant (1997). The SB zones are correlated with the Time Scale by Berggren et al. (1995).

The correlations of both Serra-Kiel et al. (1998) and Cahuzac and Poignant (1997), based on data both from the authors and from the literature, were thought as susceptible to be changes, as new data would be made available.

Here are reported the original definitions as given by Serra-Kiel et al. (1998) for the Shallow Benthic zones to which the material of this thesis is referred to.

SB1: "defined by the biostratigraphic range of *Laffitteina bibensis* and *Bangiana hanseni*. The lower boundary corresponds to the Cretaceous/Tertiary boundary. This biozone is characterized by the presence of *Laffitteina*, the only survivor among the Cretaceous forms with canal systems.

SB2: "defined by the biostratigraphic range of: *Miscellanea globularis* [= *Miscellanites globularis* in this work, see subchapter 4.5.1], *Ornatononion minutus* [=*Miscellanites minutus* in this work, see subchapter 4.5.1], *Paralockhartia eos* and *Lockhartia akbari.* The lower boundary is imprecise, located in the upper part of the Chron 26r and within P3 according to Robador et al. (1991).

SB3: "defined by the biostratigraphic range of *Glomalveolina primaeva*, *Periloculina slovenica*, *Coskinon rajkae*, *Fallotella alavensis*, *Cribrobulimina carniolica, Vania anatolica*, *Miscellanea yvettae*, *Pseudomiscellanea primitiva* [= *Miscellanites primitivus* in this work, see subchapter 4.5.1], *Ranikothalia bermudezi*, *Nummulites heberti* and *Discocyclina seunesi*. The lower boundary is imprecise, located in the lower part of the Chron 26r and within P4 according to Robador et al. (1991).

SB4: "defined by the biostratigraphic range of *Glomalveolina levis*, *Hottingerina lukasi*, *Miscellanea meandrina*, *Daviesina garumnensis*, *Dictyokathina simplex*, *Nummulites catari*, *Assilina azilensis* and *A. yvettae*. The lower boundary is located in the lower part of the Chron 25r (Serra-Kiel et al. 1994).

SB11: "defined by the biostratigraphic range of *Alveolina dainelli*, *A.* aff. *canavarii*, *A. histrica histrica*, *A. decastroi*, *A. cremae*, *Nummulites praelaevigatus*, *N. burdigalensis cantabricus*, *N. kapellosi*, *N. escheri*, *N. nitidus*, *N. archiaci*, *Assilina laxispira* and *Discocyclina fortisi simferopolensis*. The lower boundary is located in the uppermost part of the Chron 22r, practically coinciding with the base of Chron 23.1n, according to the integration of data from Bentham and Burbank (1996) and Tosquella et al. (1990). SB11 corresponds to NP13 and the lower part of NP14 (Kapellos and Schaub, 1973; Schaub 1981), and to P8 and P9 (Hillebrandt 1975, Cavelier and Pomerol 1986)."

2.2.4. The need for updating and newly define the SB zones

After more than twenty years since the establishment of the SB Zones by Serra-Kiel et al. (1998) many progresses have been done. New genera and species have been described and the systematics has been revised for many LF taxa, among which alveolinids (e.g. Fornaciari et al. 2019), nummulitids (e.g. Sirel and Deveciler 2018), and especially rotaliids (e.g. Benedetti et al. 2011, Sirel

2012, 2013, Hottinger 2014, Benedetti 2015, Acar 2019), miscellaneids (Hottinger 2009) and complex miliolids (Acar 2019). Furthermore, new data have been collected for formerly poorly known intervals (such as the Paleocene; e.g. Drobne et al. 2007, Benedetti et al. 2018; Schlagintweit and Rashidi 2019) and geographical areas (e.g. Di Carlo et al. 2010 and Pignatti et al. 2008 for the Apulian domain; Drobne et al. 2011 for the Adriatic Platform; Acar 2019 and Sirel 2003, 2009, 2015 2018 for Turkey; Cotton et al. 2016 for Armenia; Serra-Kiel et al. 2016 and Vicedo et al. 2019 for Oman; Zhang et al. 2013 and Kahsnitz et al. 2016 for Tibet; Mathur et al. 2009 for India). Therefore, it is urgent to update the SB zones with the now available data on the biostratigraphic ranges of more taxa than those mentioned in Serra-Kiel et al. (1998). Papazzoni et al. (2017a) proposed an updated biostratigraphic scheme of the SB zones and of the OZ (**Fig. 9**) but the continuous progresses yet require additional revisions. Also, it would be interesting to compare the biostratigraphic ranges of the same taxa living in different geographical area. This is not the only issue.

As mentioned above, the SB zones are based on concurrent occurrences and hence have the problem of the subjectivity in determining their boundaries. Consequently, as seen in the subchapter 2.2.3, some of them are not well constrained. The correlation with different biozonation scales, the magnetostratigraphy and the isotope stratigraphy reduces this subjectivity but some additional criteria are required in order to achieve a complete and reliable system of biozones. The biozones should maintain a definition based on different taxa to allow their recognition in sediments from different environments and regions. Nevertheless, the biozones should be based on as few as possible markers, and not assemblages of taxa to reach easier correlations (Pignatti and Papazzoni 2017).

Therefore, the current biostratigraphic research aims at:

- extending and updating the systematics (including morphometric criteria which can be used to recognize the species);
- detecting the most suitable markers for defining the boundaries of the biozones by means of their FAD (*first appearance datum*) or other bioevents (bio-horizons);
- correlating the biozones, and possibly the FAD or the bioevents used to define their boundaries, with those of different groups having a firm zonation (especially calcareous nannofossils and planktonic foraminifera), and with other stratigraphic tools (magnetostratigraphy, isotopic stratigraphy, etc.); some integrated biostratigraphic studies have already been conducted, e.g., by Scheibner and Speijer (2009), Costa et al. (2013), Cotton et al. (2016), Papazzoni et al. (2017b) and Zhang et al. (2018).

The problem of the uncertainties in the first and last appearances of the taxa always affects the evolutionary studies of the group and the understanding of whether and how the paleoenvironmental and paleoclimatic events driven the biodiversity. This is particularly important issue for the lower Paleogene, when the LF were radiating and the climate was strikingly different from the present one. The results of this thesis are a contribution aimed to clarify the time frames and to determine a sound

basis for the future investigations on evolutionary and paleoenvironmental changes occurred in shallow-water settings.

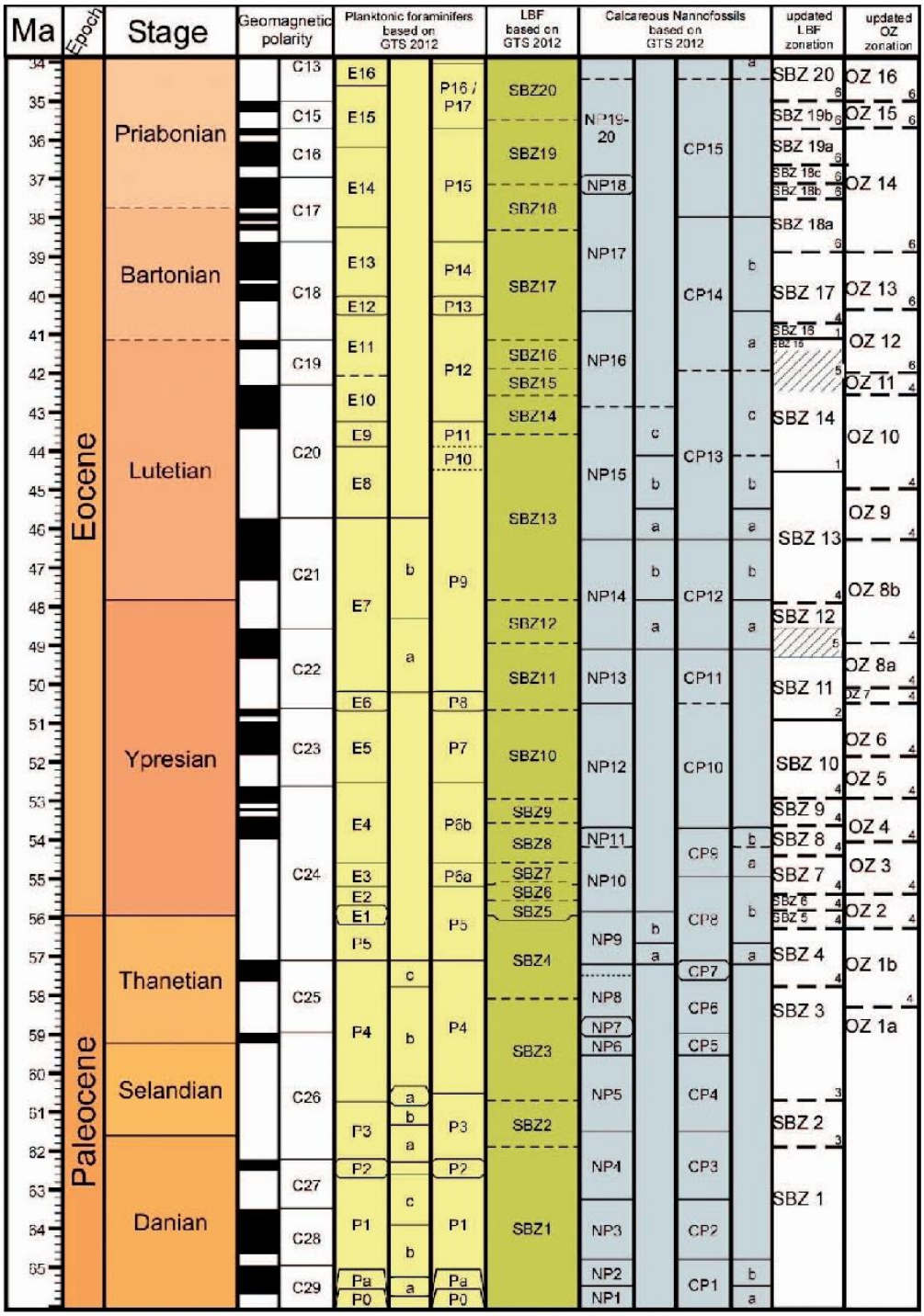

Fig. 9. Integrated biostratigraphic scheme for the Paleocene and Eocene as modified by Papazzoni et al. (2017a) from Vandenberghe et al. (2012). Numbers on boundaries of updated SBZ and OZ zonations (rightmost columns) indicate: 1 = magnetostratigraphic boundaries as proposed by Rodriguez-Pintó et al. (2012); 2 = magnetostratigraphic boundaries as proposed by Rodriguez-Pintó et al. (2013); 3 = boundaries as proposed by Serra-Kiel et al. (1998); 4 = boundaries as proposed by Özcan et al. (2014) by correlations with NP and P zones; 5 = zones of uncertain boundaries as proposed by Rodriguez-Pintó et al. (2012); 6 = Orthophragmine Zone (OZ) boundaries as proposed by Less and Özcan (2012).

2.3 THE EARLY PALEOGENE CLIMATIC AND PALEOENVIRONMENTAL EVENTS

2.3.1. The paleoclimatic events of the early Paleogene

The lower Paleogene was a crucial time for Earth's climate history, especially in the interval between the K/Pg boundary and the middle Eocene, punctuated by several paleoclimatic and paleoenvironmental events (**Fig. 10**). It was characterized by a progressive warming phase, expressed by a general decrease of the $\delta^{18}O$ values, that culminated in the Early Eocene Climatic Optimum (EECO; Zachos et al. 2001; Luciani et al. 2016). Superimposed on this trend, negative carbon isotope excursions (CIEs) witness several transient (10,000-100,000 years) environmental perturbations that determined extreme warmth and ocean acidifications and are known as hyperthemals. In the lower Paleogene, they were:

- the Dan-C2 (65.2 Ma) (Quillévéré et al. 2008, Coccioni et al. 2010);
- the Latest Danian Event (LDE) (61.7 Ma) (Quillévéré et al. 2008, Bornemann et al. 2009), equivalent to the Top Chron 27n (Westerhold et al. 2008) and to the CIE-DS1 (Arenillas et al. 2008);
- the Paleocene/Eocene Thermal Maximum (PETM) (e.g., ("BFEE", Kennett and Stott 1991, Thomas and Shackleton 1996, Schulte et al. 2013) (55.5 Ma), that was the longest (about 170 ky-long) and major event (associated to a global warming up to 10°C).

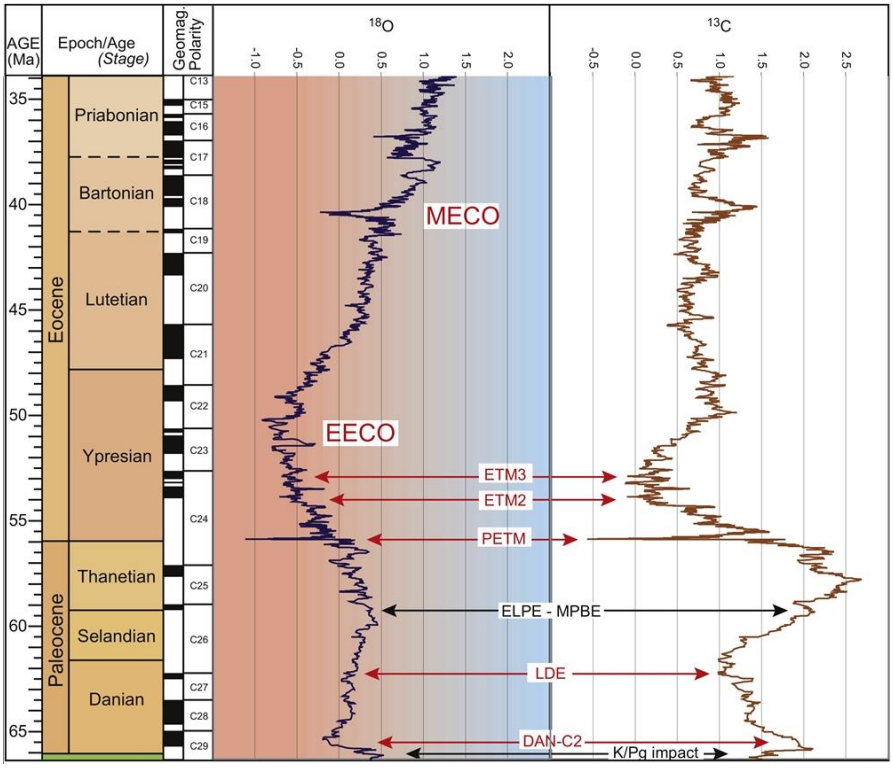

Fig. 10. Position of main lower Paleogene climatic events against the oxygen and carbon isotope curves for the Paleogene. Oxygen and carbon isotopic curves from Cramer et al. (2009). Modified from Vandenberghe et al. (2012).

All these events were probably connected with the introduction in the ocean-atmosphere system of a large mass of ^{13}C depleted carbon determining the excursion of the $\delta^{13}C$ towards negative values (Zachos et al. 2010). Studies on cores from numerous ODP sites (e.g. Bralower el al. 2002, Alegret and Thomas 2004, Bernaola et al. 2007, Westerhold et al. 2011) allowed to obtain a continuous and high-resolution stratigraphic and stable isotopic record for the lower Paleogene and discovered a correlation between the negative carbon isotope excursions and the maxima in both the long (405 kyr) and the short (100 kyr) eccentricity cycles. Therefore, these events are thought to be related to a particular orbital configuration but the exact trigger is still debated (Zachos et al. 2010) and the tempo and mode of their effects on the marine and terrestrial biota are not fully explored.

Among the different hypothesis for the trigger of the hyperthermals, there are:

- crossing of a climatic threshold associated with the long-term warming trend (De Conto et al. 2012);
- impulse of the volcanism during the formation of the North Atlantic Igneous Province (NAIP) that would have provoked a thermogenic methane release and/or a temperature increase (Svensen et al. 2004, Storey et al. 2007);
- carbon release in the atmosphere from the methane clathrate deposits in the Antarctica due to a suitable orbital configuration (De Conto et al. 2012) as methane hydrate deposits in marine sediments may expand or contract in response to climatic changes under orbital variations control (e.g. oceanic temperature), sedimentation rate and/or productivity (Zachos et al. 2010);
- desiccation of organic-matter rich large basins with consequent oxidation (Higgins and Schrag 2006): indeed, during eccentricity *maxima*, land-sea heating produces monsoon and strong precipitations that lead to intense but short wet season; when eccentricity increases, the pronounced dry season reduces organic carbon accumulation and promotes the oxidation of the already formed peat or lignite through desiccation; the release of CO_2 determines warming, amplifying season extremes. Such control on coal formation is supported in part by the massive upper Paleocene coal seams of Wyoming, whose cyclicity matches precession and eccentricity frequencies. Moreover, cores from different locations show evidences for increased erosion indicating enhanced seasonally precipitation during the hyperthermals (Zachos et al. 2010);
- cometary impact (Kent et al. 2003).

However, according to Zachos et al. (2010), carbon volcanic-related emissions, both direct and indirect (e. g. volcanic emissions or crustal organic matter burning), though potentially able to contribute to one or two excursions, could not have been the main responsible for these cycles. Moreover, according to Littler et al. (2014), the hypothesis of a cometary impact seems to be scarcely related to these phenomena which are instead connected with the orbital cyclicity. Only further integrated stratigraphic studies may help to understand timing, features and reasons of these hyperthermal events.

2.3.2. The Early Late Paleocene Event (ELPE)

In the lower Paleogene there was a major paleoenvironmental event, called Early late Paleocene Event (ELPE) or Mid Paleocene Biotic Event (MPBE) (e.g., Bralower 2002, Bernaola et al. 2007, Petrizzo 2005), dated at ~58.4 Ma. This thesis investigates the possible relation between it the LF evolution. Therefore, the ELPE is summarized here below.

According to Petrizzo (2005), who studied the lithology and the fossil assemblages on cores from the Shatsky Rise (northwestern Pacific), the ELPE occurs in correspondence of a 5-25 cm thick, dark brown clay-rich muddy level with low-diversified associations of planktonic foraminifera. As regards the nannofossil associations, here we have the first appearance of *Heliolithus kleinpelli* (marker for the base of the NP6 zone; Martini 1971) and of primitives discoasterids (both dominant components of the upper Paleocene). The planktonic foraminiferal associations are characterized by a low diversity, largely dissolved tests dominated by representatives of the genus *Igorina*. Other groups (morozovellids, acarininids, globanomalinids, subbotinids and chiloguembelinids) almost disappear in correspondence of the level while they are common below it and present in low abundances above it. These changes in faunal compositions could be the result of dissolution on the seafloor, probably due to a shoaling of the lysocline and of the carbonate compensation depth induced by oxydation of methane released from sedimentary hydrate reservoirs of CO_2. The hypothesis of dissolution is also supported by the common presence of crystals of phillipsite and fish teeth inside the clay-rich level, indicating very low sedimentation rate. Furthermore, in correspondence of the ELPE it is also registered a prominent peak in the magnetic susceptibility related to the quantity of phillipsite (Petrizzo et al. 2005).

The ELPE has been characterized also by several parameters. Zachos et al. (2010), analyzing Fe intensities, carbon and oxygen isotopes and magnetic susceptibility, found evidences of a climate control (through the runoff) in the clayey fraction and therefore in the conditions that control carbonate preservation (such as local carbonatic production and water saturation on the sea bottom). Frequencies corresponding to the Milankovitch precession and eccentricity cycles were also identified.

Nevertheless, the exact features and the nature of the ELPE are discussed. Only at Zumaia, which holds the best record for the ELPE, the onset of this event is marked by a significant negative carbon isotope excursion (a -1‰ shift in the $\delta^{13}C$), not recorded elsewhere (Bernaola et al. 2007, Westerhold et al. 2011), corresponding to a large input of CO_2 in the environments. According to Bernaola et al. (2007), this input lowered deep-sea pH, triggering a rapid shoaling of the lysocline and contributing to a greenhouse warming. However, this characterization has been inferred only at Zumaia. The duration of the event has been estimated in 52-53 kyr but its core (corresponding to the negative shift of the $\delta^{13}C$) in 10-11 kyr (Bernaola et al. 2007).

The effect of the ELPE on the marine carbonate production and on the pelagic biota are well known but the same cannot be said for the shallow water organisms. All what we known is that,

according to the current correlations between SB zones and plankton/nannoplankton zones, the ELPE occured very close to some important LF events. It corresponds roughly to the base of the Zone SB3, which coincide with the first appearance of several genera of Paleogene LF: among others *Nummulites*, *Ranikothalia*, *Glomalveolina*, *Discocyclina*, *Orbitoclypeus*, etc. Unfortunately, the lowermost occurrences of these genera are poorly constrained and the base of the SB3 itself is not yet clearly defined. Therefore, to clarify the relationship between the LF evolution and the ELPE we need a refined biostratigraphic frame. This work, aimed to detect the main bio-horizons of both pelagic and shallow water assemblages, may help in clarifying this point.

3. GEOLOGICAL SETTINGS OF THE ANALYZED SECTIONS

3.1. THE SOUTHERN ALPS

Fig. 11. Location map of the studied sections: 1 = Tabiago section; 2 = Monte Giglio section; 3 = Ardo section; 4 = Monte Postale and Pesciara sections. Modified from Papazzoni et al. (2017b).

The Tabiago, Monte Giglio, Ardo and Monte Postale sections are located in northern Italy (**Fig. 11**), in the Southern Alps, which represent the south-verging fold-and-thrust belt (Doglioni and Bosellini 1987) resulting from the polyphasic deformation of the northern passive continental margin of the Adria microplate (Bernoulli 1972).

The history of the Southern Alps can be reconstructed from the Permian, when dextral wrench movements between Gondwana and Laurasia determined widespread transcurrent faulting and graben formation. During the Early and Middle Triassic the Southern Alps were gradually flooded and differential subsidence and local uplifts formed a complex pattern of carbonate platforms and basins, which were later interested by volcanism and extensional tectonics (Bertotti et al. 1993). In the Early Jurassic the Southern Alps were divided into four major domains, from east to west the Friuli Platform, the Belluno Trough, the Trento Platform and the Lombardian Basin. At the end of the Early Jurassic, a strong subsidence led to the drowning below the photic zone of the former shallow-water Trento Platform, which became the Trento Plateau, and a rather uniform pelagic sedimentation settled on most of the Southern Alps (e.g., Bosellini et al. 1981, Winterer and Bosellini 1981, Luciani 1989). During the Late Cretaceous a tectonic inversion occurred determining the beginning of the collision between the Eurasian and the African plate and of the Ligurian-Piedmont Ocean subduction (e.g., Dal Piaz et al. 2003). The western part of the Southern Alps acted as the foredeep of a northern emerged area and was interested by thick (up to 2.5 km) deposits of siliciclastic debris known as “Cretaceous Flysch of Lombardy” derived from the erosion of the early orogenic wedge of the Alpine belt (Luciani 1989, Bersezio et al. 1993). The Trento Plateau continued to be covered by pelagic sedimentation with the deposition of the Upper Cretaceous Scaglia Rossa Formation. The Friuli Platform remained in shallow-water setting and discharged its debris in a wide slope towards the Trento Plateau (Luciani 1989) (**Fig. 12**).

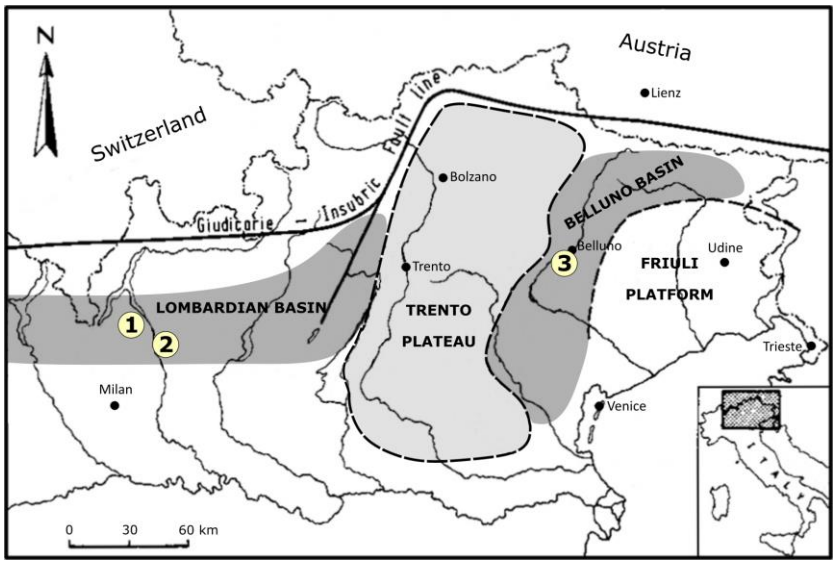

Fig. 12. The main Paleocene paleogeographic elements of the Southern Alps modified from Channel and Medizza (1981) with the locations of the Tabiago section (1), Monte Giglio section (2) and Ardo section (3).

During the early Paleogene the collision between the Eurasian and the African plate led to a major reorganization of the Southern Alps: the former Trento Plateau was uplifted and block-faulted and since the early Eocene it gradually became an area of shallow-water carbonate sedimentation, the Lessini Shelf (**Fig. 13**), also interested by volcanic activity (Luciani 1989). In the Belluno Basin, the carbonatic pelagic sedimentation persisted up to the early Eocene, when it was overlaid by siliciclastic turbidites forming the Belluno Flysch (Stefani and Grandesso 1991), representing the foredeep deposits of the west-verging Dinaric thrusts (Doglioni and Bosellini 1987).

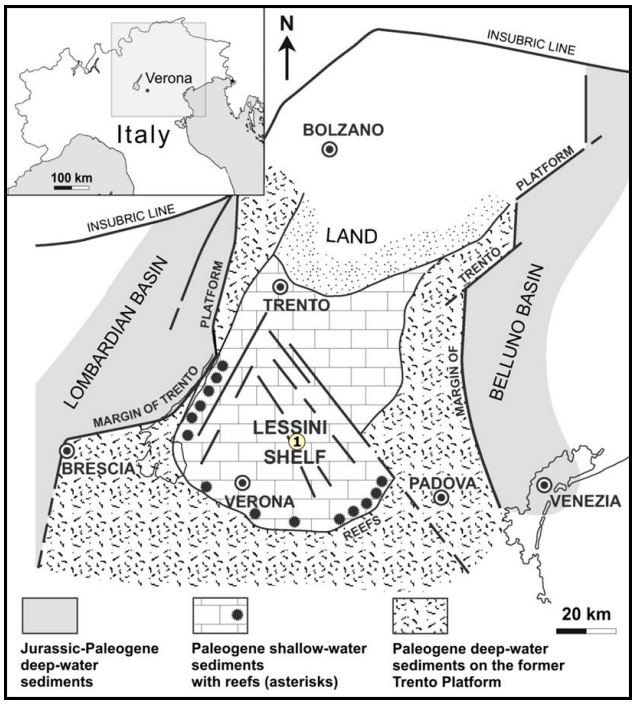

Fig. 13. The early Eocene Lessini Shelf with the location of the Monte Postale and Pesciara sections (1) of Bolca *Fossil-Lagerstätten*. Modified from Vescogni et al. (2016).

3.2. THE LOWER PALEOGENE IN THE LOMBARDIAN BASIN

In the Lombardian Basin the lower Paleogene is quite well represented. In the eastern Lombardy the K/Pg boundary is represented by the contact between the Brenno Formation (upper Campanian-upper Maastrichtian; Tremolada et al. 2008) and the Tabiago Formation (Danian-lower Lutetian), both commonly referred to the "Scaglia Lombarda" *Auctt*.

The Brenno Formation, formerly known as "Piano di Brenno" (De Alessandri 1899, Kleboth 1982), is mainly constituted by white/grey/pinkish marly limestones and secondarily by calcareous marls, regularly bedded and intercalated with thin sandstone levels.

The Tabiago Formation (Kleboth 1982) is mainly formed by calcareous marls and secondarily by marly limestones, sometimes alternated with pelitic marls, with intercalations of calciruditic/calcarenitic turbidites containing abundant benthic foraminifera. Kleboth (1982) distinguished the Montorfano member from the coeval Tabiago Formation due to its different lithofacies, mainly represented by conglomerates. The Tabiago Formation is overlain by the Lutetian-Bartonian Cibrone Formation, belonging to the Gallare Marls Group and composed by grey pelitic or siltitic marls, sometimes referred to as Scaglia (Bini et al. 2013, 2014).

The presence of the Paleocene in the Lombardian Basin was first reported by Venzo (1954), who described the Flysch of the Brianza and Bergamo areas. His record relied on micropaleontological studies on planktonic foraminifera by Selli (in Venzo, 1954). Schweighauser (1953), in a work focussed on the Vicenza province, described the characteristic benthic foraminiferal association of Cava Merone (near Camisasca, Lecco province) ascribing it to the Maastrichtian and the lower Paleocene. Bolli and Cita (1960a, b) studied the planktonic foraminifera of Paderno d'Adda, a section object of most of the previous works and successively re-sampled by Cita et al. (1968), who obtained the first integrated biostratigraphy with larger foraminifera, planktonic foraminifera and calcareous nannofossils for the Maastrichtian to middle Eocene interval in the area. The stratigraphy, sedimentology and micropaleontology of many outcrops of the Upper Cretaceous-middle Eocene of the Lombardian Basin were later extensively analysed by Kleboth (1982), who hypothesized that the area was occupied by a 1,500-2,500 m depth basin, east-westward elongated, bounded to the north by a platform from which shallow-water material was repeatedly discharged as turbidites and debris-flows. The higher detrital input in the middle and upper Paleocene created two fans: Montorfano to the west and Monte Giglio to the east, studied in detailed by Beckmann et al. (1982) who framed the section in both planktonic foraminiferal and calcareous nannofossil stratigraphy. Poletti et al. (2004) recorded orbitally-driven fertility cycles in correspondence of the limestone-marlstone alternations in Tabiago section, as in the Belluno Basin, finding a stronger control by the runoff for the first than for the latter and therefore supporting the hypothesis of the vicinity of a large land mass. Calcareous nannofossils and planktic foraminifera have been later analyzed in detail by Tremolada et al. (2008)

and Premoli Silva et al. (2010), respectively. The recent studies on the lower Paleogene of the Lombardian Basin supported Bini et al. (2013, 2014) in developing the geological map of the area.

3.3. THE LOWER PALEOGENE IN THE TRENTO PLATEAU-LESSINI PLATFORM

The area between the Lombardian Basin and the Belluno Basin in the lower Paleogene underwent important changes. In the Paleocene, this area was a basin partly occupied by a structural high, called Trento Plateau which was the former shallow-water Trento Platform, formed in the early Jurassic and drowned below the photic zone in the Middle Jurassic due to an important tectonic subsidence (Winterer and Bosellini 1981, Luciani 1989). From the Late Cretaceous, the Alpine tectonics, passing from an extensional regime to a compressive one, determined the block-faulting of the Trento Plateau in horst and graben. Therefore, the structural highs acted as centres of shallow-water carbonate production which, prograding and coalescing, eventually formed the Lessini Shelf (Bosellini 1989; Luciani 1989), whose first evidences are known from the early Eocene. Basaltic intrusions and volcanoclastites are scattered into these sediments, as the tectonics also determined volcanic activity. According to Barbieri et al. (1991), six volcanic phases occurred, one in the Paleocene and five in the early-late middle Eocene.

From the late Paleocene, the central-eastern Lessini were interested by the development of the Castelvero fault, NNW-SSE oriented, which border to the west the graben system known as "Alpone-Chiampo graben" (Barbieri et al. 1982) or "Alpone-Agno graben" (Zampieri 1995), where Bolca is located. This graben influenced the sedimentation on the Lessini Shelf, determining the deposition of pelagic carbonates and resedimented calcarenites on the eastern part (the graben), and of shallow-water marine carbonates on the western part (western Lessini) (De Zanche and Conterno 1972).

The area of the Lessini Mounts has been intensively studied in the past but the litostratigraphy still suffers the lack of formal names for the formations. The "Spileccian" stage was used by Fabiani (1912) as equivalent to the whole Paleocene and the lower Eocene but then (Fabiani 1915) he restricted it to the lower Eocene and the Spileccian was intended in this sense also later (e.g., Malaroda 1967, Ungaro 2001), while Spilecco outcrop is currently ascribed only to the uppermost Thanetian and the lowermost Ypresian (Papazzoni et al. 2014). The Chiusole Formation represents the deeper deposition of the lower Eocene.

3.4. THE LOWER PALEOGENE IN THE BELLUNO BASIN

In the Belluno Basin (NE Italy) the lower Paleogene rocks are well exposed south of Belluno, where the expanded and relatively undisturbed pelagic-hemipelagic sediments crop out in numerous sites. The K/Pg boundary in the Belluno Basin falls within the Scaglia Rossa Formation which, in this

area, is extended from the Upper Cretaceous (with a diachronous base) to the lower Eocene (Costa et al. 1996).

The Scaglia Rossa Formation is mainly represented by bedded and sometimes nodular, pinkish-reddish limestones and marly limestones, with frequent intercalations of whitish bioclastic turbidites and cherty nodules in the lower part progressively decreasing towards the upper part, where the clayey fraction becomes progressively higher (Costa et al. 1996). In the eastern part of the Belluno Basin (Ardo section included), it has been subdivided into local informal lithostratigraphic units: "Cugnan Formation", "Scaglia Cinerea" and "Marna della Vena d'Oro" (Di Napoli Alliata et al. 1970, Costa et al. 1996). The Cugnan Formation is formed by Maastrichtian-Danian Scaglia-type rocks with decimetric intercalations of greyish biocalcarenites composed of bryozoans, foraminifera, calcareous algae and corals. According to Costa et al. (1996) such beds were deposited by turbidity currents, whith the source area probably located to the SE, as testified by the renewal/persistence of carbonate productivity in some sectors of the western Friuli Platform. The "Scaglia Cinerea", deposited in the Selandian-Thanetian between the "Cugnan Formation" and the "Marna della Vena d'Oro", is composed by more or less argillaceous grey marls, with few intercalations of bioclastic turbidites, while the Marna della Vena d'Oro is formed by upper Thanetian-Ypresian argillaceous reddish marls.

These sedimentary rocks are capped by the lower-middle Eocene Belluno Flysch (e.g., Stefani and Grandesso 1991, Costa et al. 1996) representing the foredeep deposits of the west-verging Dinaric thrusts (Doglioni and Bosellini 1987).

The lower Paleogene deep-sea succession of the Belluno Basin have been studied in detail only recently (e.g., Giusberti et al. 2019). Fornaciari et al. (2007) documented the K/Pg boundary and an expanded and continuous record of the basal Danian in the Forada section by means of an integrated calcareous plankton study. Giusberti et al. (2007) documented a condensed upper Danian and Selandian and an expanded Thanetian in the same section, where the PETM has been intensively investigated (e.g., Giusberti et al. 2007, Agnini et al. 2007; Luciani et al. 2007; Giusberti et al. 2016, 2018, 2019). Other Paleocene-lower Eocene hemipelagic outcrops of the Belluno area (Teche, Cicogna and Ardo) were object of detailed stratigraphic and paleoclimatic investigations (e.g., Dallanave et al. 2009, 2010, 2012a,b, Agnini et al. 2016, D'Onofrio et al. 2016) and some of them contributed to the development of a new biozonation scheme for the low and middle latitudes Paleogene calcareous nannofossils (Agnini et al. 2014).

4. MATERIAL AND METHODS

4.1. THE STUDIED SECTIONS

4.1.1. The Tabiago section

The Tabiago section is located near the town of Tabiago (18 km south-west of Lecco, north-western Italy), where the Brenno Formation and the Tabiago Formation (in its type locality) crop out along the sides of the Milano-Lecco SS 36 highway (**Fig. 14**, **Fig. 15**).

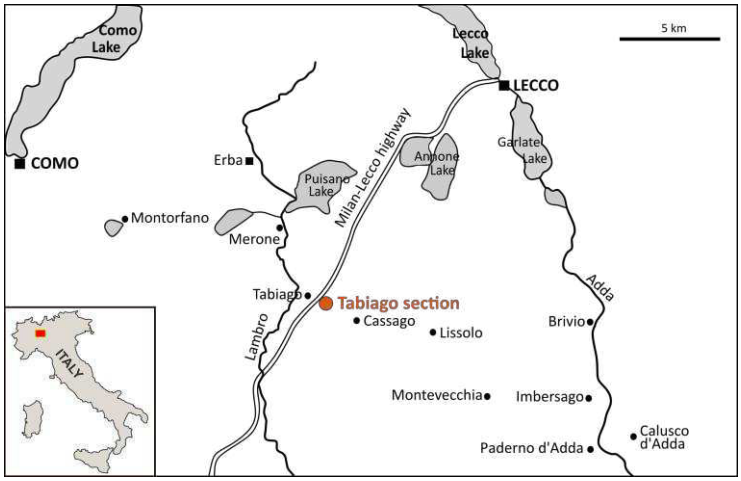

Fig. 14. Location map of the Tabiago section. Modified from Kleboth (1982).

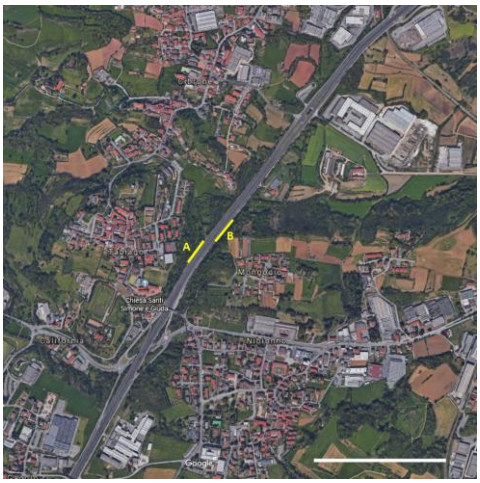

Fig. 15. The Tabiago section (in orange) as seen from Google Earth. The section is composed by: A = Milano segment; B = Lecco segment.

The Tabiago section was first mentioned by Premoli Silva and Luterbacher (1966) and it was successively dated by Kleboth (1982) by means of the planktonic foraminifera, by Tremolada et al. (2008) by calcareous nannofossils and by Premoli Silva et al. (2010), who obtained an integrated biostratigraphy with planktonic foraminifera and calcareous nannofossils. However, these studies were based on low-resolution sampling (about 1 sample every 5 m; Kleboth 1982, Tremolada et al. 2008) and none of them analysed the LF contained in the turbidites.

The part of the section here analysed is entirely included within the Tabiago Formation (Kleboth 1982), mainly made by reddish-brown marls and calcareous marls ("Scaglia" type facies) with intercalated biocalcarenitic or biocalciruditic turbidites. The section was sampled on two segments due to the impossibility to follow continuously the outcrop on only one side of the road: the "Milano" segment (19.2 m thick) represents the lower part of the section on the western side of the highway, whereas the "Lecco" segment (48.4 m thick) cover the higher part of the formation on the eastern side of the highway. The total thickness is therefore 67.6 m. The base section corresponds to

the lowermost outcrop of the Paleocene. Here were collected in total 60 samples for LF from the turbidites and 77 samples for calcareous nannofossils from the marls (**Fig. 16**, **Fig. 17**).

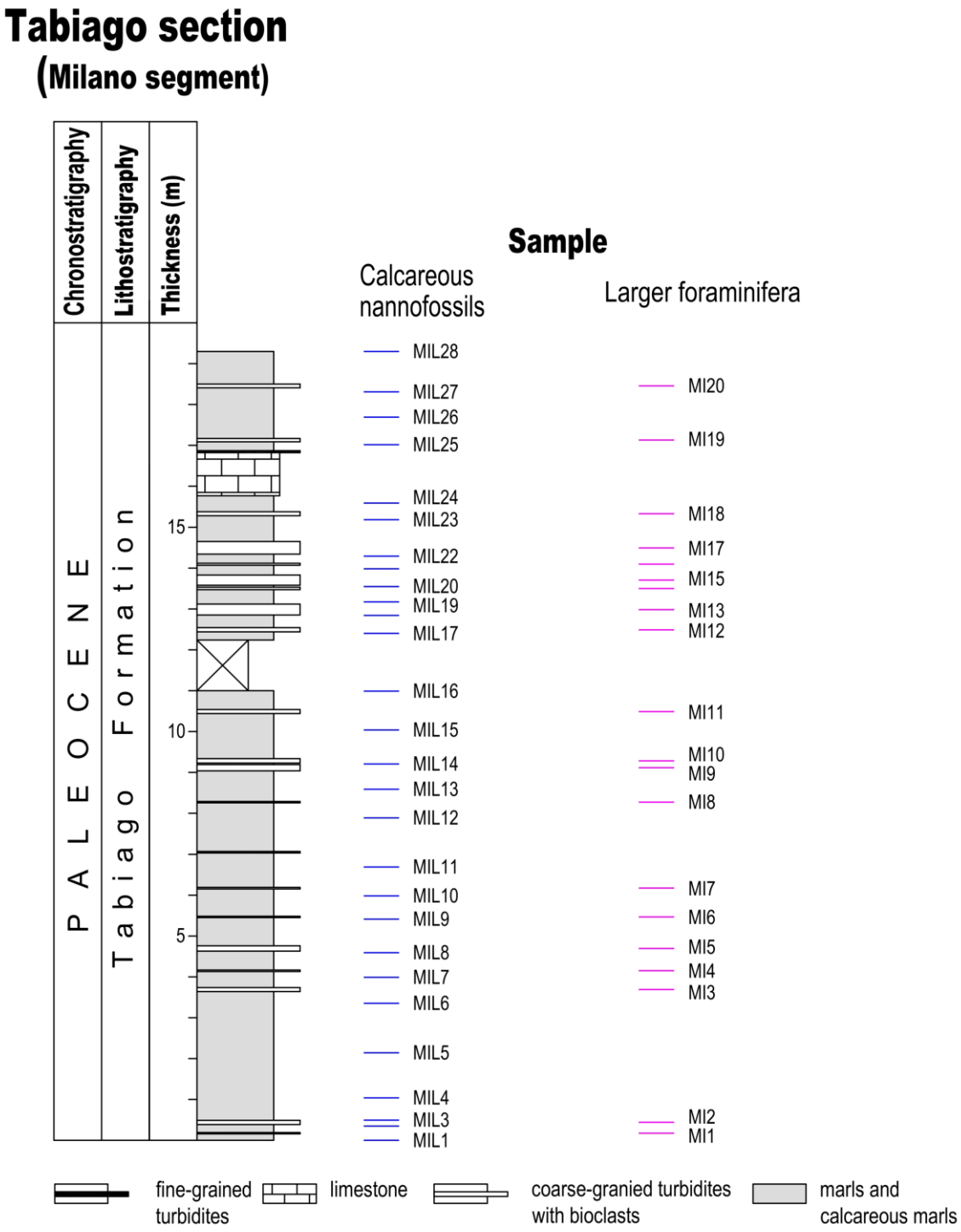

Fig. 16. Stratigraphical column of the Milano segment of the Tabiago section with the positions of the samples collected for nannofossils and larger foraminifera.

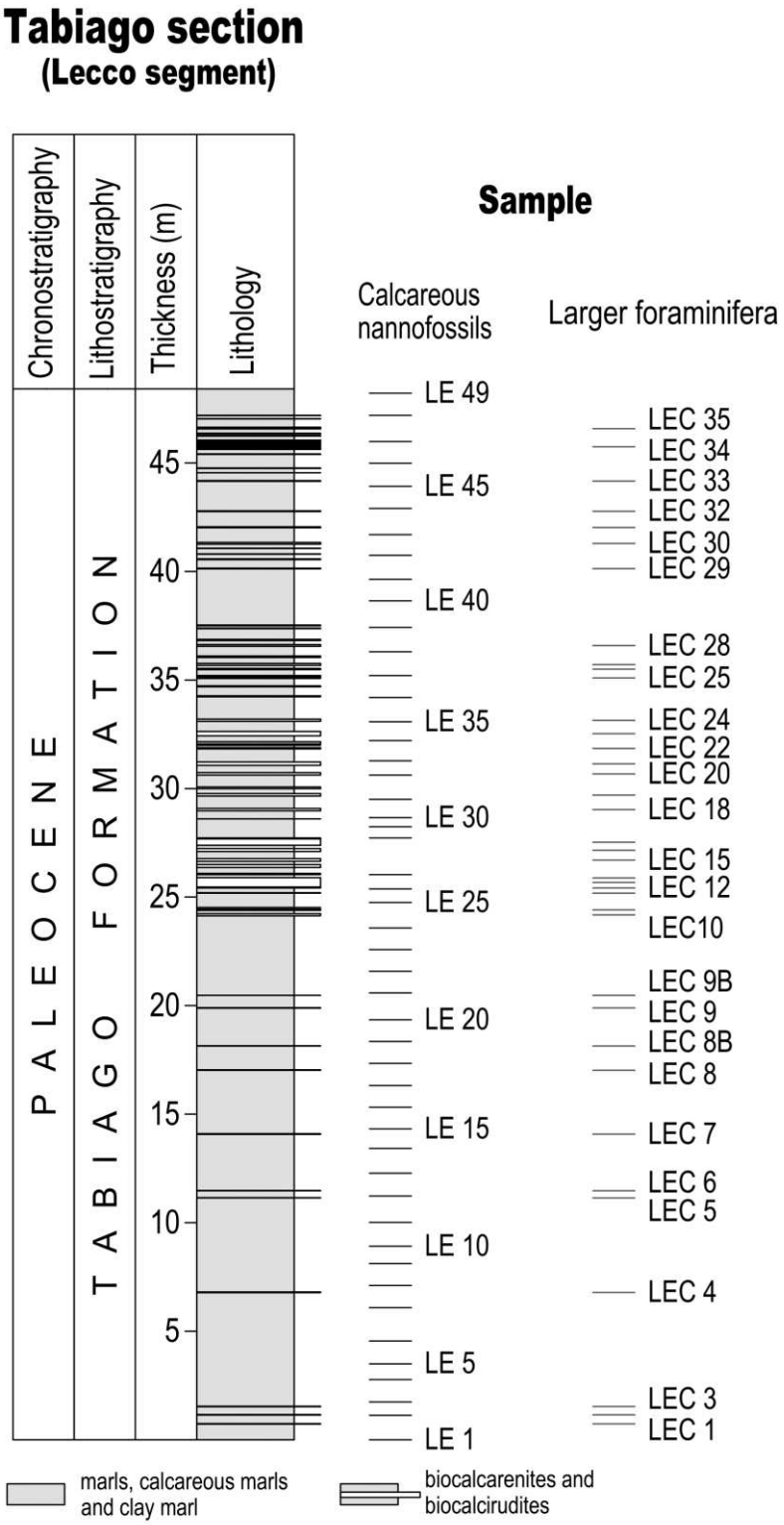

Fig. 17. Stratigraphical column of the Lecco segment of the Tabiago section with the positions of the samples collected for nannofossils and larger foraminifera.

4.1.2. The Monte Giglio section

The Monte Giglio section is located in the homonymous quarry, on the eastern side of the Adda River, north of Calusco d'Adda (17 km east of Bergamo, north-western Italy) (**Fig. 18**, **Fig. 19**).

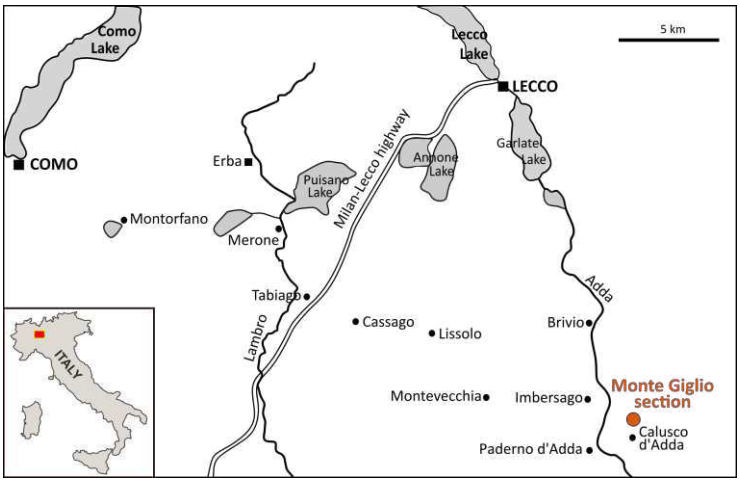

Fig. 18. Location map of the Monte Giglio section. Modified from Kleboth (1982).

Fig. 19. The Monte Giglio section (in orange) as seen from Google Earth.

Monte Giglio was first mentioned by De Alessandri (1899) in some observations about the Cretaceous of this area. At that time, it was a 412 m-high hill; currently, after more than one century of exploitation, it is an open pit mine with negative relief. Floridia (1935), in a paper about the orbitoids of the Lombardian Flysch, described the stratigraphic succession of the area, providing a geological sketch map. The first to provide biostratigraphic data for a section of the Monte Giglio quarry was Venzo (1954) who detected the Campanian-Danian interval by means of planktonic foraminifera. Moreover, he identified a *hiatus* spanning the upper Maastrichtian to basal Danian. Premoli Silva and Luterbacher (1966) considered this *hiatus* to be limited to the lower Danian. Kleboth (1982), by means of planktonic foraminifera, again recognized an upper Maastrichtian–Danian hiatus. The most complete study for Monte Giglio was published by Beckmann et al. (1982), who examined in detail the micropaleontological associations and attributed the Flysch di Bergamo to the upper Campanian, the Piano di Brenno Formation to the Maastrichtian and the Tabiago Formation to the middle Paleocene (from the *Heliolithus kleinpelli* to the *Discoaster multiradiatus* zones *sensu* Hay et al. 1967, corresponding to the NP6-NP9 zones *sensu* Martini 1971).

Unfortunately, the section originally described by Beckmann (1982) no longer exists in the quarry due to the intense exploitation activity; for this reason, we sampled a 40.7 m-thick section on the northwestern side of the quarry, considered to be more or less equivalent to the one described by Beckmann (1982). It is mainly made by reddish-brown calcareous marls and marls intercalated by whitish-greyish thick calciruditic and calcarenitic turbidites belonging to the Tabiago Formation. Most of these turbidites contain clasts of various lithologies, often with pointed angles, indicating the re-

deposition of sediments with a quite close source area. Here were collected 59 samples for LF and 51 samples for CNF (**Fig. 20**)

.

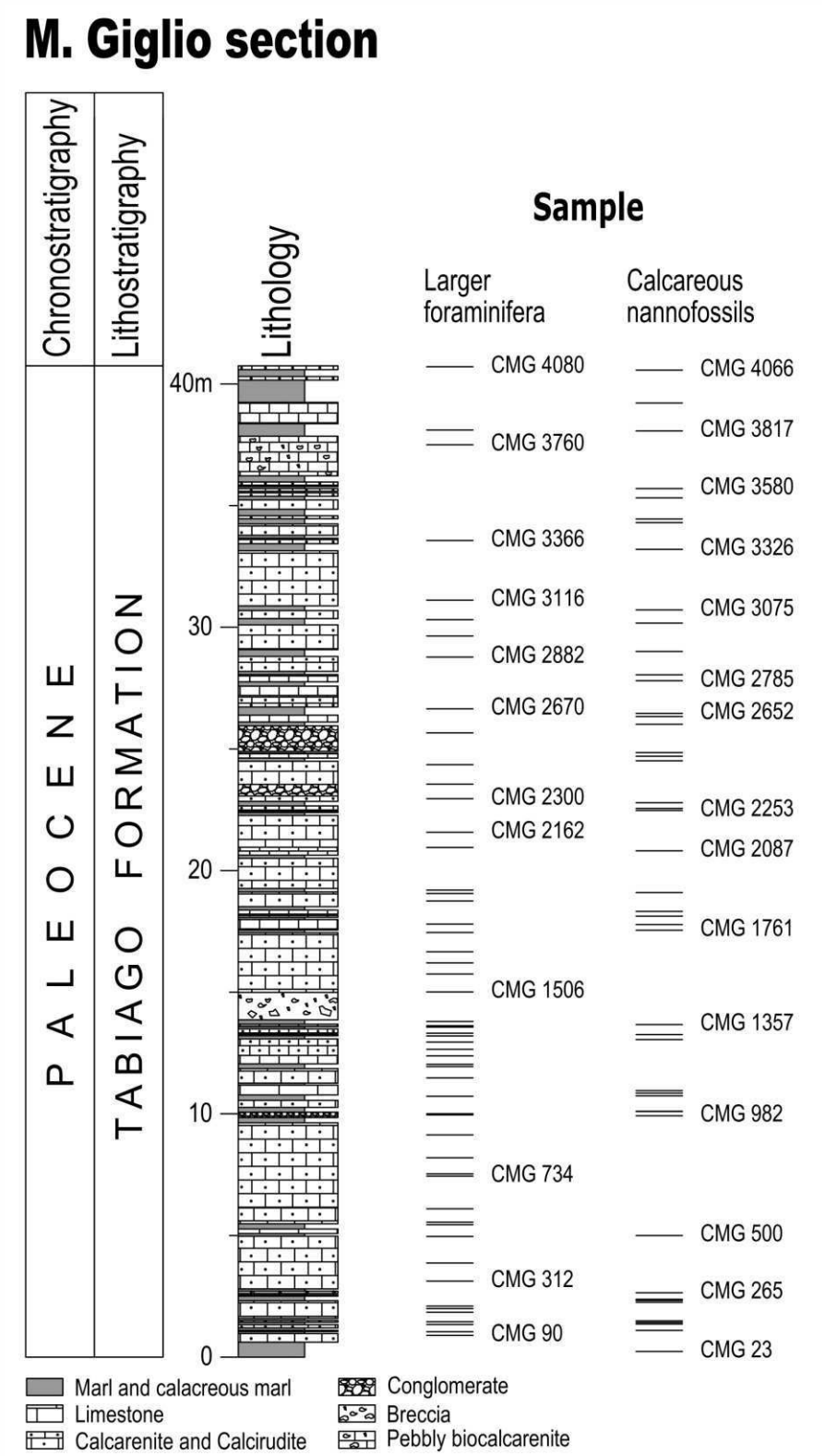

Fig. 20. Stratigraphical column of the Monte Giglio section with the positions of the samples collected for calcareous nannofossils and larger foraminifera.

4.1.3. The Ardo section

The Ardo section is located along the homonymous creek near Sant'Antonio Tortal village (13 km southwest of Belluno, north-eastern Italy) (**Fig. 21**, **Fig. 22**) where a ca. 100 m-thick Paleocene succession continuously crops out.

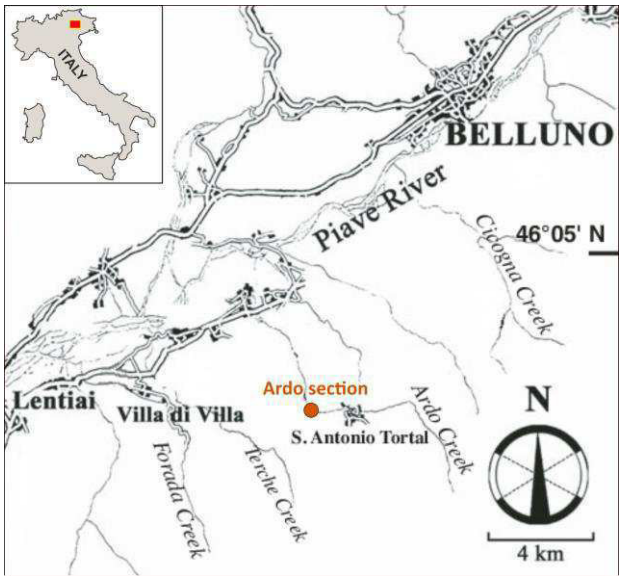

Fig. 21. Location map of the Ardo section. Modified from Giusberti et al. (2007).

Fig. 22. The Ardo section (in orange) as seen from Google Earth.

In the lower part of the section the K/Pg boundary is represented by a 1.5 cm-thick red "boundary clay" level (Agnini et al. 2005, Fornaciari et al. 2007, Agnini et al. 2104) overlaid by reddish/pinkish to grey marls and calcareous marls. Frequently intercalated calciruditic and calcarenitic greyish-whitish turbidites occur below and right above the K/Pg boundary up to 14 m ("Cugnan Formation"; Di Napoli Alliata et al. 1970, Costa et al. 1996), where the beds are organized in decimetric marly limestones-marls couplets belonging to the "Scaglia Cinerea" up to the top of the sampled section (Costa et al. 1996, Giusberti et al. 2007).

The outcrop was previously studied by Giusberti et al. (2007) who preliminary investigated the calcareous nannofossil biostratigraphy and correlated it with other Paleocene-lower Eocene sections of the Belluno Basin. Later, Dallanave et al. (2012) refined the calcareous nannofossil stratigraphy of the section and integrated it with the magnetostratigraphy for the entire Paleocene interval. The section studied by these authors spans from the uppermost Maastrichtian to the Ypresian.

For this study, the lower part of this section was resampled starting from the K/Pg boundary, namely the first 25 m characterised by bioclastic, larger foraminifera-bearing intercalations. Thirty-nine samples were collected for LF and sixty-seven for calcareous nannofossils (**Fig. 23**).

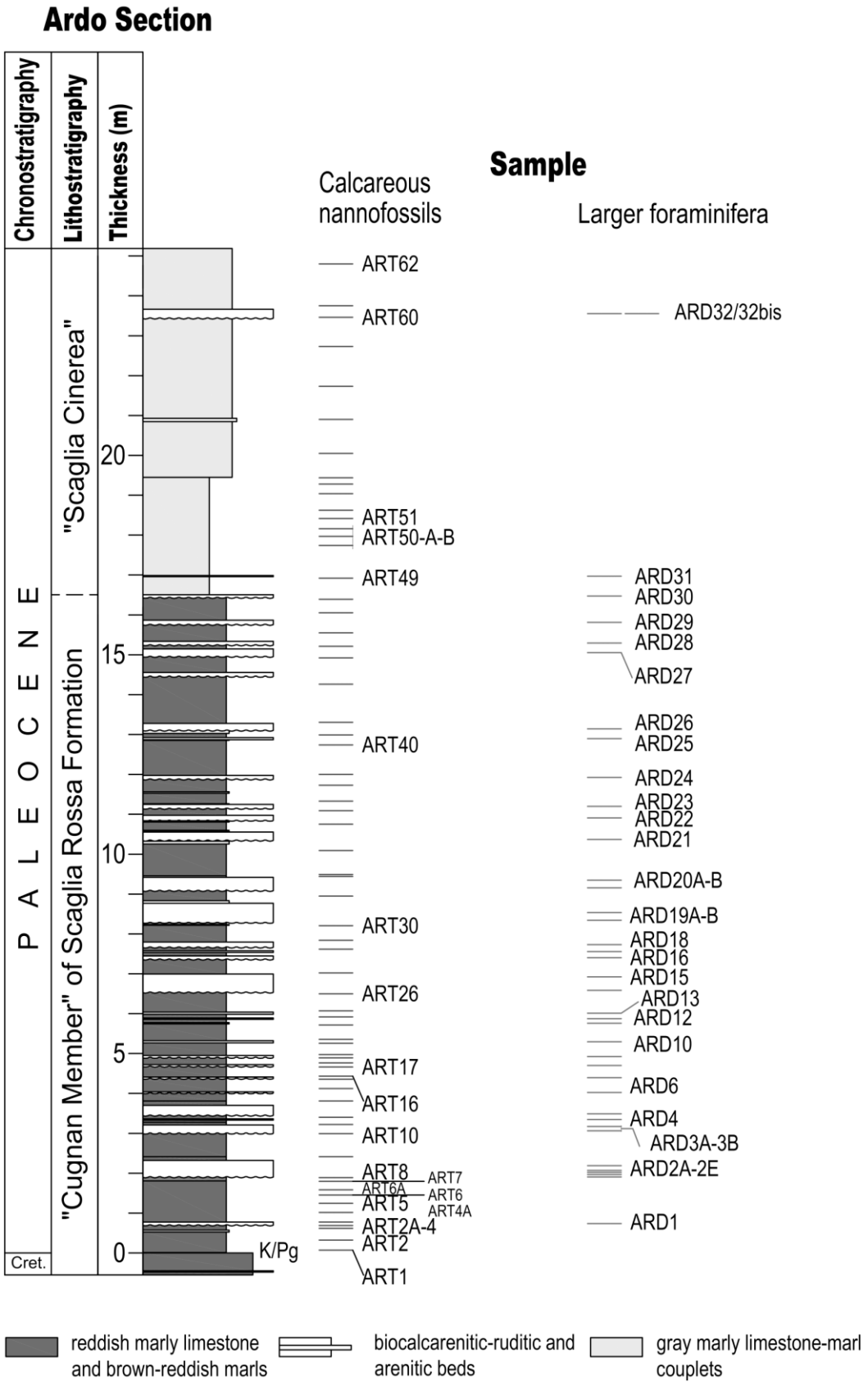

Fig. 23. Stratigraphical colum of the Ardo section with the position of the samples collected for calcareous nannofossils and larger foraminifera.

4.1.4. The Monte Postale and Pesciara sections at Bolca

The Monte Postale and Pesciara sections are located close to the village of Bolca (40 km northeast of Verona, northeastern Italy) (**Fig. 24**). Both the outcrops are formed by shallow-water limestones (alternatively massive, bedded with *Alveolina* grainstones or laminated) intercalated by thin marly layers.

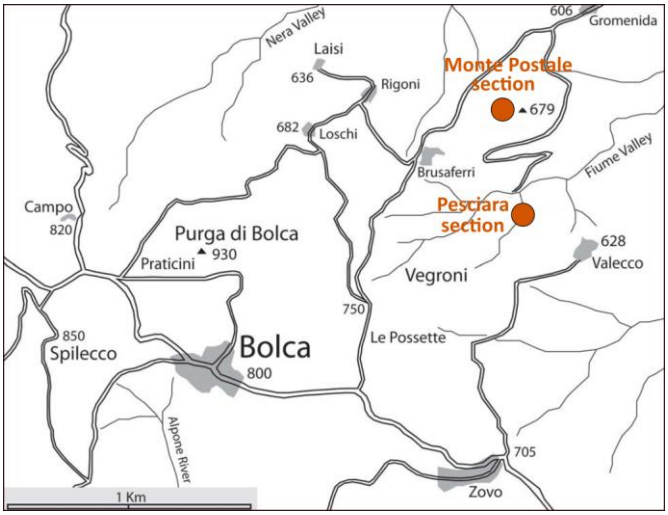

Fig. 24. Location map of the Monte Postale and Pesciara sections. Modified from Papazzoni et al. (2014).

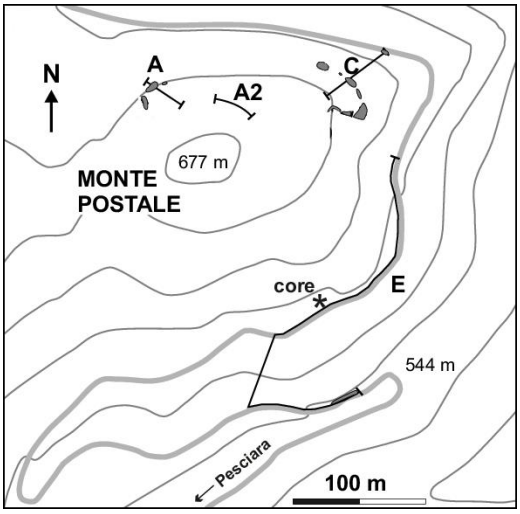

Fig. 25. The sections analyzed in Monte Postale for the description of *Alveolina postalensis*. Modified from Papazzoni et al. (2017b).

In Monte Postale, a coralgal-rim, fore-reef and lagoon deposits have been identified representing a rare example of a lower Eocene reefal depositional system (Vescogni et al., 2016), while the Pesciara is thought to be an olistolith coming from a shallow-water intraplatform basin strongly influenced both by emerged areas and pelagic environment (Schwark et al., 2009; Marramà et al., 2016). The Pesciara outcrop is surrounded by volcanoclastic tuffs hampering the reconstruction of its original position in the sedimentary succession.

The Monte Postale and Pesciara *Fossil-Lagerstätten* are famous for their exceptionally-preserved fauna and flora. The astounding fossils from here were collected and reported since the XVI century and were sent in museums and university collections all over Europe. Until the end of the XIX century, Bolca was mainly cited for its macrofossils but the basis for the geological knowledge of the area were also established (especially by Munier-Chalmas, 1891) and with the coming of the modern geology Bolca became object of several stratigraphers' and biostratigraphers' studies. Fabiani (1912, 1914, 1915) gave the first detailed geological description of the area and defined his "Spileccian" stage (after the Spilecco hill) as equivalent to the whole Paleocene and lower Eocene; Schweighauser (1953) was the first to study the larger foraminifera from Monte Postale, later analyzed by Hottinger (1960) The most recent synthesis of the geology of the area has been provided by Dal Degan and Barbieri (2005) but the lithostratigraphic units should be revised.

The limestones forming the Monte Postale and Pesciara, informally known with different names, have been considered as part of the Calcari di Spilecco Formation dated to the Paleocene-early Eocene by Bosellini et al. (1967). Successively Malaroda (1954) assigned the uppermost part of Monte Postale to the Lutetian on the basis of the mollusc fauna, whereas Hottinger (1960) attributed them to the Cuisian (=upper Ypresian) on the basis of the LF (alveolinid) assemblages. Papazzoni et al. (2017b) finally clarified the age of Monte Postale which, by means of LF and calcareous nannofossils integrated biostratigraphy, turned out to belong to the SB11, CNE 5-?6 (=NP13-?14a) Zones, that is middle Cuisian (upper Ypresian). The LF assemblages of the Pesciara limestone, already studied by Hottinger (1960) and Schaub (1981), have been also attributed to the SB11 Zone (Trevisani et al. 2005, Papazzoni and Trevisani 2006). The volcanoclastic tuffs presumably belong to the third volcanic phase recognized by Barbieri et al. (1991) in the Lessini area.

For the description of *Alveolina postalensis* Fornaciari, Giusberti & Papazzoni 2019, we mostly used the material analyzed by Papazzoni et al. (2017b) and Papazzoni et al. (2013) aimed at determining the biostratigraphy of the Monte Postale and of the Pesciara, respectively. Among this already analyzed material and some more, 74 specimens from different sections of Monte Postale (whose locations are reported in **Fig. 25**), eight from the Pesciara section, one from the Pesciara core and four from the tuffs were selected in thin sections from 40 different samples. For the section and for the core, the stratigraphical columns with the position of each sample are reported in **Fig. 26**.

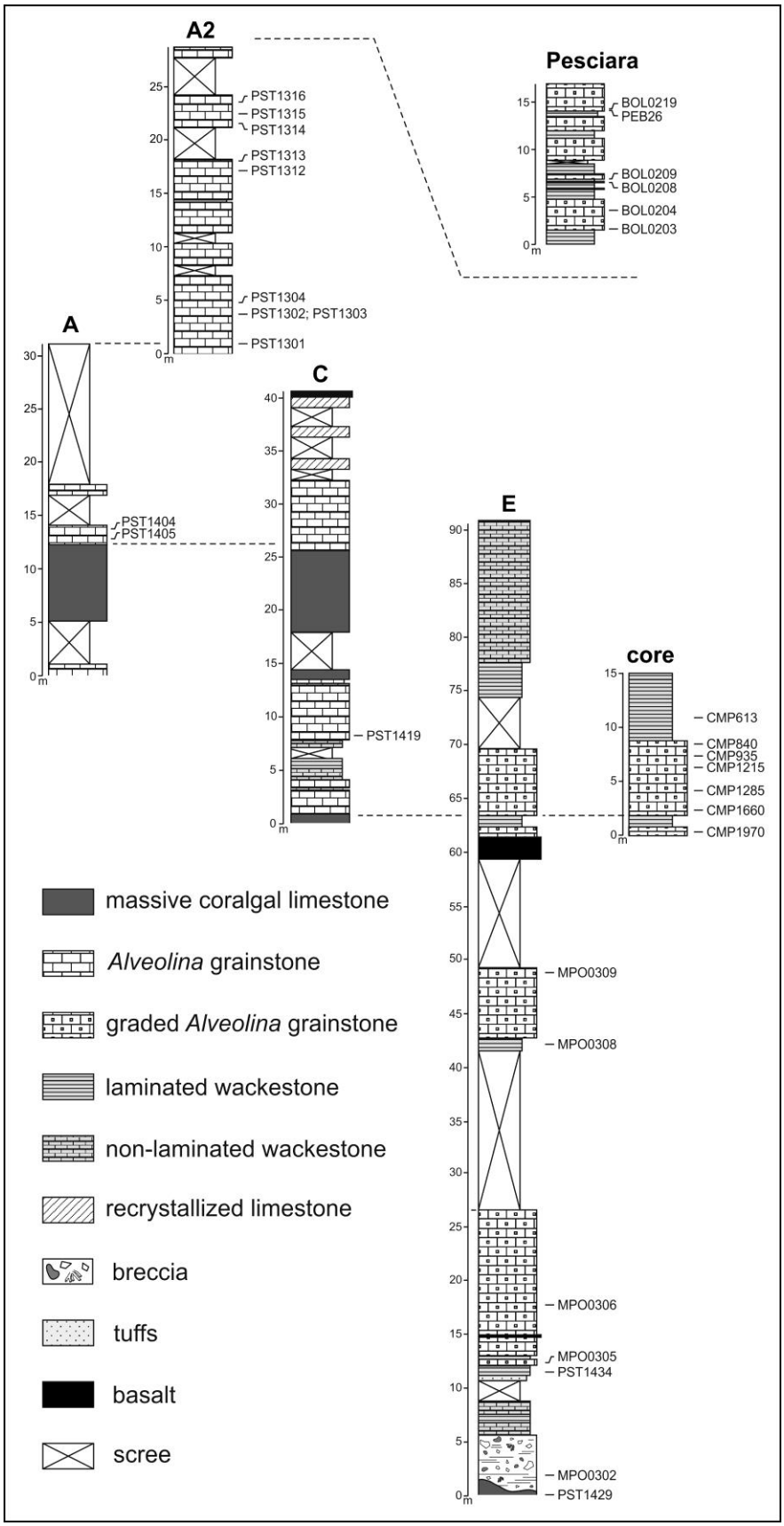

Fig. 26. Stratigraphic columns of Monte Postale sections (A, A2, C, E and core; after Papazzoni et al., 2017a, modified) and Pesciara (after Papazzoni & Trevisani, 2006, modified) sections, showing the position of the samples containing *A. postalensis* n. sp. From Fornaciari et al. (2019).

4.5. THE LARGER FORAMINIFERA ANALYSES

For the larger foraminifera associations of Tabiago, Monte Giglio and South Ardo sections, 158 samples in total were studied.

The thin sections (4.5 x 6.0 cm) of all this material were analysed at the optical microscope and digitally photographed. The preservation of the specimens is quite good in the Tabiago and the South Ardo sections, and moderate/bad in the Monte Giglio section, where several specimens are broken and/or partly recrystallized. The alveolines of the Monte Postale section are well preserved, even if some show signs of bioerosion. The diagnostic features of the best specimens were measured by means of the image analyses software JMicroVision 1.27©. For the description of *A. postalensis*, a morphometrical and biometrical approach was performed. It should be remarked that quantitative determinations on the LF are scarce because they require to select useful cuts of the specimens and they are time-consuming.

The taxa of the assemblages of the Tabiago, Ardo and Monte Giglio sections were determined following mainly Accordi et al. (1998), Sirel (1999, 2009, 2012, 2015), Hottinger (2009, 2014), and Di Carlo (2010). *A. postalensis* was compared to the similar species of the group *A. levantina* referring to Hottinger (1960), Scotto di Carlo (1966), Hottinger (1974), and Drobne (1977).

4.5.1. Taxonomical remarks

The taxonomy used in the present thesis for some Miscellaneidae and some Rotaliidae taxa deserves some explanatory notes.

Family Miscellaneidae Sigal *in* Pivetaeu 1952

In this thesis we refer to the classification of the Miscellaneidae used by Hottinger (2009). He established the subfamily Miscellaniteinae. By so doing, the Miscellaneidae are divided into two subfamilies, the Miscellaneinae Kacharava *in* Rauzer-Chernousova & Furzenko 1959, and the Miscellaniteinae Hottinger 2009. Hottinger (2009) grouped all the miscellaneids with a single interiomarginal intercameral foramen in the first subfamily, whereas all the miscellaneids with multiple intercameral foramina in the latter. Hottinger (2009) assigned several species formerly ascribed to the genus *Miscellanea* Pfender 1935 (emended by Smout 1954) to a new genus, *Miscellanites*, with type species *Miscellanea iranica* Rahaghi 1983. The genus *Miscellanites* is distinguished from the genus *Miscellanea* by the multiple intercameral foramina.

Species *Miscellanites globularis* (Rahaghi 1978)

The species *Miscellanites globularis* is used instead of *Miscellanea globularis* as Hottinger (2009) re-assigned *Miscellanea globularis* Rahaghi 1978 to the new genus *Miscellanites* Hottinger 2009 for the reasons mentioned above.

Species *Miscellanites minutus* (Rahaghi 1983)

Rahaghi 1983 established the species *Miscellanites minutus*. Hottinger (2009) re-assigned this species and some specimens identified as *Miscellanea* aff. *juliettae* and *Miscellanea* cf. *juliettae* by Pignatti at al. (2008) to the new genus *Miscellanites* Hottinger 2009 for the reasons mentioned above. Therefore the species *Miscellanites minutus* is here used instead of *Miscellanea minuta* Rahaghi 1983.

Furthermore, in Serra-Kiel et al. (1998), it is mentioned the species *Ornatononion minutus* (Rahaghi 1983) but the work by Hottinger and Tambareau cited in the references, which should have assigned *Miscellanea minuta* to the genus *Ornatononion*, has never been published. The genus *Ornatononion* was later established by Hottinger (2009) who, however, did not assigned *Miscellanea minuta* to the genus *Ornatononion* but to the genus *Miscellanites*. Consequently, the species *Ornatononion minutus* is here retained as invalid.

Species *Miscellanites primitivus* (Rahaghi 1983)

Hottinger (2009) assigned the species *Miscellanea primitiva* Rahaghi 1983 to the genus *Miscellanites* for the reasons mentioned above. Sirel (2009) established the genus *Akbarina* referring to the same type species, as *Akbarina primitiva* (Rahaghi, 1983). As Hottinger (2009) was published in September and Sirel (2009) in December the same year, the name *Miscellanites* maintains its priority over *Akbarina*. Therefore, the genus *Miscellanites* is here used instead of the junior synonym genus *Akbarina*.

In Serra-Kiel et al. (1998), it is mentioned the species *Pseudomiscellanea primitiva* (Rahaghi 1983) which, similarly to *Ornatononion minutus*, has never been described because the work by Hottinger and Tambareau cited in the references has never been published. Consequently, the species *Pseudomiscellanea primitiva* is invalid.

Family Rotaliidae Ehrenberg 1839

Genus *Elazigina* Sirel 2012

The genus *Elazigina* Sirel 2012 is here used instead of the junior synonym of the genus *Plumokathina* Hottinger 2014. Sirel (2012) established the genus *Elazigina*, with type species *Kathina subsphaerica* Sirel 1972. *Plumokathina* was used as *nomen nudum* in Peybernes et al. (2000) and it was formally erected only by Hottinger (2014). The type species is *Plumokathina dienii* Hottinger 2014. However, *Elazigina subsphaerica* (Sirel 1972) and *Plumokathina dienii* Hottinger 2014 share the same generic

characters. Therefore, considering that the genus *Elazigina* has been established before *Plumokathina*, the Principle of Priority (art. 23 ICZN) allows to consider *Plumokathina* Hottinger 2014 as a junior synonym of *Elazigina* Sirel 2012.

Species *Cuvillierina sireli* Inan 1988

Sirel 1998 assigned the species *Cuvillierina sireli* Inan 1988 to a new genus, *Pseudocuvillierina* on the basis of "the lack of septal and umbilical flap" characterizing *Cuvillierina*. Hottinger (2014) re-assigned the species to the genus *Cuvillierina* observing that "all foraminifera with a so-called double-septum [e.g. rotaliids], that is with a intraseptal interlocular space, have *per definitionem* a septal flap forming the posterior septal wall of the respective chamber." In this thesis, the genus *Pseudocuvillierina* is therefore considered invalid following Hottinger (2014).

4.5.2. The quote of the samples, of the first occurrences and of the SB boundaries

All the indicated occurrences correspond to the mean between the quote of the analysed sample and the quote of the sample below ("Approximated height of the occurrences" in Tabs. 1-3). Consequently, the first occurrences (FO) correspond to the quote between the uppermost sample in which the species doesn't occur and the lowermost sample in which the species occurs. In this way, we introduce an approximation to reduce the interval of uncertainty where no LF samples could be collected (e.g. due to the lack of shallow-water turbidites).

Similarly, the boundaries of the SB zones are defined in this thesis by taking the quote between the uppermost sample assigned to the lower SB zone and the lowermost sample assigned to the upper SB zone. The associated error has been also calculated.

Both for first occurrences and for the SB zones boundaries, the LF-barren samples were not considered for calculating the quote.

4.6. THE CALCAREOUS NANNOFOSSIL ANALYSES

The analyses of the calcareous nannofossils have been conducted by the co-tutor of the present thesis, Prof. Eliana Fornaciari, of the University of Padova (Italy).

The analyses of 48 samples from Tabiago, 40 from Ardo and 48 from M. Giglio were performed in order to obtain the calcareous nannofossil biostratigraphic framework of the investigated sections. The calcareous nannofossil samples were prepared from unprocessed material as smear slides and examined using a light microscope at ~1250X magnification. The stratigraphic distribution pattern of index taxa was assessed by mean of semiquantitive countings following the methods developed by Backman and Shackleton (1983), Rio et al. (1990), and Gardin and Monechi (1998). Specifically, (1) specimens of index taxa were counted in a prefixed area (1 mm^2); and (2) specimens of rare but biostratigraphically useful taxa (i.e., discoasterids and *Coccolithus pelagicus*) were counted in an area of about 6–7 mm^2, which is roughly equivalent to three vertical traverses. At Monte Giglio also the quantitative counting method (Thierstein et al., 1977; Rio et al., 1990) was applied calculating the abundance of selected taxa taking into account at least 300 specimens.

The taxonomy used is that of Aubry (1984, 1988, 1989, 1990, 1999), Perch-Nielsen (1985) and Romein (1979), apart from the *Ericsonia robusta* plexus for which we preferred to follow the taxonomic concept proposed by Garzarella and Raffi (2018). Calcareous nannofossil zonations are according to Martini (1971) and Agnini et al. (2014).

4.7. THE SHAW DIAGRAMS

In collaboration with Prof. Eliana Fornaciari, University of Padova (Italy)

The Shaw diagram is a graphic technique developed by Shaw (1964) and later used by Rio et al. (1990) and Luciani et al. (in press) to compare sequences of bio-horizons or other geological events observed in two or more stratigraphic sections. It allows to test ranking and spacing among the events, to observe changes in the sedimentation rates and in the stratigraphic completeness and expansion of the sections analyzed. Specifically, the "Shaw diagram" is a scatter graph in which the scale units are the depth or thickness of successions and in which the sequence of events in one section is paralleled to the same sequence of events documented in a section considered a standard reference.

In this thesis, we compare the Ardo and the Monte Giglio sections with the Tabiago section. Specifically, in the Ardo-Tabiago Shaw diagram the "master" section is the Ardo section. Only the first 25 m of the Ardo section previously investigated by Dallanave et al. (2012) for calcareous nannofossil biomagnetostratigraphy have been resampled and studied for both LF and calcareous nannofossil because they are rich in shallow-water turbidites. Therefore, the data from the base of the section to the base of *Fasciculithus tympaniformis* belong to the present work, while the calcareous nannofossil events above the latter are from Dallanave et al. (2012).

The Ardo section, located in the same geographic area of Tabiago, spans the same stratigraphic interval and records a good magnetostratigraphy (Dallanave et al., 2012). Instead, in the M. Giglio-Tabiago Shaw diagram the "master" section is M. Giglio.

The best fit for the resulting separated homologous points is a so-called "line of correlation". The events that intercept or coarsely fall in close proximity to the line of correlation can be considered as reasonably synchronous. Changes in the slope of the line suggest variations of sedimentation accumulation rates.

5. ANALYSES AND DISCUSSION OF THE PALEOCENE SECTIONS

5.1. THE TABIAGO SECTION

5.1.1. The LF biostratigraphy of the Tabiago section

The distribution of the recorded LF species in the Tabiago section is reported in **Table 1**.

	Height (cm)	Approximated height of the occurrences (cm	*Assilina* sp.	*Assilina azilensis*	*Cocaorata orali*	*Coskinon* sp.	*Cuvillierina sireli*	*Daviesina* sp.	*Daviesina intermedia*	*Daviesina praegarumnensis*	*Daviesina salsa*	*Discocyclina* sp.	*Elazigina* sp.	*Elazigina dienii*	*Elazigina lenticula*	*Globoflarina* sp.	*Glomalveolina* sp.	*Idalina* sp.	*Kayseriella decastroi*	*Kathina aquitanica*	*Keramosphaerinidae*	Miscellaniteinae undet.	*Miscellanites* sp.	*Miscellanea juliettae*	*Miscellanites* cf. *primitivus*	*Miscellanites primitivus*	*Orbitoclypeus* sp.	*Orbitoclypeus multiplicatus haymanaensis*	*Orbitoclypeus shopeni* cf. *ramaraoi*	*Orbitoclypeus shopeni ramaraoi*	*Orduella sphaerica*	*Ornatononion moorkensii*	*Paralockhartia eos*	*Paraspirolina* sp.	*Planorbulina cretae*	*Ranikothalia* sp.	*Rotalia* sp.	*Slovenites praecursorius*	*Slovenites pembaphis*	*Stomatorbina binkhorsti*	*Thalmannita* aff. *madrugaensis*	*Thalmannita madrugaensis*	Undetermined Nummulitidae	Undetermined orthophragmines	Agglutinated conical forms	Miliolidea	Orbitolinids (Cretaceous)	Planktonics (Cretaceous)
LECCO SEGMENT																																															
LEC35	4658	4538										X																														X				
LEC34	4575																																													
LEC33	4417	4348																																								X	X			
LEC32	4278	4241	X									X			X															X						?					X	X		X	
LEC31	4203	4167	X												X															X	X											X				
LEC30	4130	4072										X																														X				
LEC29	4013	3782	X	X				X			X	X			X													X		X						X						X	X			
LEC28	3659																																													
LEC27	3572																																													
LEC26	3550	3530																												X												X				
LEC25	3510	3413																										?	X													X	X			
LEC24	3315	3284				X						X	X		X										X											X						X	X	X		
LEC23	3253	3219			X					X					X								X		X											X				X		X	X			
LEC22	3185	3150											X		X		X																				X				X		X	X			
LEC21	3114	3091			X								X		X																												X				
LEC20	3067	3019											X		X																X					X										
LEC19	2970	2937			X		X					X			X		?																				X				X		X	X			
LEC18	2903	2822			X								X		X										X											X							X			
LEC17	2740	2728										X	X		X	X																											X	X			
LEC16	2716	2691				X	X						X		X	X					X														X	X			X			X			
LEC15	2666	2627			X	X				?					X				X																	X							X	X			
LEC14B	2587	2518				X						X																					X			X							X				
LEC14	2449	2496										X													X										X	X						X		X		
LEC13	2543	2481										X																														X				
LEC12	2519																																													
LEC11	2442																																													
LEC10	2419	2204										X														X											X						X				
LEC9B	2048																																													
LEC9	1989	1846			X							X	X																							X						X				
LEC8B	1814																																													
LEC8	1703	1556																																								X				
LEC7	1408	1278							X																																	X				
LEC6	1147	1131			X																																			X						
LEC5	1114	897			X																																			X						
LEC4	679	416			X					X			X	X								X											X	X					X		X		X		
LEC3	153	134			X																																					X				
LEC2	115	94																								X																				
LEC1	73	37			X																																			X						
MILANO SEGMENT																																														
MI20	1840	1777			X																			X												X				X						
MI19	1713	1622																						X												X				X		X	X			X
MI18	1530	1452			X		X																	X										X		X				X		X	X			X
MI17	1460																																													
MI16	1409																																													
MI15	1373	1362			X		X										?								X								X		X	X	X		X	X		X	X			X
MI14	1350	1320					X																												X				X		X	X			X
MI13	1289	1269			X		X																																X		X	X			X
MI12	1249	1101			X		X														X													X				X		X	X			
MI11	1046																																													
MI10	925																																													
MI9	953	890			X													X																						X			X	X			
MI8	827	722			X																																		X	X			X			
MI7	617	543																																						X	X			X			
MI6	546																																													
MI5	468	442																																						X				X	X			X
MI4	415	392			X																																		X				X				X
MI3	369	193			X																																		X				X	X			
MI2	41																																													
MI1	17	9			X																														X					X	X			X	

Table 1. Distribution of the LF taxa in the Tabiago section. The grey lines correspond to LF-barren intervals.

From the base of the Tabiago Milano section up to 7.22 m the assemblage is composed almost exclusively by *Cocoarota orali* (Pl. 1, fig. B), *Planorbulina cretae* and *Stomatorbina binkhorsti* (Pl. 10, fig. E), which are present throughout the section and, according to the literature, span the whole Paleocene. *Cocoarota orali* is reported from the Maastrichtian to the lower Lutetian (Inan 2003), *Planorbulina cretae* from the Campanian (Omaña et al. 2009) to the present (Meriç et al., 2008), *Stomatorbina binkhorsti* from the Maastrichtian to the Thanetian (Sirel 2012). Reworked Cretaceous planktonic foraminifera are frequent. The only benthic foraminifera with a certain degree of complexity is represented by *Thalmannita* aff. *madrugaensis* (Pl. 10, fig. F = FO), characterized by features similar to those of *Thalmannita madrugaensis* but with a smaller equatorial diameter (ranging from 0.31 to 0.60 mm, with a mean of 0.46 mm) than the latter one (from 0.54 to 1.00 mm in Hottinger, 2014; pl. 9.1).

At 8.90 m, *Kayseriella decastroi* (Pl. 4, fig. F = FO) occurs together with *Cocoarota orali* and *Stomatorbina binkhorsti*. *Kayseriella decastroi* has been erected and firstly described by Sirel (1999) and ascribed to the upper Danian. However, in the paper by Sirel (1999) the Selandian was not recognized and most probably included within the so-called "Danian". Inan and Inan (2008) reported *K. decastroi* from the Selandian, therefore from the SB2 according to Serra-Kiel et al. (1998). Sirel (2012, 2015), instead, recorded it from the upper SB1 to the lower SB2 but it is not clear on what he bases the attribution to the SB1, as no marker species of this biozone co-occurs with *K. decastroi* in the analysed sections. Therefore, *K. decastroi* can be considered as a reliable marker for the SB2, as already reported in Di Carlo et al. (2010). The samples below the first occurrence (FO) of *K. decastroi*, lacking of biostratigraphically significant species, are assumed to be in the SB1. The boundary SB1/SB2, consequently, is placed at 8.90 (± 0.63) m.

From 11.01 m upwards, the diversity increases as rotaliids and miscellaneids appear along with the previously recorded *Cocoarota orali*: *Cuvillierina sireli* (Pl. 1, figs. D-E = FO; Pl. 1, figs. F-H), *Paralockhartia eos* (Pl. 8, figs. E-G = FO; Pl. 8, fig. H) and undetermined Miscellaniteinae. Miscellaniteinae are recognized to appear in the SB2 (Serra-Kiel et al. 1998, Hottinger 2009, Sirel 2012), of which *P. eos* is a marker species (according to Serra-Kiel et al. 1998 and to Hottinger 2014). At 13.62 m, *Ornatononion moorkensii* (Pl. 7, figs. E-F = FO), *Paraspirolina* sp., *Rotalia* sp. and *Slovenites praecursorius* (Pl. 10, figs. A-B = FO) appear along with the already recorded *Cuvillierina sireli*. The assemblage is still consistent with the SB2, being *O. moorkensii* and *S. praecursorius* both SB2 marker species according to Hottinger (2009, 2014 respectively) and having *Paraspirolina* been recorded by Accordi et al. (1998) from the upper SB1 to the SB3. As regards the biostratigraphic distribution of the genus *Rotalia,* Hottinger (2014: p. 31, 32) mentions material belonging to a level assigned to the SB3, whereas in his fig. 1.3 its range starts in the Ilerdian. Therefore, the uncertainty about this range persists. It should be noticed that Accordi et al. (1998) recorded *Rotalia* cf. *hensoni* from the upper SB1, which is consistent with the presence of *Rotalia* sp. in SB2 in the Tabiago section. Therefore, the genus *Rotalia* probably arose earlier than indicated by Hottinger (2014).

At the top of the Milano segment, the Miscellaniteinae become more abundant and are here ascribed to *Miscellanites* cf. *primitivus* (Pl. 5, figs. F-H = FO; Pl. 6, fig. A). At 0.94 m of the Tabiago Lecco section, *Orduella sphaerica* (Thanetian according to Sirel 1999; SB2 and lower SB3 in Sirel 2009, 2012) appears. At 4.16 m, the SB2 can still be recognized due to the presence of *Elazigina dienii* (Pl. 2, figs. F-G = FO) and *Ornatononion moorkensii* (Pl. 7, fig. G), both identified by Hottinger (2014) as marker species of this biozone. At this quote, also *Daviesina praegarumnensis* (Pl. 2, fig. D = FO; Pl. 2, fig. E) (recorded by Hottinger 2014 in SB2 and SB3), *Miscellanites* sp. and *Thalmannita madrugaensis* (Plate 10, fig. H = FO) (with an equatorial diameter of 0.67 mm, consistent with the dimensions of this species according to Hottinger, 2014) are present.

At 12.78 m, a significant change in the assemblage occurs as the sample is very rich in orthophragminids (Pl. 8, fig. C = FO), testifying the SB3 Zone (see Serra-Kiel et al. 1998), whose base has to be placed at 12.78 (± 0.13) m. At 12.78 m, also *Daviesina intermedia* (Pl. 2, fig. C = FO) is found. Hottinger (2014: p. 136) wrote that this species is found in the SB3, but the distribution of the species indicated in fig. 1.3 is SB4 and SB5: this latter distribution is most probably a mistake. *Kathina aquitanica* (Pl. 4, fig. E = FO), marker species of the SB3 (Hottinger 2014), also concurs to determine the SB3 at 26.27 m. More taxa consistent with this biozone were found: *Ranikothalia* sp. (Pl. 9, fig. A = FO; Pl. 9, figs. B-C, D) (which is present since the SB3 in Serra-Kiel et al. 1998) from 18.46 m, *Orbitoclypeus* sp. (Pl. 6, fig. G = FO) (from SB3 in Serra-Kiel et al. 1998) at 24.96 m, *Miscellanites primitivus* (Pl. 6, fig. B = FO; Pl. 6, fig. C) (SB2 in Sirel 2012, SB3 in Hottinger 2009) from 24.96 m, *Coskinon* sp. (Pl. 1, fig. C) (SB2 and SB3 in Serra-Kiel et al. 1998) from 25.18 and *Elazigina lenticula* (Pl. 3, figs. D-H; Pl. 4, fig. A) (SB3 and SB4 in Hottinger 2014) from 26.27 m, *Cuvillierina sireli* and *Globoflarina* sp. (SB2, ?SB3 in Serra-Kiel et al. 1998, SB2 – lower SB3 in Accordi et al. 1998 and in Di Carlo et al. 2010, upper SB1 – lower SB2 in Sirel 2012) from 26.91 m, *Slovenites pembaphis* (Pl. 9, fig. G = FO) (SB3 – SB5 in Hottinger 2014) at 26.91 m, *Glomalveolina* sp. (Pl. 4, fig. C = FO) (from SB3 in Accordi et al. 1998, Serra-Kiel et al. 1998) at 31.50 m and *Miscellanea juliettae* (Pl. 4, fig. G = FO) (SB3 in Hottinger 2009) at 32.19 m. Furthermore, at 29.37 m, we find a specimen of *Thalmannita madrugaensis* (equatorial diameter = 0.64 mm).

The distribution of *Miscellanites* sp. and *Miscellanites* cf. *primitivus* in the Tabiago section is particularly interesting. According to Hottinger (2009) the only Miscellaniteinae in the SB2 is *Ornatononion moorkensii* and *M. primitivus* is ascribed to the SB3. The presence of *M. primitivus* in SB2, though, had been already indicated by Sirel (2012) who considered it (under the name of *Akbarina primitiva*) limited to this biozone. Consorti and Köroğlu (2019) as well observed *Miscellanites minutus* and *Miscellanites primitivus* only in the SB2, in Turkey. The analyses of the Tabiago section indicate that the presence of the Miscellaniteinae in SB2 is not limited to *O. moorkensii* and that *M*. cf. *primitivus* occurs both in SB2 and in SB3.

The presence of *Cuvillierina sireli* within the SB3 should be discussed due to its problematic distribution. Indeed, it has been reported by Serra-Kiel et al. (1998) from SB2, SB3, and tentatively

SB4, by Inan and Inan (2008) from the Selandian and the Thanetian, by Sirel (2009; 2012) from SB2 and by Hottinger (2014) from the Ilerdian in his fig. 1.3, whereas in his pls. 8.7 and 8.8 it is attributed to a generic Paleocene. The occurrence of *Cuvillierina sireli* in the Tabiago section is consistent with a SB2-SB3 range.

An interesting observation regards also *Thalmannita* aff. *madrugaensis* and *Thalmannita madrugaensis*. The specimens we indicated as *Thalmannita* aff. *madrugaensis* in the lower part of Milano segment have the same features as *T. madrugaensis* but a smaller equatorial diameter than its average one (according to Hottinger 2014), which is instead shown by the specimens of *Thalmannita madrugaensis* in the Lecco segment. The only species known from literature belonging to the genus *Thalmannita* is *T. madrugaensis*, which has been recorded in SB 1 by Sirel (2009, 2012), in SB2 and SB3 by Accordi et al. (1998) and by Serra-Kiel et al. (1998), in SB3 and SB4 by Hottinger (2014). The data from this section indicate the presence of two forms of *Thalmannita* along the Paleocene: *Thalmannita* aff. *madrugaensis*, having a smaller equatorial diameter (mean equatorial diameter=0.47 mm), in the SB1, and of *Thalmannita madrugaensis*, having a larger equatorial diameter (mean equatorial diameter=0.66 mm), in the SB2 and in the SB3.

At 37.82 m, the first occurrences of *Assilina* sp., *Assilina azilensis* (Pl. 1, fig. A = FO) and *Daviesina salsa* allow to recognize the SB4, whereas the samples at 36.59 m and at 35.72 m are devoid of LF, and those at 35.50 m and at 35.10 m can be ascribed neither to the SB3 nor to the SB4 because they contain only species distributed in both biozones, as *Orbitoclypeus* cf. *shopeni ramaraoi* (Pl. 7, fig. B-C = FO), *O. shopeni ramaraoi* (Pl. 7, fig. D), *O. multiplicatus haymanaensis* (Pl. 6, fig. H and Pl. 7, fig. A = FO), *Ranikothalia* sp. (Less et al. 2007; Serra-Kiel et al. 1998). Therefore, the base of the SB4 has been located at 35.33 (± 0.24) m.

The turbidites at the top of the section are mainly formed by siliciclastic debris and we can assume that the top of the section still in the SB4 Zone.

5.1.2. Integrated biozonation of the Tabiago section

The integrated biostratigraphy (**Fig. 27** for Milano segment, **Fig. 28** for the Lecco segment) shows that in the Tabiago section the boundary SB1/ SB2 at 8.90 (± 0.63) m of the Milano segment, defined on the base of the first occurrence of *Kayseriella decastroi*, is placed roughly in correspondence with the base common (Bc) of *Prinsius martinii* within the CNP4 (NP2-NP3) Zone, tying soundly to the calcareous nannofossil biostratigraphy the base of SB2 in the investigated section. It should be remarked that in the Tabiago section the first occurrence of *Elazigina dienii*, is not observed at the base of SB2 as expected, but in higher position above the base (B) of *Fasciculithus tympaniformis* (CNP7; Base NP5 Zones). In contrast, at Ardo the first occurrence of *E. dienii* is between the Top common (Tc) of *Prinsius dimorphosus* and the base (B) of *Prinsius martini* (upper CNP3 Zone).

The boundary SB2/SB3 at 12.78 (± 0.13) m in the Lecco segment, established on the base of the first occurrence of the orthophragminids, has been detected between the top (T) of *Fasciculithus pileatus* and the base (B) of *Heliolithus cantabriae* and it is therefore included in the upper CNP7 and in the upper NP5.

The boundary SB3/SB4 at 35.33 (± 0.24) m in the Lecco segment occurs close to the base (B) of *Discoaster multiradiatus* which marks the base of CNP11 and NP9 Zones respectively.

In the Lecco segment, the top (T) of *Fasciculithus pileatus* has been found at 10.62 m, shortly below the first occurrence of the orthophragmines. Although not used in the zonal schemes, the top of *F. pileatus* is largely reported in the literature. Specifically, both Berggren et al. (1995) and Agnini et al. (2007) associated this event to the middle part of Chron C26r. Gradstein et al. (2012) estimated the age of the top of *F. pileatus* at 60.73 Ma, in the middle of Chron C26r.

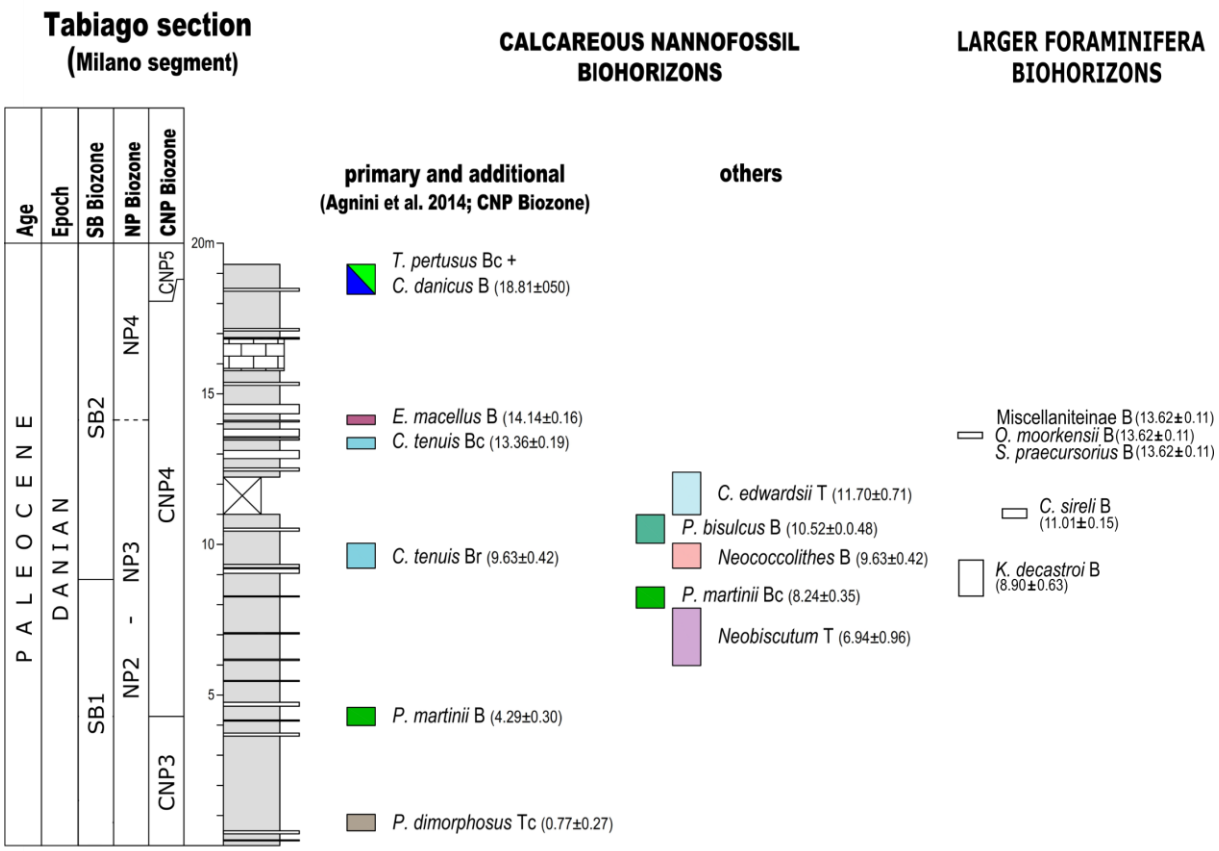

Fig. 27. Integrated LF and calcareous nannofossils on the Milano segment of the Tabiago section.

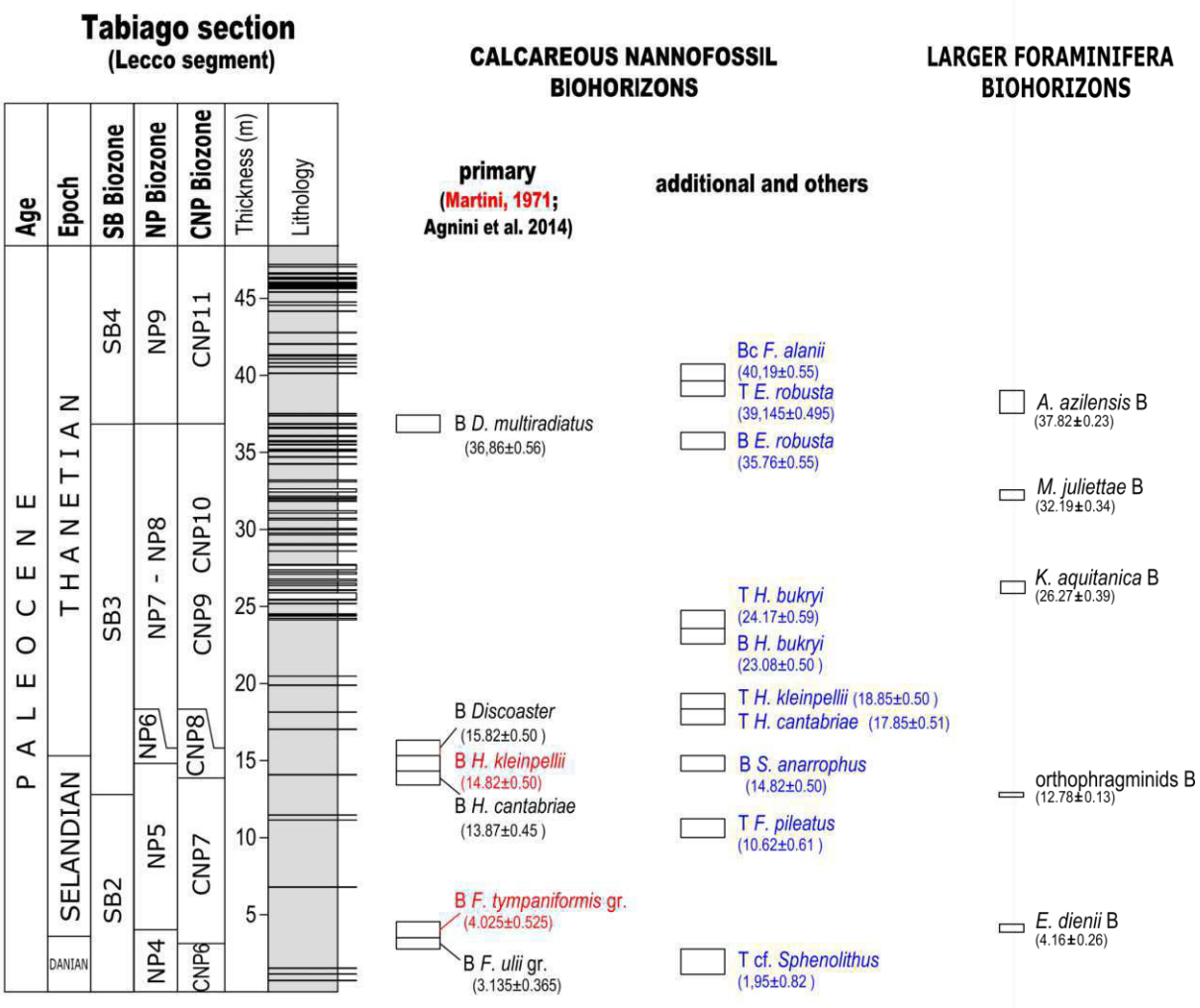

Fig. 28. Integrated LF and calcareous nannofossil biostratigraphy of the Lecco segment of the Tabiago section.

5.2. THE ARDO SECTION

5.2.1. The LF biostratigraphy of the Ardo section

The LF of the Ardo section are quite diversified and their distribution is reported in **Table 2**.

	Height (cm)	Approximated height of the occurrences (cm)	*Cocoarota orali*	*Cuvillierina sireli*	*Daviesina* sp.	*Daviesina praegarumnensis*	*Elazigina dienii*	*Globoflarina* sp.	*Haymanella paleocenica*	*Idalina sinjarica*	*Miscellanites* sp.	*Miscellanites globularis*	*Miscellanites minutus*	*Miscellanites primitivus*	*Orduella sphaerica*	*Ornatononion moorkensii*	*Planorbulina cretae*	*Rotorbinella* sp.	*Slovenites pembaphis*	*Slovenites praecursorius*	*Stomatorbina binkhorsti*	*Thalmannita* aff. *madrugaensis*	*Thalmannita madrugaensis*	Small unidentified miscellaneids	Small unidentified rotaliids	Agglutinated conical forms	Miliioloidea	Planktonics (Cretaceous)	Orbitoidids (Cretaceous)	*Sirtina* sp. (Cretaceous)
ARD 32, 32BIS	2355	1968	X				X			X								X		X						X	X			
ARD 31	1697																													
ARD 30	1647																													
ARD 29	1581	1555		X			X	X			X		X								X					X	X			
ARD 28	1529	1517					X				X									X							X			
ARD 27	1505	1398	X		X		X	X		X		X			X	X			X								X			
ARD 26	1314																													
ARD 25	1290	1205	X				X				X									X						X	X			
ARD 24	1193																													
ARD 23	1120	1106		X			X						X	X												X	X			
ARD 22	1091	1064		X									X												X	X	X			
ARD 21	1037	986																								X	X			
ARD 20B	935	925	X	X										X												X	X			
ARD 20A	915	884		X														X			X					X	X			
ARD 19B	853	844																								X	X			
ARD 19A	834	804	X	X			X		X				X				X									X	X			
ARD 18	773	757					X											X								X	X	X		
ARD 17	756																													
ARD 16	741	716		X																										
ARD 15	692	676					X						X																	
ARD 14	659	630				X	X													X			X					X		
ARD 13	601	595	X				X				X										X		X			X	X			
ARD 12	588	529					X																			X	X			
ARD 11	576																													
ARD 10	529																								X					
ARD 9	493																													
ARD 8	470	455																		X	X			X		X				
ARD 7	439	421																		X	X					X	X	X		
ARD 6	403	376	X																		X		X		X	X				
ARD 5	349	333	X																		X				X	X				
ARD 4	335																													
ARD 3B	317	312	X																									X		
ARD 3A	306	263	X														X			X	X			X	X		X	X	X	
ARD 2E	219	213	X																						X		X			
ARD 2D	207	204	X																	X				X	X	X	X		X	
ARD 2C	200	198	X																	X					X	X				
ARD 2B	196	194	X																	X					X	X	X			
ARD 2A	191	96	X														X			X	X			X	X	X	X		X	
ARD 1	74																													

Table 2. Distribution of the LF taxa in the Ardo section. The grey lines correspond to LF-barren intervals.

From the base of the section to 4.55 m, the association of benthic foraminifera is formed by *Cocoarota orali*, *Planorbulina cretae*, *Stomatorbina binkhorsti*, *Thalmannita* aff. *madrugaensis,* reworked Cretaceous specimens (mostly *Globotruncana* sp., but also *Sirtina* sp. and orbitoidids) and

unidentified forms. The latter are small specimens of benthic foraminifera, some of them trochospiral with an umbo, probably rotaliids, and some other planispiral with ornamentations, possibly miscellaneids, which cannot be ascribed to any known species. They could be either reworked Cretaceous species or Paleocene early rotaliids. In the latter case, they would indicate that the beginning of the rotaliids diversification started earlier than thought. Further investigations are required, especially in the Cretaceous turbidites outcropping near the studied Ardo section, to assess the age of these specimens (but this goes beyond the purposes of this thesis). Apart from these small forms, the association of the lower part of the Ardo section is very similar to the one of the Tabiago section and in this case as well no markers for the SB1 has been recorded.

Only from 5.29 m upwards it is possible to recognize a SB2 marker species, *Elazigina dienii* (Pl. 2, fig. H = FO; Pl. 3, figs. A-B), which becomes a stable component of the assemblages up to the top of the section. Below this level, there are three samples devoid of LF. The samples below this "barren" interval, lacking any marker species, are assumed to belong to the SB1. Therefore, the boundary SB1/SB2 is established at 5.29 (± 0.59) m. Unfortunately, *Kayseriella decastroi*, whose first occurrence was used for the base of the SB2 in the Tabiago section, is not present here.

Slightly above the base of the SB2, the Miscellaniteinae appear in the Ardo section with *Miscellanites* sp. at 5.95 m, together with *Daviesina praegarumnensis* (see subchapter 5.1.1) and *Slovenites praecursorius* (see subchapter 5.1.1) at 6.30 m, *Miscellanites minutus* (Pl. 5, figs. B-C = FO; Pl. 5, figs. D-E) (SB3 in Hottinger 2009) at 6.76 m, *Cuvillierina sireli* (Pl. 2, fig. A-B) (see subchapter 5.1.1) at 7.17 m, *Rotorbinella* sp. (Pl. 9, fig. E = FO; Pl. 9, fig. F) (Cretaceous–SB4 in Hottinger 2014) at 7.57 m, *Haymanella paleocenica* (Pl. 4, fig. D = FO) (Danian in Sirel 1999, SB1 in Sirel 2009, SB1 – low SB2 in Sirel 2012) from 8.04 m, *Miscellanites primitivus* (Pl. 6, fig. D = FO; Pl. 6, fig. E-F) (see subchapter 5.1.1) at 9.25 m; *Globoflarina* sp. (Pl. 4, fig. B = FO) (see subchapter 5.1.1), *Idalina sinjarica* (SB3 in Accordi et al. 1998, SB3 – SB6 in Serra-Kiel et al. 1998, SB2 – SB3 in Sirel 2015, SB3 – SB5 in Di Carlo et al. 2019), *Miscellanites globularis* (Pl. 5, fig. A = FO) (?SB2, SB3 in Hottinger 2009), *Orduella sphaerica* (Thanetian, in Sirel 1999, SB2 and low SB3 in Sirel 2009), *Ornatononion moorkensii* (Pl. 7, fig. H = FO) (see subchapter 5.1.1) and *Slovenites pembaphis* (Pl. 9, fig. H = FO) (SB3 – SB5 in Hottinger 2014) from 13.98 m. They are all present in the same interval associated with *Elazigina dienii* which, together with *Slovenites praecursorius* (Pl. 10, fig. C-D) and *Ornatononion moorkensii*, is considered a marker of the SB2 Zone (Hottinger 2009, 2014) (see subchapter 5.1.1).

Some of these species present in the SB2 Zone of the Ardo section deserve further considerations as they testify biostratigraphic ranges extend lower than what previously recorded: in particular, the first occurrences of *Miscellanites minutus*, *M. primitivus* and *Slovenites pembaphis* are recorded in SB2, in contrast to what reported in Hottinger (2009; 2014). As already seen in the Tabiago section (see subchapter 5.1.1), the appearance of the Miscellaniteinae in SB2 is not limited to

one genus or two (*O. moorkensii* and tentatively *Miscellanites globularis*) as indicated by Hottinger (2009).

Furthermore, *Idalina sinjarica* is recorded in the SB2 Zone. This species was placed by Serra-Kiel et al. (1998) from SB3 to SB6, by Accordi et al. (1998) in SB3, by Di Carlo et al. (2019) from SB3 to SB5, by Inan and Inan (2008) in the Selandian, and by Sirel (2012) from SB2 to SB3. Both in the Ardo and in the Tabiago sections it occurs only in the SB2.

Finally, it is reported the presence of *Thalmannita* aff. *madrugaensis* (Pl. 10, fig. G) with an equatorial diameter ranging from 0.28 to 0.59 mm and a mean value of 0.4 mm) in the SB1 and of *Thalmannita madrugaensis* (with an equatorial diameter ranging from 0.5 to 0.66 mm and a mean value of 0.57 mm) in the SB2. The distinction between *Thalmannita* aff. *madrugaensis* and *Thalmannita madrugaensis* according to their equatorial diameters is therefore possible both in the Ardo and in the Tabiago section (see subchapter 5.1.1).

5.2.2. Integrated biozonation of the Ardo section

The integrated biostratigraphy (**Fig. 29**) shows that in the Ardo section the SB1/SB2 boundary at 5.29 (± 0.59) m, recognized according to the first occurrence of *Elazigina dienii*, occurs in the interval between the top common (Tc) of *P. dimorphosus* and the base (B) of *Prinsius martini***,** in the uppermost CNP3 (upper NP3).

This result, together with the one from the Tabiago section, allows to redefine the position of the boundary SB1/SB2, lowering the boundary to the uppermost part of the biozone CNP3. Furthermore, we can correlate our data with the magnetostratigraphic data obtained by Dallanave et al. (2012) along the same section, showing that the SB1/SB2 boundary falls in the middle part of the Chron C28n.

In the Ardo section the first occurrence of *Cuvillierina sirelii* has been detected between the base common (Bc) of *Prinsius martinii* and the base (B) of *Prinsius bisulcus.* The same relative position of the first occurrence of *C. sirelii* has been observed in the Tabiago section (Milano segment). This suggests that this event has a good potential to become a bio-horizon useful for LF biostratigraphy. Specifically, it could be used as an additional marker of the base of the SB2 Zone.

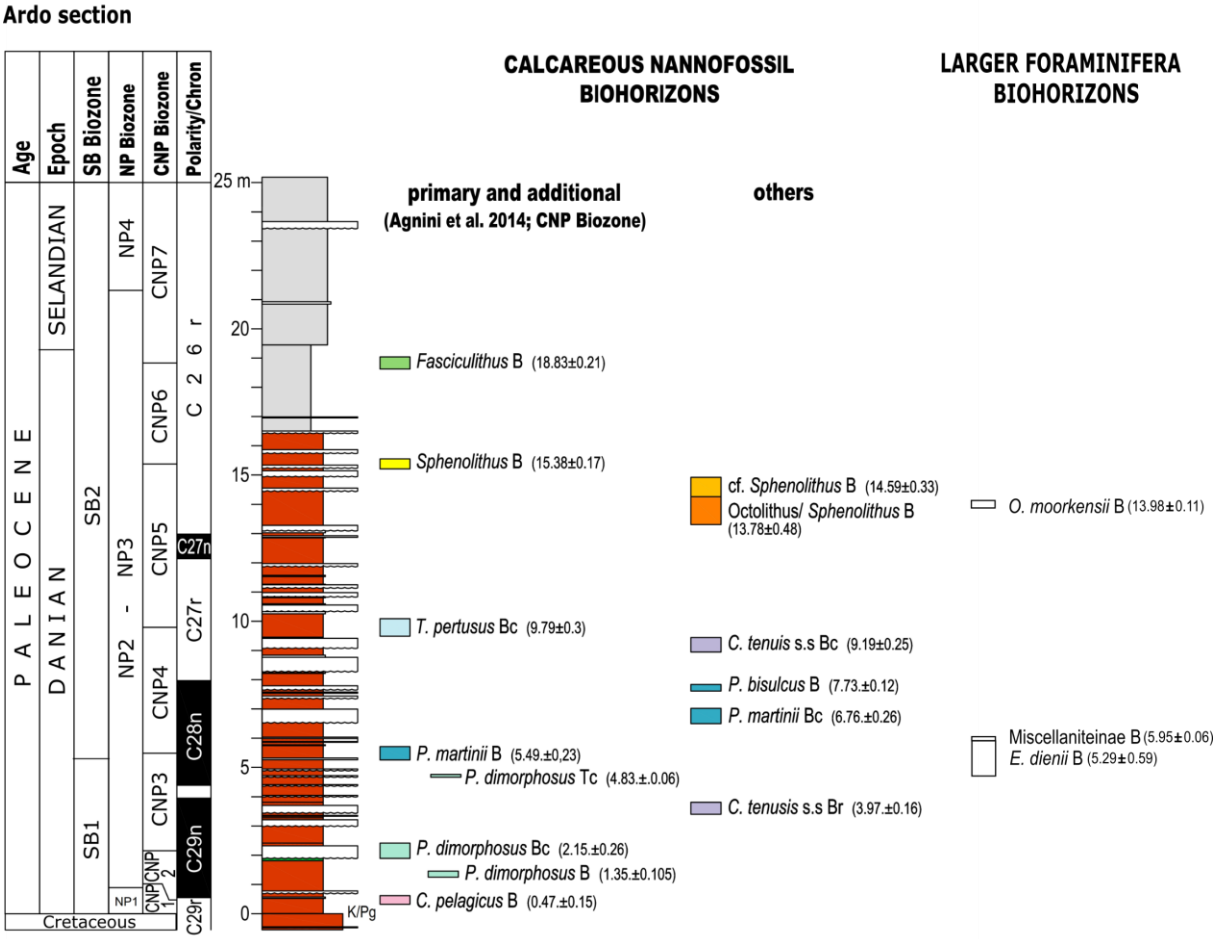

Fig. 29. Integrated LF and calcareous nannofossils biostratigraphy of the Ardo section.

5.3. THE MONTE GIGLIO SECTION

5.3.1. The LF biostratigraphy of the Monte Giglio section

The LF assemblages of the Monte Giglio section are contained in turbidites with a high percentage of clastic components (both carbonatic and siliciclastic) and are frequently broken or abraded. Nevertheless, there are enough preserved specimens allowing to obtain interesting biostratigraphic information. The distribution of the recorded LF species in the Monte Giglio section is reported in **Table 3**.

The base of the section contains only planktonic foraminifera, mainly of the Paleocene and some reworked from the Cretaceous. However, the lower portion of the section can be ascribed to the SB2 due to the presence of *Elazigina dienii* (Pl. 3, fig. C) from 0.53 m and of *Paralockhartia eos* from 0.98 m, both being marker species of the SB2 according to Hottinger (2014). Starting from 1.93 m, *Ornatononion moorkensii* (Pl. 8, fig. A-B = FO) (see subchapter 5.1.1) and *Slovenites praecursorius* (see subchapter 5.1.1), confirming the attribution to the SB2, are also recorded, along with *Cuvillierina sireli* (see subchapter 5.1.1) and *Thalmannita* sp. (whose specimens are too incomplete to be determined at the specific level). At 4.66 m, *Idalina sinjarica* (see subchapter 5.2.1) becomes part of the SB2 assemblage. From 5.50 m, the Miscellaneidae start to appear and from this sample upwards the association becomes very diversified, being composed by the already recorded *Elazigina dienii*, *Paralockhartia eos, Ornatononion moorkensii, Slovenites praecursorius* and *Cuvillierina sireli* to which are added *E. lenticula* (SB3 – SB6 in Hottinger 2014) and *Miscellanea juliettae* (see subchapter 5.1.1) from 6.50 m, *M. yvettae* (Pl. 4, fig. H = FO) (SB3 in Hottinger 2009) from 11.10 m, *Kathina selveri* (SB3 – SB4 in Hottinger 2014) and *Anatoliella ozalpiensis* (SB 2 in Serra-Kiel et al. 2016) from 12.16 m, *Rotorbinella detrecta* (SB1 – lower SB3? In Hottinger 2014) from 13.44 m, *Rotalia* sp. (see subchapter 5.1.1) from 19.13 m, *Kathina* sp. (from the SB3 in Hottinger 2014) at 21.27 m.

These co-occurrences need to be discussed on the base of where we decided to locate the SB2/SB3 boundary. We propose herein that it is more reliable to recognize the SB3 on the base of the occurrence of the orthophragminids instead that on the base of the rotaliids, whose biostratigraphic distributions are not firmly established. The appearance of the orthophragminids, indeed, is with no doubt in the SB3 Zone (Serra-Kiel et al. 1998). In the Monte Giglio section, they are present from 29.64 m (Pl. 8, fig. D = FO). Therefore, the boundary SB2/SB3 is placed at 29.20 m. Consequently, the association recorded underneath this boundary, is assigned to the SB2. Another confirmation of this assignment is the co-occurrence of some of these species with *E. dienii* and *O. moorkensii* for which the reworking hypothesis can be discarded. Some species recorded in the Monte Giglio section deserve attention, as *Elazigina lenticula*, *Kathina* sp., *Kathina selveri*, *Miscellanea juliettae* and *M. yvettae* turn out to be present already in the SB2 Zone. The *Paralockartia eos* at 10.00 m is contained in a lithoclast, therefore not part of the contemporary assemblage.

The occurrences of *Cuvillierina sireli* and *Rotalia* sp. (see subchapter 5.1.1) in the SB2 in the Monte Giglio section are consistent with what already observed both in the Tabiago Milano and in the Ardo sections.

	Height (cm)	Approximated height of the occurrences (cm	*Anatoliella* cf. *ozalpiensis*	cf. *Cincoriola ovoidea*	*Cocaorata orali*	*Cuvillierina sireli*	*Daviesina praegarumnensis*	*Elazigina* sp.	*Elazigina dienii*	*Elazigina lenticula*	*Idalina sinjarica*	*Kathina* sp.	*Kathina selveri*	Keramosphaerinidae	*Medocia* sp.	*Miscellanea* cf. *juliettae*	*Miscellanea juliettae*	*Miscellanea yvettae*	Miscellaneidae undet.	*Orduella sphaerica*	Orthophragmines	*Ornatononion moorkensii*	*Paralockhartia eos*	*Planorbulina cretae*	cf. *Redmondina henningtoni*	*Rotalia* sp.	*Rotorbinella detrecta*	*Slovenites pembaphis*	*Slovenites praecursorius*	*Stomatorbina binkhorsti*	*Thalmannita* sp.	Agglutinated conical forms	Miliolòidea	Planktonics (Cretaceous)	Orbitoids (Cretaceous)	Rudists (Cretaceous)
CMG4080	4070	3940																			X			X								X				
CMG3820	3810	3780			X																X															
CMG3760	3750	3553																			X															
CMG3366	3356	3234			X		?			X																										
CMG3116	3111	3071					X			X											X											X				
CMG3036	3031	2998								X											X											X				
CMG2969	2964	2920					?			X								X			X			X												
CMG2882	2877	2771			X																					X					X	X			
CMG2670	2665	2616			X			X		X															X											
CMG2571	2566	2501			X					?							X							X												
CMG2440	2435	2395								?																				X		X				
CMG2360	2355	2325						X	X	X		?							X					X		X					X	X			
CMG2300	2295	2226								X							X		X												X	X			
CMG2162	2157	2127			X					X		X							X						X							X				
CMG2102	2096	2008		X						X			?				X		X																	
CMG2101	2095													X						X																
CMG1925	1920	1913						X	X	X									X					X		X					X	X			
CMG1912	1906	1891			X					X							X							X										X	
CMG1880	1875	1810			X					X														X												
CMG1785	1780																																			
CMG1750	1745	1706								X									X													X				
CMG1671	1666	1643			X	X				X														X								X				
CMG1625	1620	1598			X					X					X	X		X	X					X						X						
CMG1580	1575	1538				X				X								X	X											X		X	X			
CMG1506	1501	1441								X							X																			
CMG1370	1380	1371			X			X		X				X																		X	X			
CMG1352	1362	1361			X					X																						X				
CMG1349	1359	1358			X	X				X																										
CMG1347	1357	1344			X			X		X										X						X				X	X				
CMG1320	1331	1326			X			X		X														X				X			X	X			
CMG1310	1320	1308			X		X												X												X	X	X		
CMG1285	1295	1280						X		X														X												
CMG1255	1265	1252							X															X								X				
CMG1229	1238	1216	X		X			X	X	X			X											X								X				
CMG1184	1194	1171			X			X	X	X									X					X							X	X			
CMG1138	1148	1110						X										X							X						X				
CMG1062	1072	1036				X		X		X																							X			
CMG990	1000	957																					X								X				
CMG986	996																																			
CMG904	914	867						X	X	X							X					X		X									X			
CMG810	820	782			X			X		X																						X				
CMG743	743	744			X	X		X	X	X							X					X		X					X	X		X				
CMG734	744	650				X			X													X											X			
CMG600	610																															X				
CMG545	555	550						X	X										X					X								X			X	
CMG535	545	466			X				X		X																			X		X	X			
CMG497	496																																			
CMG387	387	299			X				X															X					X			X				X
CMG312	312																															X				
CMG210	210	205			X				X																					X		X	X			
CMG200	200	193			X	X			X												X							X	X	X	X		X			
CMG185	185	166			X			X	X															X						X						X
CMG146	146	126			X				X														X								X	X				
CMG134	134																																			
CMG105	105	98			X				X														X								X	X				
CMG90	90	53							X																							X	X			
CMG15	15	8																																X			

Table 3. Distribution of the LF taxa in the Monte Giglio section.

Furthermore, as observed in these sections (see subchapters 5.1.1 and 5.1.2), *Idalina sinjarica* is present only in the SB2 in the Monte Giglio section as well. However, its lack from the SB3 could be due to the provenance of the bioclasts in the turbidites, which hardly involve the inner platform environments suitable for the porcelaneous foraminifera.

As regards *Thalmannita* sp., it is here recorded in the SB2, confirming the distribution of this genus in this biozone as already observed in the Tabiago and in the Ardo sections (see subchapters 5.1.1 and 5.1.2). Eventually, *Cocoarota orali* and *Stomatorbina binkhorsti* are spread throughout the section, while reworked Cretaceous planktonic foraminifera, orbitoidids and rudists fragments are found especially in the lower part of the section.

5.3.2. Integrated biozonation of the Monte Giglio section

The integrated biostratigraphy (**Fig. 30**) shows that in the Monte Giglio section the boundary SB2/SB3 occurs at 29.20 (± 0.43) m, defined according to the first occurrence of the orthophragmines, is above the top (T) of *Fasciculithus pileatus* which occurs at 26.17 m. The B of orthophragmines which marks the base of the SB3 is therefore included in the CNP7 and in the NP5 as in the Tabiago section.

This suggests that these two bio-horizons are suitable marker for the base of the SB3 Zone and they could provide one of the best references in the development of an integrated biostratigraphic framework.

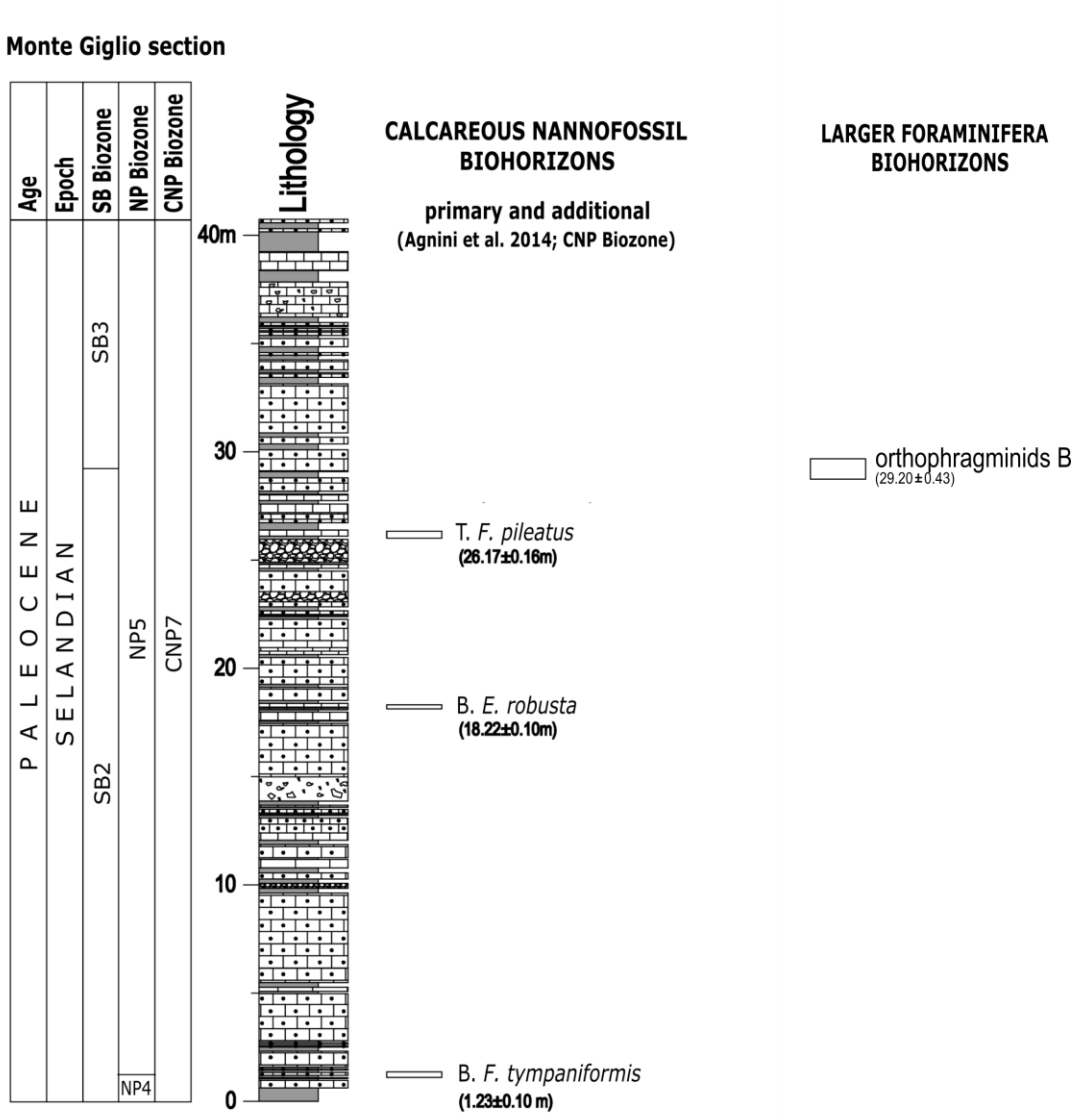

Fig. 30. Integrated LF and calcareous nannofossils biostratigraphy of the Monte Giglio section.

5.4. GENERAL DISCUSSION ON THE THREE PALEOCENE SECTIONS

5.4.1. SB marker taxa and bio-horizons

In the analysed sections, the biozones are recognized according to the following bio-horizons:

- **SB1:** primary bio-horizon: last occurrence of the Cretaceous LF (orbitoidids); additional bio-horizon: *Thalmannita* aff. *madrugaensis* FO;
- **SB2:** primary bio-horizon: *Kayseriella decastroi* FO; additional bio-horizons: *Elazigina dienii* FO, *Ornatononion moorkensii* FO*, Paralockhartia eos* FO, *Slovenites praecursorius* FO; subfamily Miscellaniteinae FO;
- **SB3:** primary bio-horizon: orthophragmines FO; additional bio-horizons: *Ranikothalia* sp. FO, *Kathina aquitanica* FO;
- **SB4:** primary bio-horizons: *Assilina* sp. FO, *Assilina azilensis* FO and *Daviesina salsa* FO;

The comparison among the sections highlights that there is usually no homotaxia of markers. More specifically, in the Tabiago section the base of the SB2 Zone is marked by *Kayseriella decastroi* FO, whereas in the Ardo section it is established according to *Elazigina dienii* FO as *K. decastroi* does not occur at all in the latter section. Furthermore, in Tabiago *E. dienii* is rarer and occurs higher than in the Ardo section. It's difficult to establish if this is due to an actual difference in the timing of appearance or if it is an apparent difference, as turbidites may have involved different part of the platform corresponding to different life-environments for LF.

The biozones defined by Serra-Kiel et al. (1998) (see subchapter 2.2.3) are here updated according to the distribution in the sections under study.

In the Tabiago and in the Ardo sections, *Laffitteina bibensis* and *Bangiana hanseni*, considered as SB1 marker species by Serra-Kiel et al. (1998), were not found. However, *Thalmannita* aff. *madrugaensis* might be considered as a marker species. Indeed, the observations from the Tabiago and Ardo sections demonstrate that two morphotypes can be identified: *Thalmannita* aff. *madrugaensis* in the SB1 and *Thalmannita madrugaensis* in the SB2 and in the SB3, distinguished on the basis of their equatorial diameter, below 0.50 mm for the first and above 0.50 mm for the latter. Accordingly, this suggests a phyletic line with *Thalmannita* aff. *madrugaensis* as the possible ancestor of *Thalmannita madrugaensis.* The increased size passing from SB1 to SB3 fits well with the Cope's rule (Guex 2003, Benedetti and Pignatti 2009), as repeatedly verified in other LF lineages.

According to Serra-Kiel et al. (1998) the SB2 Zone was defined by means of the ranges of *Miscellanea globularis* (=*Miscellanites globularis* in Hottinger 2009), *Ornatononion minutus* (=*Miscellanites minutus* in Hottinger 2009), *Paralockhartia eos* and *Lockhartia abkari*. The occurrence of the Miscellaneidae in SB2, recorded in the analysed sections, is consistent with the

definition by Serra-Kiel and also the distribution of *P. eos* in the sections under study is fitting the original definition of this biozone.

Serra-Kiel et al. (1998) defined the SB3 on the basis of the ranges of *Glomalveolina primaeva*, *Periloculina slovenica*, *Coskinon rajkae*, *Fallotella alavensis*, *Cribrobulimina carniolica*, *Vania anatolica*, *Miscellanea yvettae* (=*Miscellanites yvettae* in Hottinger 2009), *Pseudomiscellanea primitiva* (=*Miscellanites primitivus* in Hottinger 2009), *Ranikothalia bermudezi*, *Nummulites heberti* and *Discocyclina seunesi*. Unfortunately, in the sections under study most of these species are completely lacking, and given that the biostratigraphic ranges of several rotaliids and miscellaneids species are not well defined, the most reliable and recognizable event is the first occurrence of orthophragminids (exemplified by *Discocyclina seunesi* by Serra-Kiel et al. 1998). This event, indeed, can be easily recognized because it corresponds to the appearance of a large foraminiferal group (=families Discocyclinidae + Orbitoclypeidae), not of a genus or a species, characterized by a clearly different morphology in comparison with the previous forms. As they appear, they are quite frequent, as well.

For some of the species recorded the stratigraphic range does not fit with what reported in literature. In particular, data from the sections under study shows that *M. yvettae* is not limited to SB3 because it extends to the SB2 Zone as well. Therefore, this species cannot be used as marker for the SB3 Zone.

Finally, the SB4 Zone was defined by Serra-Kiel et al. (1998) on the basis of the biostratigraphic ranges of *Glomalveolina levis*, *Hottingerina lukasi*, *Miscellanea meandrina*, *Daviesina garumnensis*, *Dictyokathina simplex*, *Nummulites catari*, *Assilina azilensis* and *Assilina yvettae*. Among the analysed sections, only the Tabiago Lecco section contains the SB4 Zone. Unfortunately, the assemblage is quite poor and does not contain most of the marker species.

5.4.2. Distribution in the SB zones of the LF taxa from Tabiago, Ardo and Monte Giglio

In the analysed section, the following species are recorded in the following biozones (identified as in the subchapter 5.4.1) :

- **SB1:** *Cocoarota orali*, *Planorbulina cretae*, *Stomatorbina binkhorsti*, *Thalmannita* aff. *madrugaensis*;
- **SB2:** *Anatoliella* cf. *ozalpiensis*, *Cocoarota orali, Cuvillierina sireli*, *Daviesina* sp., *Daviesina praegarumnensis*, *Elazigina dienii*, *E. lenticula*, *Globoflarina* sp., *Haymanella paleocenica, Idalina* sp.*, Idalina sinjarica*, *Kayseriella decastroi, Kathina* sp., *K. selveri*, *Lockhartia* sp., *Medocia* sp., *Miscellanea juliettae*, *M. yvettae*, *Miscellanites* sp., *M. globularis*, *M. minutus*, *M. primitivus*, *Orduella sphaerica*, *Ornatononion moorkensii*, *Paralockhartia eos*, *Paraspirolina* sp., *Planorbulina cretae*, *Rotalia* sp., *Rotorbinella* sp., *R. detrecta*, *Slovenites pembaphis*, *S. praecursorius*, *Stomatorbina binkhorsti*, *Thalmannita madrugaensis*;

- **SB3:** *Cocoarota orali*, *Coskinon* sp., *Cuvillierina sireli*, *Daviesina intermedia*, *D. praegarumennsis*, *Elazigina lenticula*, *Glomalveolina* sp., *Globoflarina* sp., *Kathina aquitanica*, *K. selveri*, *Miscellanea yvettae*, *Miscellanea juliettae*, *Miscellanites primitivus*, *Orduella sphaerica*, orthophragmines, *Planorbulina cretae*, *Ranikothalia* sp., *Slovenites pembaphis*, *Stomatorbina binkhorsti*, *Thalmannita madrugaensis*.
- **SB4:** *Assilina* sp., *Assilina azilensis*, *Cocoarota orali*, *Daviesina* sp., *Daviesina salsa*, *Elazigina lenticula*, orthophragmines, *Ranikothalia* sp.

Therefore, it is possible to update the distributions reported since now in the literature (**Figs. 31**, **32**).

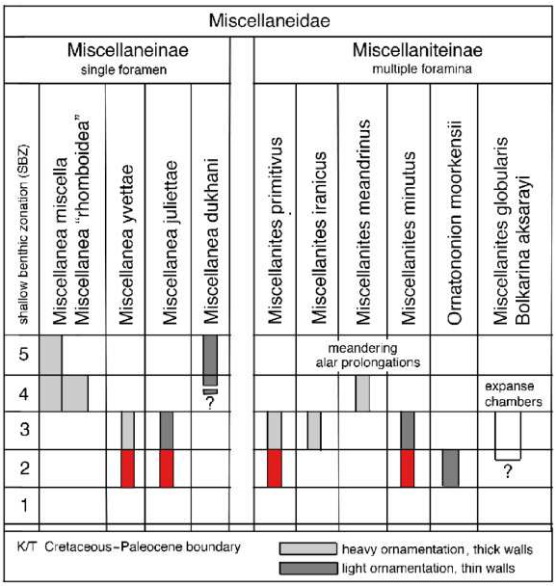

Fig. 31. Stratigraphic distribution of the taxa belonging to the Miscellaneidae from Hottinger (2009), modified according to the data (in red) from the present thesis.

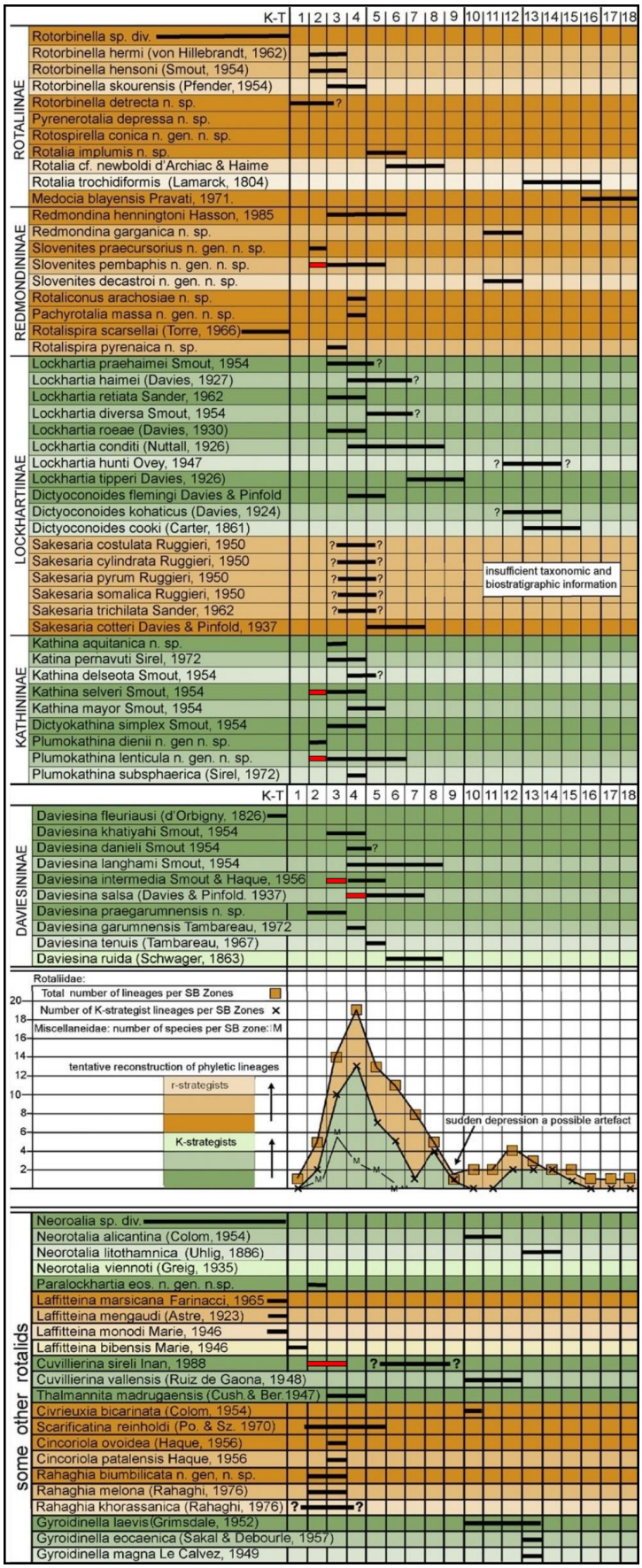

Fig. 32. Stratigraphic distribution of the taxa belonging to the Rotaliidae from Hottinger (2014), modified according to the data (in red) from the present thesis.

5.4.3. The calibration of the Paleocene SB boundaries

The larger foraminifera and the calcareous nannofossils data from the three sections are in good mutual agreement, and allow assessing the position of the SB1/SB2 and SB2/SB3 boundaries, marked as uncertain in the correlation scheme by Serra-Kiel et al. (1998).

Serra-Kiel et al. (1998), draw the base of SB2 in the lower part of the Chron C26r within the NP4 Zone. Instead, the data from Tabiago and Ardo sections stress that the SB1/SB2 boundary is included in the uppermost CNP3 (upper NP3 of Martini 1971) Zone (Agnini et al. 2014) and associated to the middle part of the Chron C28n (**Fig. 33**). Previously, Baceta et al. (2004), studying few sections in SW Pyrenees, placed the SB1/SB2 boundary in an interval which encompass the upper NP2 and the lower NP3 and the Chrons C29n and C28r. Unfortunately, the authors did not substantiate this outcome. Hence this work first supplies evidences supported by data that SB1/SB2 boundary is older than reported in the literature. Specifically, according to Cande and Kent (1995) and Ogg and Smith (2004) the base of SB2 is about 2 Ma older than suggested by Serra-Kiel et al. (1998).

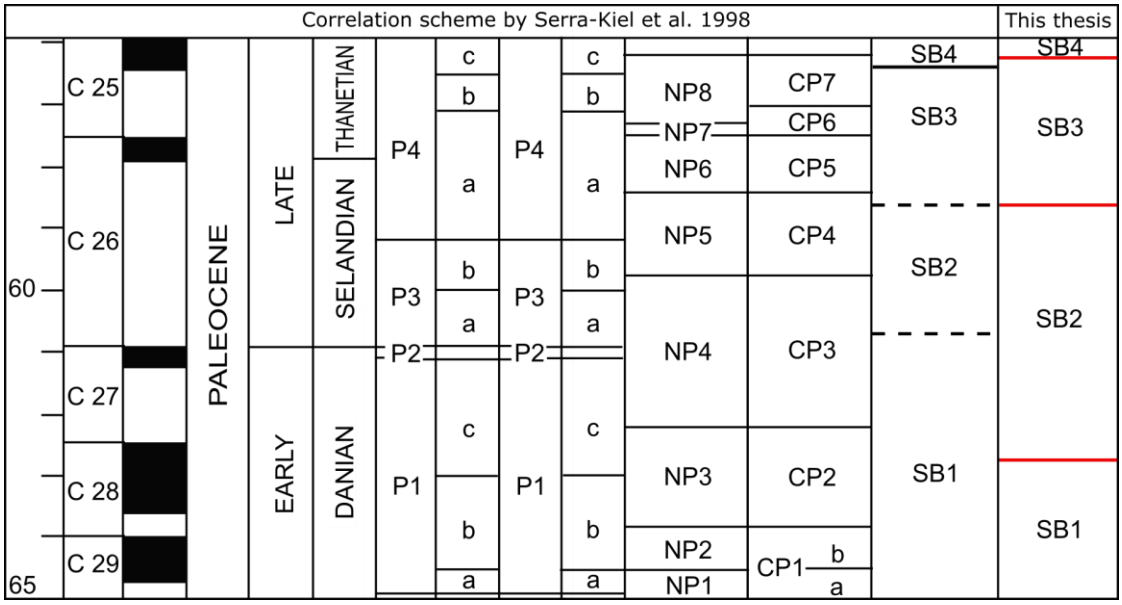

Fig. 33. Comparison between the position of the boundaries obtained by the presente thesis with the correlation scheme by Serra-Kiel et al. (1998).

This implies that the beginning of the generic diversification of the LF, occurring at the base of the SB2 (Serra-Kiel et al., 1998; Hottinger 2001), started about 2 Ma earlier than previously supposed.

Again, it should be highlighted that the *Cuvillierina sireli* FO, observed both in Tabiago and Ardo section between the base common (Bc) of *Prinsius martinii* and the base (B) of *Prinsius bisulcus*, seems to be a reliable event for biostratigraphic correlations within the SB2 Zone. Therefore, *Cuvillierina sireli* FO could be potentially useful as additional bio-horizon approximating the base of the SB2 Zone when the primary markers (*K. decastroi, E. dienii*) are absent.

The position of the base of the SB3 Zone can be inferred by the biostratigraphic data obtained from the sections of Tabiago and Monte Giglio. In both the sections, the SB2/SB3 boundary is included in the upper CNP7 (Agnini et al. 2014) and in the upper NP5 (Martini 1971) which well correlates with Serra-Kiel et al. (1998) scheme, where the SB2/SB3 boundary is also correlated to the upper NP5. Therefore, the base of the SB3 established by the orthophragminids FO, in turn close to the top (T) of *Fasciculithus pileatus* within the upper CNP7 (NP5 *pars*) is consistent with the original correlation scheme by Serra-Kiel et al. (1998). According to the data from the Tabiago section, both the bio-horizons fall below the Early Late Paleocene Event (ELPE), marked by the first appearance of *Heliolithus kleinpelli* at the base of the NP6, and therefore the radiation of the some of the most important genera of LF (*Discocyclina*, *Glomalveolina*, *Orbitoclypeus*, *Ranikothalia*) cannot be correlated to this event.

In the present work, the SB3/SB 4 cannot be accurately established because the only data available are from the Tabiago section, where an interval of 6.98 m contains assemblages without clear markers allowing the distinction of these two biozones. For sake of simplicity, the base of the SB4 Zone has been placed in the middle of this interval that is roughly correlated with the CNP10/CNP11 (Agnini et al. 2014) and NP8/NP9 (Martini 1971) boundaries, slightly above the boundary reported by Serra-Kiel et al. (1998), i.e. between the upper part of the NP8 and the lower part of the NP9.

In short, the data from this thesis allow proposing a LF and calcareous nannofossils integrated biostratigraphic reference scheme for the Paleocene of the western Neotethys (**Fig. 34**).

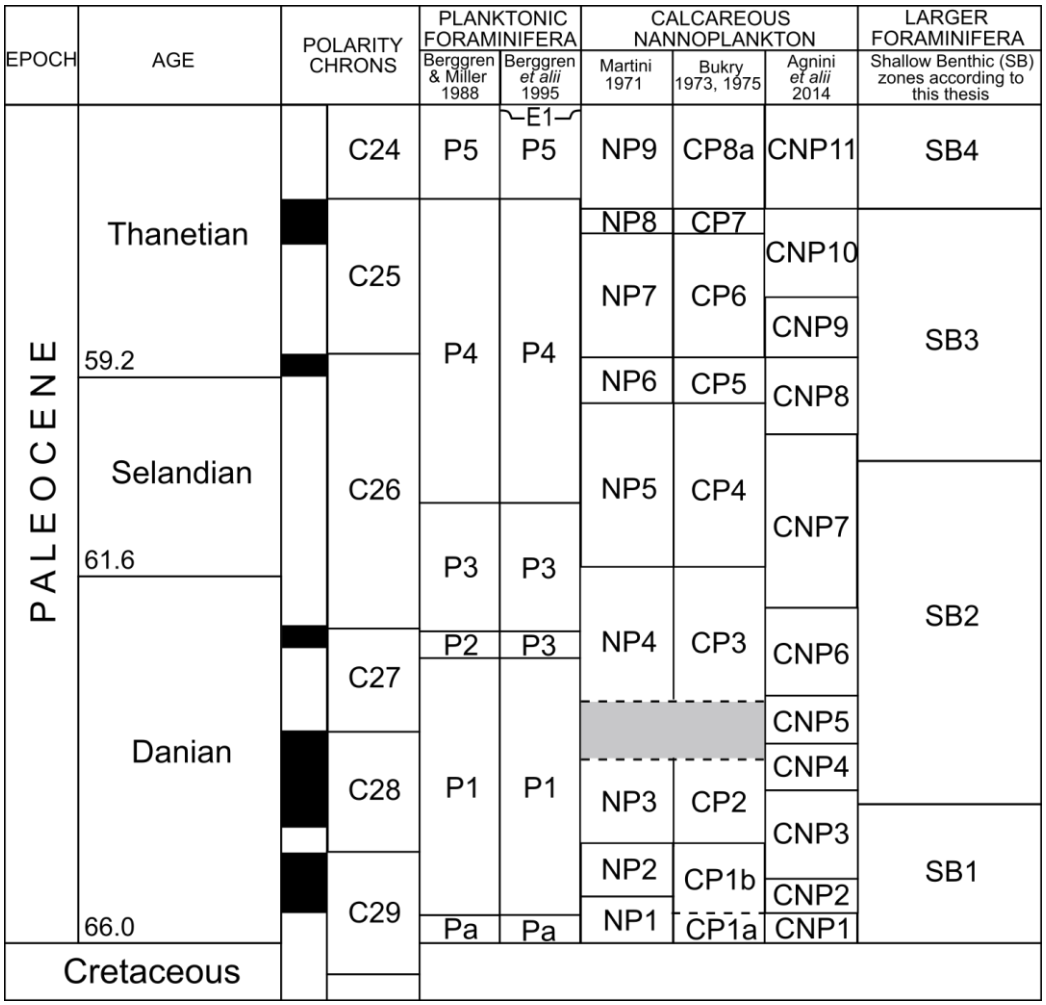

Fig. 34. Integration of the SB biozonation obtained by the present thesis with the calcareous nannoplankton zones by Agnini et al. (2014) and with the time-scale by Vandenberghe et al. (2012).

5.5. CHRONOLOGY AND SEDIMENTS-ACCUMULATION RATE IN THE INVESTIGATED SECTIONS

In collaboration with Prof. Eliana Fornaciari, University of Padova (Italy)

In order to estimate the chronology of the recorded bio-horizons and the derived mean accumulation rates of the investigated sections, we firstly evaluate through the Shaw diagram the degree of synchroneity of events between the Tabiago and Ardo sections (**Fig. 35**).

The Shaw diagram highlights that all the bio-horizons observed, with the exception of *C. pelagicus* and *E. robusta* Bases, intercept or are in close proximity to the line of correlation. The bio-horizons intercepting the correlation line can be assumed synchronous between the two compared sections unlike the two bio-horizons located far away from the best-fit correlation line can be deemed diachronous. The Shaw diagram shows, not unexpectedly, a break of the best correlation line to the shift between Milano and Lecco segments at the Tabiago composite section. Below the break the correlation line slope is 0.30 ($y = 0.30 x + q$), evidencing that the Milano segment is two time more expanded with respect the equivalent interval at the Ardo. The lower sediment accumulation rate in the first 10 m at Ardo was possibly due, at least in part, to the erosion produced by the thicker bioclastic beds. In the Lecco segment the abrupt changes from 1.95 ($y = 1.95x - q$) to 5.42 ($y = 5.42x - q$) of the correlation line slope across NP5/NP6 boundary and from 5.42 to 1.26 ($y = 1.26 x + q$) across NP6/NP7 boundary indicates that the NP 6 at Tabiago is fairly condensed. Overall the mean accumulation rate of the Lecco segment is about half with respect the same interval at the Ardo. The higher mean accumulation rate at Ardo is probably caused by an enhanced terrigenous input during the deposition of Scaglia Cinerea (e.g., Giusberti et al. 2007). In short, the average sedimentation rate switches between Ardo and Tabiago approximately at the Danian-Selandian transition.

At Ardo, we extrapolated the age of the recorded bioevents taking into account as chronologic control points the magnetic polarity reversals retrieved in the section, which permit evaluating the derived mean sedimentation rates. These points are calibrated at the geomagnetic polarity time scale of Cande and Kent (1995; CK95). We estimated the age of every bio-horizons by means of the estimated average sedimentation rate, the relative distance of events to nearest youngest geomagnetic polarity boundary and the calibrated age of this last.

In **Table 4** we reported the ages and relative positions of the bioevents at the Ardo in relation to magnetochrons. It should be remarked that, not surprisingly, the obtained ages roughly confirm the Dallanave et al. (2012) data. Successively, in the Ardo-Tabiago Shaw diagram we interpolated the bio-horizons recorded only at Tabiago (*K. decastroi* FO, orthophragminids FO and *F. pileatus* T) with the line correlation. Afterwards, we projected orthogonally this events on the Ardo section in order to evaluate their positions within the magnetochrons and consequently the ages.

Biohorizon	ARDO					
	Thickness (m)	SAMPLE	Position to chron top		Age (Ma) CK95	Age (Ma) Gradstein et al. (2012)
*T *Ericsonia robusta* morph. B	90.26 ± 0.40	/	C24r	0.05	55.78	56.95
*B *Fasciculithus alanii*	90.26 ± 0.40	/	C24r	0.05	55.78	56.95
*B *Discoaster multiradiatus*	86.06 ± 0.20	/	C25n	0.10	55.95	57.16
FO *Assilina azilensis*	**85.75**	/	**C25n**	**0.131**	**55.96**	**57.17**
*B *Ericsonia robusta* morph. B	80.41 ± 1.35	/	C25n	0.60	56.19	57.43
*T *Heliolithus kleinpellii*	62.23 ± 0.02	/	C25r	0.65	57.15	58.51
*T *Heliolithus cantabriae*	61.29 ± 0.05	/	C25r	0.70	57.20	58.56
*B *Discoaster mohleri*	55.74 ± 0.38	/	C25r	0.97	57.51	58.91
*B *Heliolithus kleinpellii*	43.54 ± 0.43	/	C26r	0.14	58.34	59.66
*B *Sphenolithus anarrhopus*	40.59 ± 0.55	/	C26r	0.22	58.58	59.91
*B *Heliolithus cantabriae*	39.97 ± 0.08	/	C26r	0.24	58.64	59.96
FO orthophragminids	**37.85 ± 2.125**	/	**C26r**	**0.302**	**58.82 ± 0.18**	**60.14 ± 0.178**
T *Fasciculithus pileatus*	34.00 ± 1.24	/	C26r	0.410	59.14 ± 0.10	60.46 ± 0.10
B *Fasciculithus tympaniformis*	21.32 ± 0.42	ART57-ART58	C26r	0.77	60.22 ± 0.04	61.52 ± 0.03
B *Fasciculithus (=F. ulii)*	18.83 ± 0.21	ART52-ART53	C26r	0.84	60.43 ± 0.02	61.73 ± 0.02
B *Sphenolithus*	15.38 ± 0.17	ART45-ART46	C26r	0.93	60.72 ± 0.01	62.02 ± 0.01
B *Toweius pertusus*	9.79 ± 0.30	ART33-ART34	C27r	0.55	61.95 ± 0.09	63.05 ± 0.07
Bc *Cruciplacolithus tenuis* s.s.	9.20 ± 0.25	ART31-ART32	C27r	0.69	62.12 ± 0.07	63.19 ± 0.06
B *Prinsius bisulcus*	7.73 ± 0.11	ART28-ART29	C28n	0.04	62.55 ± 0.04	63.54 ± 0.04
FO *Cuvillierina sirelii*	**7.16 ± 0.24**	**ARD15-ARD16**	**C28n**	**0.20**	**62.73 ± 0.08**	**63.73 ± 0.08**
FO *Kayseriella decastroi*	**7.02 ± 0.14**	/	**C28n**	**0.20**	**62.78 ± 0.05**	**63.78 ± 0.047**
Bc *Prinsius martinii*	6.76 ± 0.26	ART26-ART27	C28n	0.32	62.86 ± 0.08	63.87 ± 0.09
FO *Elazigina dieniii*	**5.29 ± 0.59**	**ARD8-ARD12**	**C28n**	**0.74**	**63.34 ± 0.19**	**64.36 ± 0.20**
B *Prinsius martinii*	5.49 ± 0.23	ART23-ART21	C28n	0.68	63.27 ± 0.07	64.30 ± 0.08
Tc *Praprinsius dimorphosus*	4.83 ± 0.06	ART18-ART19	C28n	0.87	63.49 ± 0.02	64.52 ± 0.02
Bc *praeprinsisus dimorphosus*	2.15 ± 0.26	ART8-ART9	C29n	0.53	64.39 ± 0.06	65.34 ± 0.06
B *Praeprinsius dimorphosus*	1.35 ± 0.11	ART5-ART6	C29n	0.76	64.57 ± 0.02	65.52 ± 0.02
B *Coccolithus pelagicus*	0.47 ± 0.15	ART2-ART2A	C29r	0.15	64.79 ± 0.06	65.74 ± 0.08

Table 4. Age estimations of selected bio-horizons in the Ardo section based on the GPTS of CK95 and Gradstein et al. (2012). In red the supposed position of taxa not observed in the Ardo section (see the text for discussion). * Data from Dallanave et al. (2012).

Biohorizon	MONTE GIGLIO				
	Thickness (m)	SAMPLE	Position to chron top	Age (Ma) CK95	Age (Ma) Gradstein et al. (2012)
FO orthophragminids	**29.20 ± 0.43**	**CMG2969-CMG2882**	/	**59.32**	**60.63**
T *Fasciculithus pileatus*	26.17 ± 0.16	CMG 2638-CMG 260	/	59.42	60.73
B *Fasciculithus tympaniformis*	1.23 ± 0.13	CMG 136-CMG 110	/	60.20	61.51

Table 5. Age estimations of selected bio-horizons in the Monte Giglio section based on the GPTS of CK95 and Gradstein et al. (2012).

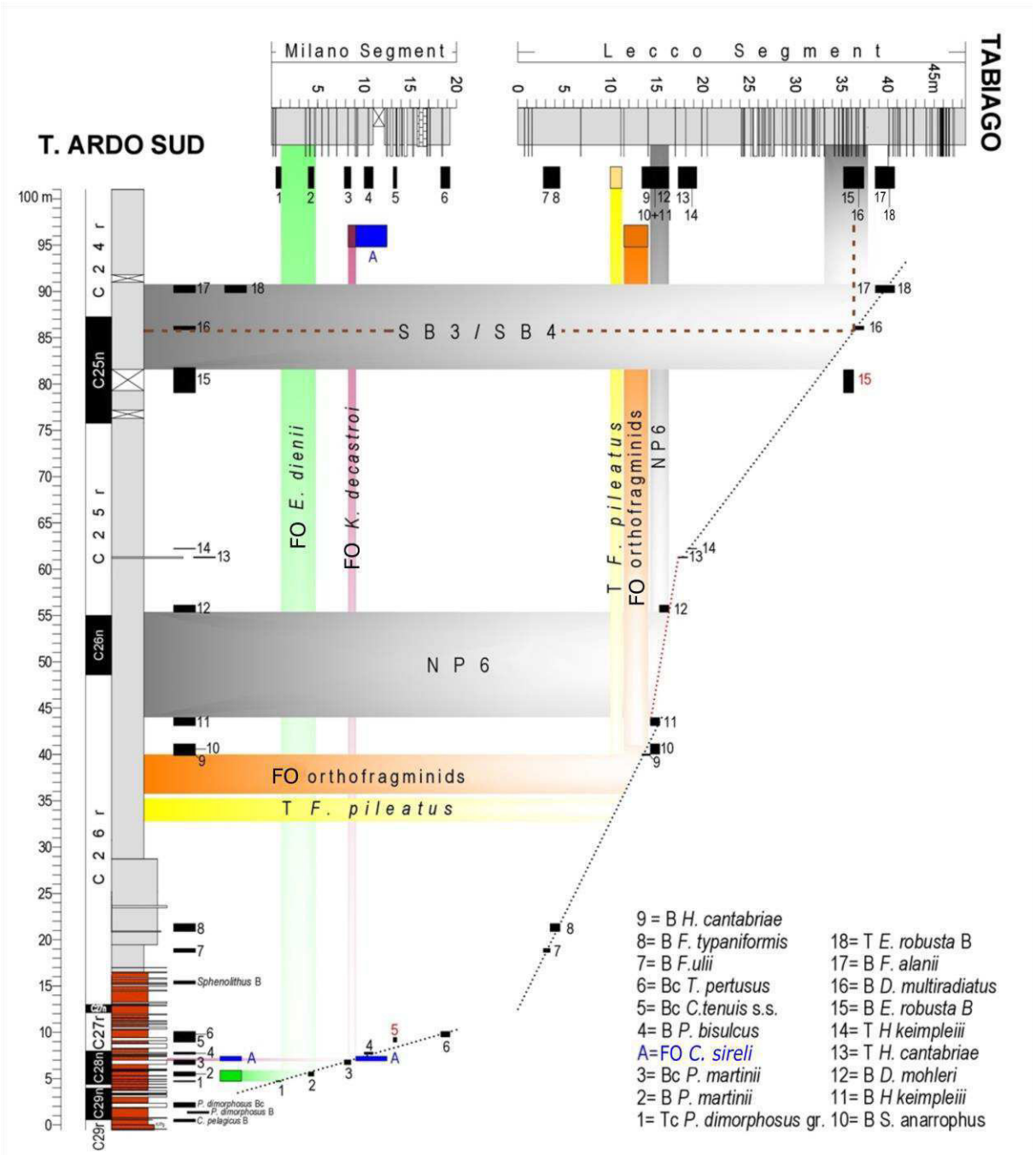

Fig. 35. Shaw diagram Tabiago Milano and Lecco – Ardo sections.

The obtained data suggest that the *K. decastroi* FO is associated to the upper part of Chron C28n with an assumed age of 62.78 ± 0.05 Ma and the orthophragminids FO and *F. pileatus* T to the mid C26r Chron with an age estimated of 58.82 ± 0.18 Ma and 59.14 ± 0.10 Ma, respectively. The position of the SB3/SB4 boundary at Tabiago displays a large associated error preventing an accurate positioning of the SB3 base that straddles upper Chron C25n-lower Chron C24r with a mean age of 55.96 Ma. It should be noted that the position and the age of the orthophragminids first occurrence is affected both by the very low accumulation rate within NP6 and the associated error of the position of this event in the Lecco segment.

In order to better constrain the age of orthophragminids FO, first we prepared the M. Giglio-Lecco segment Shaw diagram (**Table 5**, **Fig. 36**) to test the synchronicity of the Base of orthophragminids. Indeed, at Tabiago we were able to detect more accurately the relative position of this event.

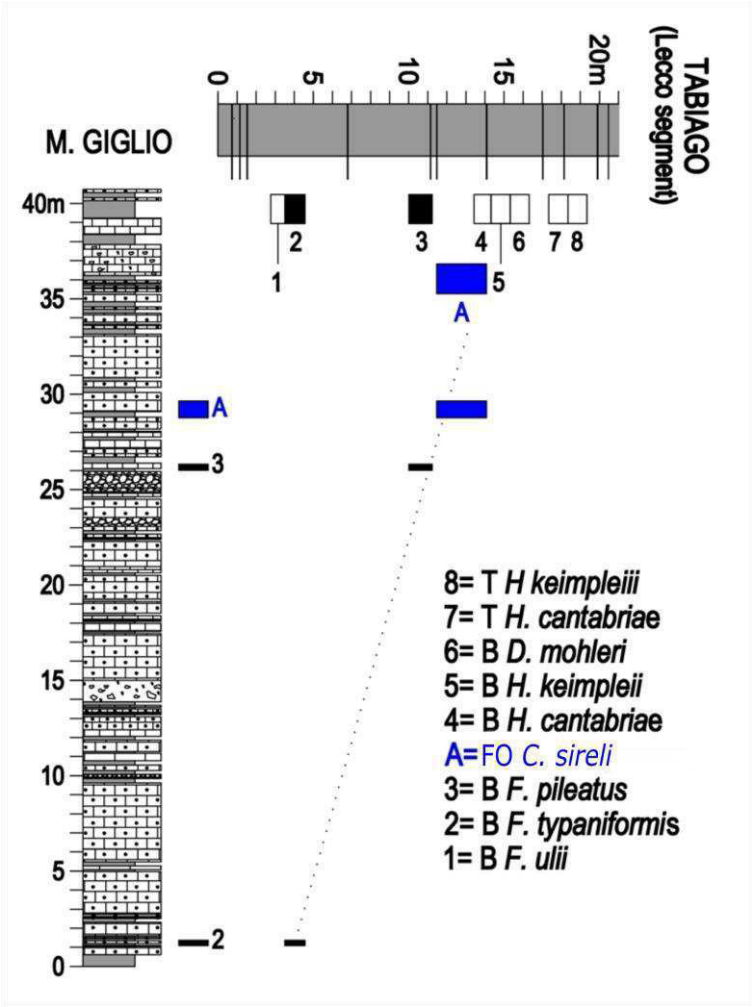

Fig. 36. Shaw diagram Tabiago Lecco - Monte Giglio sections.

The most important points of the M. Giglio-Lecco Shaw Diagram are the *F. tympaniformis* B and the *F. pilatus* T. Indeed, these calcareous nannofossil events are proved reliable with consistent ages over wide areas (e.,g., Agnini et al ., 2014; Gradstein et al., 2012). The correlation line generated partially intercepts the bio-horizon defined by the orthophragminids FO suggesting that the event is synchronous between the two compared section. Once it has been ascertained that the three considered events are synchronous, the age of orthophragminids FO has been indirectly assumed by means of the mean accumulation rate calculated between the calcareous nannofossil events whose ages have been calibrated in Agnini et al. (2014; for the base of *F. tympaniformis*) and in Berggren et al. (1995; for the Top of *F. pileatus*). The estimated age of the orthophraminids FO is 59.32 Ma according to Cande and Kent (1995) and 60.63 Ma according to Gradstein et al. (2012). The relative positions of this event which marks the base of the SB3 in relation to the magnetochrons is mid Chron C26r confirming the previous calibrations of the base of SB3.

6. A NEW SPECIES OF *Alveolina* FROM BOLCA

6.1. THE LF ASSEMBLAGES OF MONTE POSTALE AND PESCIARA DI BOLCA

The Monte Postale and the Pesciara di Bolca, even if world-famous for their exceptionally preserved fishes, include several levels containing rich *Alveolina* assemblages. In the Monte Postale section the alveolinids are preserved in the bedded grainstones-rudstones alternated with the coralgal rudstones, the laminated fish-bearing mudstones, and the *Alveolina-Nummulites* packstones, representing the sand bars, the coralgal rims, the back-reef lagoon, and the fore-reef, respectively (Vescogni et al. 2016). In the Pesciara section, there are thick biocalcarenitic-biocalciruditic beds alternating with the laminated fish-bearing limestones; these coarser-grained limestones often contain abundant *Alveolina* tests. Thin intercalations of re-sedimented grainstones-packstones with alveolines and miliolids could locally occur inside the laminated beds (Papazzoni and Trevisani 2006).

The large foraminiferal assemblage at Monte Postale has been described by Papazzoni et al. (2017b) and ascribed to the SB11 Zone (middle Cuisian = upper Ypresian; Serra-Kiel et al., 1998) according to the presence of the marker species *Alveolina cremae*, *A. dainelli*, and *A. decastroi*. Other species recorded and consistent with this biozone are *Alveolina distefanoi* (SB10–SB11), *A. fornasinii* (SB9–SB10), *A. rutimeyeri* (SB10– SB11) and *A. rugosa* (upper SB10–lower SB12). Also *Alveolina frumentiformis* (SB12–upper SB13) was identified; as its presence was limited to the top of the Monte Postale section and in co-occurrence with several SB11 marker species, it was inferred that its range has to be extended to the upper SB11. The presence of *Alveolina* cf. *schwageri*, marker of the SB10, is attributed to reworking, given that it has been collected within a slump.

In Papazzoni et al. (2017b), the larger foraminiferal assemblage was correlated to the calcareous nannofossils, demonstrating that the Monte Postale section spans the SB11 and the CNE5 (Agnini et al. 2014), equivalent to the NP13 (Martini 1971), with a possible transition to the CNE6 in its uppermost part.

The larger foraminiferal assemblages of the Pesciara, instead, were object of the study by Papazzoni and Trevisani (2006), which assigned it to the SB11 as well because of the occurrence of *Alveolina* ex gr. *canavarii*, *A. cremae*, *A. decastroi*. Other recorded taxa consistent with this biozone are *A. distefanoi* (SB10–SB11), *A. levantina* (upper SB11–SB12), *A. rugosa* (upper SB 10–lower SB12), *Nummulites pratti* (SB11–lower SB12), *N. praelucasi* (SB 10–SB 11).

Relying on Medizza (1975), who recognized the *Discoaster sublodoensis* (=NP14) calcareous nannofossil zone in the uppermost part of the outcrop, Papazzoni and Trevisani (2006) restricted the age of the Pesciara to the uppermost SB11 and the lowermost NP14 (=CNE 6). Further studies, aimed at the integrated LF and calcareous nannofossils biostratigraphy, are in progress on the Pesciara outcrop and on the recently drilled cores.

Both Papazzoni et al. (2017) for the Postale assemblage and Papazzoni and Trevisani (2006) for the Pesciara assemblage remarked the presence of a form differing from the others, not assigned to any known species and provisionally named *Alveolina* aff. *croatica*, differing from *Alveolina croatica* Drobne 1977 for the size of the proloculus and its smaller overall size, with a lower number of whorls. Fornaciari et al. (2019) analysed the morphology and the biometric parameters of this morphotype, examined several diagnostic sections from the Monte Postale and Pesciara sections and cores, and measured and compared it with the known species. Given the significant differences, the new species *Alveolina postalensis* Fornaciari, Giusberti and Papazzoni, 2019 was erected.

DISCLAIMER: the study of this new species is part of the present PhD thesis, therefore it is reported here below. I have to mention that the description of the new species in the following could not be considered in any way as a formal one or an emendation to the original description of Fornaciari et al. (2019).

6.2. ANALYSES OF *Alveolina postalensis* Fornaciari, Giusberti and Papazzoni 2019

The specimens have been analysed taking into account morphological and biometrical features (proloculus diameter, axial diameter, equatorial diameter), whose values are listed in **Table 6.**

Pesciara tuffs																							
Sample	**Specimen**	**Pd**	**Ax1**	**Eq1**	**EI1**	**Ax2**	**Eq2**	**EI2**	**Ax3**	**Eq3**	**EI3**	**Ax4**	**Eq4**	**EI4**	**Ax5**	**Eq5**	**EI5**	**Ax6**	**Eq6**	**EI6**	**Ax7**	**Eq7**	**EI7**	**Ax8**
BPEV2-06	IPUM 29155	490	0.72	0.63	1.14	1.10	0.84	1.31	1.75	0.99	1.77	1.60	1.20	1.33	3.74	1.50	2.49	-	-	-	-	-	-	-
BPEV7-01	IPUM 29156	480	-	-	-	-	-	-	-	-	-	-	-	-	-	-	-	-	-	-	-	-	-	-
PEV4-10	IPUM 29157	500	-	-	-	-	-	-	-	-	-	-	-	-	-	-	-	-	-	-	-	-	-	-
PEV5-02	IPUM 29158	700	0.90	0.80	1.13	1.47	1.02	1.44	2.42	1.22	1.98	3.23	1.56	2.07	-	-	-	-	-	-	-	-	-	-
mean		**543**	**0.81**	**0.72**	**1.13**	**1.29**	**0.93**	**1.38**	**2.09**	**1.11**	**1.88**	**2.42**	**1.38**	**1.70**	**3.74**	**1.50**	**2.49**	-	-	-	-	-	-	-
Pesciara																								
Sample	**Specimen**	**Pd**	**Ax1**	**Eq1**	**EI1**	**Ax2**	**Eq2**	**EI2**	**Ax3**	**Eq3**	**EI3**	**Ax4**	**Eq4**	**EI4**	**Ax5**	**Eq5**	**EI5**	**Ax6**	**Eq6**	**EI6**	**Ax7**	**Eq7**	**EI7**	**Ax8**
BOL0219	IPUM 29159	440	-	-	-	-	-	-	-	-	-	-	-	-	-	-	-	-	-	-	-	-	-	-
PEB26	IPUM 29160	400	0.57	0.50	1.14	0.94	0.63	1.49	1.34	0.74	1.81	1.92	0.91	2.11	2.32	1.04	2.23	-	-	-	-	-	-	-
BOL0209	IPUM 29161	860	-	-	-	-	-	-	-	-	-	-	-	-	-	-	-	-	-	-	-	-	-	-
BOL0209	IPUM 29162	640	-	-	-	-	-	-	-	-	-	-	-	-	-	-	-	-	-	-	-	-	-	-
BOL0208	IPUM 29163	520	-	-	-	-	-	-	-	-	-	-	-	-	-	-	-	-	-	-	-	-	-	-
BOL0204	IPUM 29164	580	-	-	-	-	-	-	-	-	-	-	-	-	-	-	-	-	-	-	-	-	-	-
BOL0203	IPUM 29165	650	0.93	0.71	1.31	1.64	0.85	1.93	2.02	1.01	2.00	2.60	1.20	2.17	3.32	1.40	2.37	4.02	1.62	2.48	4.80	1.87	2.57	5.42
BOL0203	IPUM 29166	720	-	-	-	-	-	-	-	-	-	-	-	-	-	-	-	-	-	-	-	-	-	-
mean		**601**	**0.75**	**0.61**	**1.22**	**1.29**	**0.74**	**1.71**	**1.68**	**0.88**	**1.91**	**2.26**	**1.06**	**2.14**	**2.82**	**1.22**	**2.30**	**4.02**	**1.62**	**2.48**	**4.80**	**1.87**	**2.57**	**5.42**
Pesciara core																								
Sample	**Specimen**	**Pd**	**Ax1**	**Eq1**	**EI1**	**Ax2**	**Eq2**	**EI2**	**Ax3**	**Eq3**	**EI3**	**Ax4**	**Eq4**	**EI4**	**Ax5**	**Eq5**	**EI5**	**Ax6**	**Eq6**	**EI6**	**Ax7**	**Eq7**	**EI7**	**Ax8**
CABO9.5	IPUM 29167	570	0.74	0.62	1.19	1.18	0.78	1.51	1.72	0.93	1.85	2.44	1.09	2.24	2.75	1.20	2.29	3.16	1.30	2.43	3.64	1.40	2.60	-
Monte Postale																								
Sample	**Specimen**	**Pd**	**Ax1**	**Eq1**	**EI1**	**Ax2**	**Eq2**	**EI2**	**Ax3**	**Eq3**	**EI3**	**Ax4**	**Eq4**	**EI4**	**Ax5**	**Eq5**	**EI5**	**Ax6**	**Eq6**	**EI6**	**Ax7**	**Eq7**	**EI7**	**Ax8**
PST1316	IPUM 29168	397	-	-	-	-	-	-	-	-	-	-	-	-	-	-	-	-	-	-	-	-	-	-
PST1316	IPUM 29169	404	0.55	-	-	0.85	0.58	1.47	1.23	0.72	1.71	1.60	0.81	1.98	2.08	0.98	2.12	2.49	-	-	2.84	-	-	3.26
PST1316	IPUM 29170	738	-	-	-	-	-	-	-	-	-	-	-	-	-	-	-	-	-	-	-	-	-	-
PST1316	IPUM 29171	476	0.66	0.60	1.10	1.20	0.76	1.58	1.52	0.95	1.60	2.48	1.25	1.98	3.20	-	-	3.40	-	-	-	-	-	-
PST1315	IPUM 29172	526	-	-	-	-	-	-	-	-	-	-	-	-	-	-	-	-	-	-	-	-	-	-
PST1315	IPUM 29173	475	-	-	-	-	-	-	-	-	-	-	-	-	-	-	-	-	-	-	-	-	-	-
PST1315	IPUM 29174	377	-	-	-	-	-	-	-	-	-	-	-	-	-	-	-	-	-	-	-	-	-	-
PST1315	IPUM 29175	420	-	-	-	-	-	-	-	-	-	-	-	-	-	-	-	-	-	-	-	-	-	-
PST1314	IPUM 29176	431	-	-	-	-	-	-	-	-	-	-	-	-	-	-	-	-	-	-	-	-	-	-
PST1314	IPUM 29177	570	0.73	-	-	0.91	-	-	1.50	0.88	1.70	2.26	1.14	1.98	2.87	1.33	2.16	3.36	1.53	2.20	-	-	-	-
PST1313	IPUM 29178	410	-	-	-	-	-	-	-	-	-	-	-	-	-	-	-	-	-	-	-	-	-	-
PST1312	IPUM 29179	633	-	-	-	-	-	-	-	-	-	-	-	-	-	-	-	-	-	-	-	-	-	-
PST1304	IPUM 29180	410	-	-	-	-	-	-	-	-	-	-	-	-	-	-	-	-	-	-	-	-	-	-
PST1304	IPUM 29181	378	-	-	-	-	-	-	-	-	-	-	-	-	-	-	-	-	-	-	-	-	-	-
PST1304	IPUM 29182	450	-	-	-	-	-	-	-	-	-	-	-	-	-	-	-	-	-	-	-	-	-	-
PST1303	IPUM 29183	590	-	-	-	-	-	-	-	-	-	-	-	-	-	-	-	-	-	-	-	-	-	-
PST1302	IPUM 29184	490	-	-	-	-	-	-	-	-	-	-	-	-	-	-	-	-	-	-	-	-	-	-
PST1302	IPUM 29185	649	-	-	-	-	-	-	-	-	-	-	-	-	-	-	-	-	-	-	-	-	-	-
PST1301	IPUM 29186	754	-	-	-	-	-	-	-	-	-	-	-	-	-	-	-	-	-	-	-	-	-	-
PST1404	IPUM 29187	585	-	-	-	-	-	-	-	-	-	-	-	-	-	-	-	-	-	-	-	-	-	-
PST1405	IPUM 29188	783	-	-	-	-	-	-	-	-	-	-	-	-	-	-	-	-	-	-	-	-	-	-
PST1405	IPUM 29189	419	-	-	-	-	-	-	-	-	-	-	-	-	-	-	-	-	-	-	-	-	-	-
PST1405	IPUM 29190	416	-	-	-	-	-	-	-	-	-	-	-	-	-	-	-	-	-	-	-	-	-	-
PST1405	IPUM 29191	674	-	-	-	-	-	-	-	-	-	-	-	-	-	-	-	-	-	-	-	-	-	-
PST1405	IPUM 29192	550	0.84	0.66	1.27	1.24	0.84	1.48	1.72	1.02	1.69	2.39	1.18	2.03	-	-	-	-	-	-	-	-	-	-
CMP613	IPUM 29193	560	-	-	-	-	-	-	-	-	-	-	-	-	-	-	-	-	-	-	-	-	-	-
PST1419	IPUM 29194	618	-	-	-	-	-	-	-	-	-	-	-	-	-	-	-	-	-	-	-	-	-	-
PST1419	IPUM 29195	560	-	-	-	-	-	-	-	-	-	-	-	-	-	-	-	-	-	-	-	-	-	-
PST1419	IPUM 29196	634	-	-	-	-	-	-	-	-	-	-	-	-	-	-	-	-	-	-	-	-	-	-
PST1419	IPUM 29197	526	-	-	-	-	-	-	-	-	-	-	-	-	-	-	-	-	-	-	-	-	-	-
PST1419	IPUM 29198	525	-	-	-	-	-	-	-	-	-	-	-	-	-	-	-	-	-	-	-	-	-	-
CMP840	IPUM 29199	740	1.07	0.80	1.34	1.48	1.05	1.41	2.18	1.36	1.60	2.72	1.50	1.81	-	-	-	-	-	-	-	-	-	-
CMP935	IPUM 29200	694	-	-	-	-	-	-	-	-	-	-	-	-	-	-	-	-	-	-	-	-	-	-
CMP935	IPUM 29201	457	-	-	-	-	-	-	-	-	-	-	-	-	-	-	-	-	-	-	-	-	-	-
CMP935	IPUM 29202	620	1.01	0.86	1.17	1.52	1.05	1.45	2.14	1.22	1.75	2.70	-	-	-	-	-	-	-	-	-	-	-	-
CMP1215	IPUM 29203	711	0.97	0.77	1.26	1.69	0.93	1.82	2.56	1.09	2.35	3.15	1.26	2.50	-	-	-	-	-	-	-	-	-	-
CMP1215	IPUM 29204	568	-	-	-	-	-	-	-	-	-	-	-	-	-	-	-	-	-	-	-	-	-	-
CMP1285	IPUM 29205	602	-	-	-	-	-	-	-	-	-	-	-	-	-	-	-	-	-	-	-	-	-	-
CMP1660	IPUM 29206	687	-	-	-	-	-	-	-	-	-	-	-	-	-	-	-	-	-	-	-	-	-	-
CMP1970	IPUM 29207	645	-	-	-	-	-	-	-	-	-	-	-	-	-	-	-	-	-	-	-	-	-	-
MPO0309	IPUM 29208	740	-	-	-	-	-	-	-	-	-	-	-	-	-	-	-	-	-	-	-	-	-	-
MPO0308	IPUM 29209	492	-	-	-	-	-	-	-	-	-	-	-	-	-	-	-	-	-	-	-	-	-	-
MPO0308	IPUM 29210	533	-	-	-	-	-	-	-	-	-	-	-	-	-	-	-	-	-	-	-	-	-	-
MPO0308	IPUM 29211	558	-	-	-	-	-	-	-	-	-	-	-	-	-	-	-	-	-	-	-	-	-	-
MPO0307	IPUM 29212	565	-	-	-	-	-	-	-	-	-	-	-	-	-	-	-	-	-	-	-	-	-	-
MPO0307	IPUM 29213	742	-	-	-	-	-	-	-	-	-	2.62	1.50	1.75	3.58	1.70	2.11	4.30	2.00	2.15	4.6	-	-	-
MPO0307	IPUM 29214	445	-	-	-	-	-	-	-	-	-	-	-	-	-	-	-	-	-	-	-	-	-	-
MPO0307	IPUM 29215	652	-	-	-	-	-	-	-	-	-	-	-	-	-	-	-	-	-	-	-	-	-	-
MPO0306	IPUM 29216	545	-	-	-	-	-	-	-	-	-	-	-	-	-	-	-	-	-	-	-	-	-	-
MPO0306	IPUM 29217	581	-	-	-	-	-	-	-	-	-	-	-	-	-	-	-	-	-	-	-	-	-	-
MPO0305	IPUM 29218	494	0.66	0.54	1.22	0.93	0.71	1.31	1.39	0.88	1.58	1.97	1.05	1.88	2.60	1.25	2.08	3.16	1.47	2.15	-	-	-	-
PST1434	IPUM 29219	596	-	-	-	-	-	-	-	-	-	-	-	-	-	-	-	-	-	-	-	-	-	-
PST1434	IPUM 29220	640	-	-	-	-	-	-	-	-	-	-	-	-	-	-	-	-	-	-	-	-	-	-
PST1434	IPUM 29221	542	-	-	-	-	-	-	-	-	-	-	-	-	-	-	-	-	-	-	-	-	-	-
PST1434	IPUM 29222	611	-	-	-	-	-	-	-	-	-	-	-	-	-	-	-	-	-	-	-	-	-	-
PST1434	IPUM 29223	631	-	-	-	-	-	-	-	-	-	-	-	-	-	-	-	-	-	-	-	-	-	-
MPO0302	IPUM 29224	710	0.88	-	-	1.11	0.96	1.16	1.98	1.08	1.83	3.20	1.44	2.22	3.80	1.63	2.33	4.17	1.92	2.17	4.60	2.2	2.09	-
PST1429	IPUM 29225	585	-	-	-	-	-	-	-	-	-	-	-	-	-	-	-	-	-	-	-	-	-	-
PST1429	IPUM 29226	509	0.73	-	-	1.09	0.85	1.28	1.60	1.09	1.47	2.46	1.29	1.91	3.36	1.48	2.27	4.22	1.67	2.53	4.87	1.81	2.69	-
PST1429	IPUM 29227	532	-	-	-	-	-	-	-	-	-	-	-	-	-	-	-	-	-	-	-	-	-	-
PST1429	IPUM 29228	637	-	-	-	-	-	-	-	-	-	-	-	-	-	-	-	-	-	-	-	-	-	-
mean		**565**	**0.81**	**0.71**	**1.23**	**1.20**	**0.86**	**1.44**	**1.78**	**1.03**	**1.73**	**2.50**	**1.24**	**2.00**	**3.07**	**1.40**	**2.18**	**3.59**	**1.72**	**2.24**	**4.23**	**2.01**	**2.39**	**3.26**
All specimens																								
		Pd	**Ax1**	**Eq1**	**EI1**	**Ax2**	**Eq2**	**EI2**	**Ax3**	**Eq3**	**EI3**	**Ax4**	**Eq4**	**EI4**	**Ax5**	**Eq5**	**EI5**	**Ax6**	**Eq6**	**EI6**	**Ax7**	**Eq7**	**EI7**	**Ax8**
minimum		**377**	0.55	0.50	1.10	0.85	0.58	1.31	1.23	0.72	1.58	1.60	0.81	1.33	2.08	0.98	2.08	2.49	1.30	2.15	2.84	1.40	2.57	3.26
maximum		**860**	1.07	0.86	1.34	1.69	1.05	1.82	2.56	1.36	2.35	3.20	1.56	2.50	3.80	1.70	2.49	4.30	2.00	2.53	4.80	1.87	2.69	5.42
mean		**568**	**0.80**	**0.68**	**1.21**	**1.22**	**0.85**	**1.47**	**1.80**	**1.01**	**1.78**	**2.46**	**1.23**	**2.00**	**3.06**	**1.35**	**2.25**	**3.59**	**1.64**	**2.30**	**4.31**	**1.82**	**2.49**	**4.34**
stand. dev.		**110**	0.16	0.12	0.08	0.27	0.15	0.20	0.40	0.18	0.21	0.52	0.21	0.26	0.58	0.24	0.13	0.62	0.25	0.17	0.81	0.21	0.27	1.53

Table 6. Measured parameter for each speciments of *Alveolina postalensis* Fornaciari, Giusberti and Papazzoni 2019. The specimens are grouped according to the locality and listed in stratigraphic order (except for the Pesciara tuffs, for which no relative position could be determined). Pd=proloculus diameter (μm); Axn=axial diameter (mm) at the n-th whorl; Eqn=equatorial diameter (mm) at the n-th whorl; EIn=elongation index at the n-th whorl.

From the Table 6, the mean values of the biometric features have been obtained and compared to those of similar species belonging to the *Alveolina levantina* group (*A. levantina*, *A.* aff. *levantina*, transitional forms between *A. levantina* and *A. hottingeri*, *A. hottingeri*, *A. croatica*) reported in literature (Scotto di Carlo 1966, Hottinger 1960, Hottinger 1974, Drobne 1977) (**Table 7**). To do this, it was sometimes necessary to measure the specimens illustrated in the figures/plates by the authors because the texts didn't reported the values of every biometric parameter.

Species	Author, year (page of description)	Specimen	Pd	n. of whorls	Ax	Eq	EI	Ax7	Eq7	EI7
A. levantina Hottinger, 1960	Hottinger, 1960 (p. 154)	pl. 10, fig. 12 (right)*	550	6	-	1.15	-	-	-	-
		pl. 10, fig. 13*	400	11/12	4.50	2.45	1.84	3.20	1.35	2.37
		pl. 14, fig. 7	300	12	4.40	2.20	2.00	2.50	1.00	2.50
	Hottinger, 1974 (p. 46-47)	pl. 51, fig. 2 low	500	11	8.00	1.90	4.21	4.50	1.05	4.29
		pl. 51, fig. 2 high	700	10	8.50	2.80	3.04	5.20	1.20	4.33
		pl. 51, fig. 3	650	6	4.20	1.20	3.50	4.10	1.20	3.42
	Drobne, 1977 (p. 57)	pl. 14, fig. 1	600	7	3.45	1.25	2.76	3.45	1.25	2.76
		pl. 14, fig. 2	400	14	6.45	3.00	2.15	2.45	1.15	2.13
		p. 59, fig. 32a	400	13	6.60	2.35	2.81	4.00	1.35	2.96
A.* aff. *levantina Hottinger, 1960	Scotto di Carlo, 1966 (p. 72)	tav. LVIII (X), fig. 2	430; 400 **	10	5.80	1.87	3.10	3.86	1.50	2.57
		tav. LIX (XI), fig. 2	600	7/8	-	2.00	-	-	-	-
		tav. LX (XII), fig. 3	500	9	-	1.94	-	-	-	-
Transitional forms between *A. levantina* and *A. hottingeri*	Drobne, 1977 (p. 57)	pl. 14, fig. 3	750	10	8.50	2.40	3.54	6.85	1.57	4.36
		pl. 14, fig. 4	500	11	10.25	2.60	3.94	5.60	1.15	4.87
		pl. 14, fig. 5	375	13	10.00	2.45	4.08	3.35	0.90	3.72
A. hottingeri Drobne, 1977	Drobne, 1977 (p. 57)	pl. 14, fig. 7	600	11/12	10.35	1.90	5.45	5.30	1.08	4.93
		pl. 14, fig. 8	500	13	15.25	2.20	6.93	8.75	1.08	8.14
		p. 59, fig. 32b	550	13	6.30	1.95	3.23	6.00	0.92	6.52
		p. 59, fig. 32c	-	10	14.01	1.35	10.38	9.25	1.20	7.71
A. croatica Drobne, 1977	Drobne, 1977 (p. 58)	pl. 14, fig. 9	600	12	6.70	2.55	2.63	3.70	1.47	2.52
		pl. 14, fig. 10	1000	12/13	-	3.55	-	-	-	-
		pl. 14, fig. 11	750	10	8.60	2.05	4.20	7.00	1.15	6.09
		pl. 14, fig. 12	1000	11	9.00	2.00	4.50	5.75	1.05	5.48
		p. 60, fig. 33	1100	7	7.95	2.05	3.88	7.95	2.05	3.88
***A. postalensis* n. sp.**	This work	IPUM 29155	490	5	3.74	1.50	2.49	-	-	-
		IPUM 29158	700	4	3.23	1.56	2.07	-	-	-
		IPUM 29160	400	5	2.32	1.04	2.23	-	-	-
		IPUM 29165	650	8	5.42	-	-	-	-	-
		IPUM 29167	570	7	3.64	1.40	2.60	3.64	1.40	2.60
		IPUM 29169	404	8	3.26	-	-	2.84	-	-
		IPUM 29171	476	6	3.40	-	-	-	-	-
		IPUM 29177	570	6	3.36	1.53	2.20	-	-	-
		IPUM 29192	550	4	2.39	1.18	2.03	-	-	-
		IPUM 29199	740	4	2.72	1.50	1.81	-	-	-
		IPUM 29202	620	4	2.70	-	-	-	-	-
		IPUM 29203	711	4	3.15	1.26	2.50	-	-	-
		IPUM 29213	742	7	4.60	-	-	4.60	-	-
		IPUM 29218	494	6	3.16	1.47	2.15	-	-	-
		IPUM 29224	710	7	4.60	2.20	2.09	4.60	2.20	2.09
		IPUM 29226	509	7	4.87	1.81	2.69	4.87	1.81	2.69

Table 7. Values of the parameters measured on single specimens of *Alveolina* figured in the literature (*A. levantina*, *A.* aff. *levantina*, transitional forms *A. levantina-A. hottingeri*, *A. hottingeri* and *A. croatica*) or measured by Fornaciari, Giusberti and Papazzoni (2019) on *Alveolina postalensis*. Pd=proloculus diameter (μm); Ax=axial diameter (mm); Eq=equatorial diameter (mm); EI=elongation index; Ax7=axial diameter (mm) at the 7th whorl; Eq7=equatorial diameter (mm) at the 7th whorl; EI7=elongation index at the 7th whorl.
*Reported as "*Alveolina levantina* group". **Twin proloculi. From Fornaciari et al. (2019).

By means of the **Table 8**, the collected data have been summarized in order to allow an easy comparison between the new species and the similar species.

	A. levantina Hottinger, 1960					***A. aff. levantina*** Hottinger, 1960	**Transitional forms between *A. levantina* and *A. hottingeri***	***A. hottingeri*** Drobne, 1977	***A. croatica*** Drobne, 1977	***A. postalensis* n. sp.**
References	Hottinger (1960)	Hottinger (1974)	Drobne (1977)			Scotto di Carlo (1966)	Drobne (1977)	Drobne (1977)	Drobne (1977)	this work
			middle Cuisian	upper Cuisian	Cuisian to Lutetian					
Proloculus diameter (µm)	360-450 (1) 300-550 (2)	max. 1000 (1) 500-700 (2)	550 (1) 600 (2)	400-550 (1) 400 (2)	max. 500 (1) 400 (2)	350-450 (max. 600) (1) 400-600 (2)	350-650 (often 400-600) (1) 375-750 (2)	400-650 (1) 500-600 (2)	500-1000 (1) 600-1100 (2)	377-860 -
Number of whorls	- 6-12 (2)	max. 14 (1) 6-11 (2)	max. 10 (1) 7 (2)	max. 15 (1) 14 (2)	max. 13 (1) 13 (2)	- 7-10 (2)	7-14 (often 11-12) (1) 10-13 (2)	max. 13 (1) 10-13 (2)	- 7-13 (2)	max. 8 -
Axial diameter (mm)	max. 5.0 (1) 4.40-4.50 (2)	- 4.20-8.50 (2)	> 3.5 (1) 3.45 (2)	5.5-8.2 (1) 6.45 (2)	max. 9.0 (1) 6.60 (2)	- 5.80 (2)	6.5-14.3 (1) 8.50-10.25 (2)	7.3-15.2 (1) 6.30-14.01 (2)	- 6.70-9.00 (2)	2.32-5.42 -
Equatorial diameter (mm)	- 1.15-2.45 (2)	- 1.20-2.80 (2)	1.3 (1) 1.25 (2)	2.3-3.2 (1) 3.00 (2)	- 2.35 (2)	- 1.87-2.00 (2)	1.6-2.8 (1) 2.40.2.60 (2)	1.2-2.3 (1) 1.90-2.20 (2)	- 2.00-3.55 (2)	1.04-2.20 -
Elongation index EI	2.0-3.0 (1) 1.84-2.00 (2)	3.0-4.0 (1) 3.04-4.21 (2)	2.7-3.5 (1) 2.76 (2)	2.1-3.2 (1) 2.15 (2)	3.5 (1) 2.81 (2)	- 3.10 (2)	3.7-5.5 (1) 3.54-4.08 (2)	4.5-10.6 (1) 3.23-10.38 (2)	- 2.63-4.50 (2)	1.81-2.69 -
Description	Oval, slightly fusiform test; internal whorls elongated and pointed, external ones more rounded.	Fusiform test with rounded poles, more fusiform if tightly coiled and more oval otherwise.	Elongated and tightly coiled test, external chamberlets higher than wide.	Fusiform test, 10 to 15 whorls, younger whorls more tightly coiled and elongated than the older ones.	Test tightly coiled in all the stages.	Fusiform test, large and ovoidal or subrectangular chamberlets, sometimes larger in the first whorls, many whorls, elongated.	Very elongated test, first 4-7 whorls very tight and with very small chamberlets, very frequent additional chamberlets.	Fusiform test with elongated from the first whorls, chamberlets becoming larger towards the periphery.	Ovoidal test with rounded poles, elongated first whorls, tight spire, subrectangular chamberlets.	Ovoidal test with rounded poles, elongation increasing since the first whorls, tight spire, rounded to subrectangular chamberlets, distinctly larger chamberlets in the first whorl.

Table 8. Comparison among the megalospheric form of *A. levantina*, *A*. aff. *levantina*, transitional forms *A. levantina*-*A. hottingeri*, *A. hottingeri*, *A. croatica* and *A. postalensis* Fornaciari, Giusberti and Papazzoni (2019).
(1) Data reported in the descriptions by the authors (see the row of References).
(2) Data obtained by the measures of the figured specimens in the figures/plates of the authors (see the row of References).
From Fornaciari et al. (2019).

The plot of the axial diameter vs the equatorial diameter at the 7th whorl has been find useful to distinguish the new species from the other species under investigation **(Fig. 37)**.

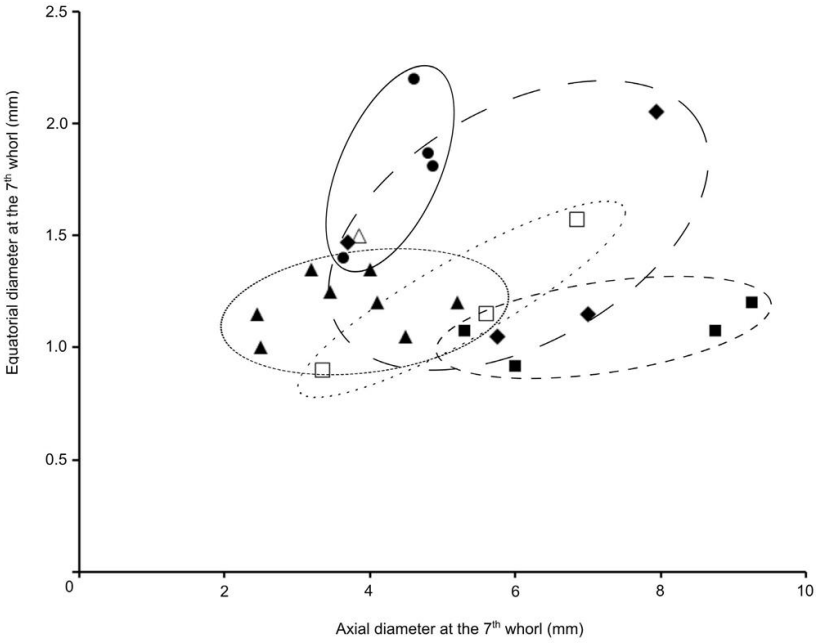

Fig. 37. Plot of axial vs equatorial diameters at the 7th whorl: ● *Alveolina postalensis* Fornaciari, Giusberti and Papazzoni 2019; ♦ *A. croatica* Drobne; ▲ *A. levantina* Hottinger; Δ *A.* aff. *levantina* Hottinger; □ transitional forms between *A. levantina* and *A. hottingeri*; ■ *A. hottingeri* Drobne. From Fornaciari et al. (2019).

It was also important to plot the elongation index vs the number of whorls (**Fig. 38**), corresponding to the ontogeny pattern, which is also clearly distinct.

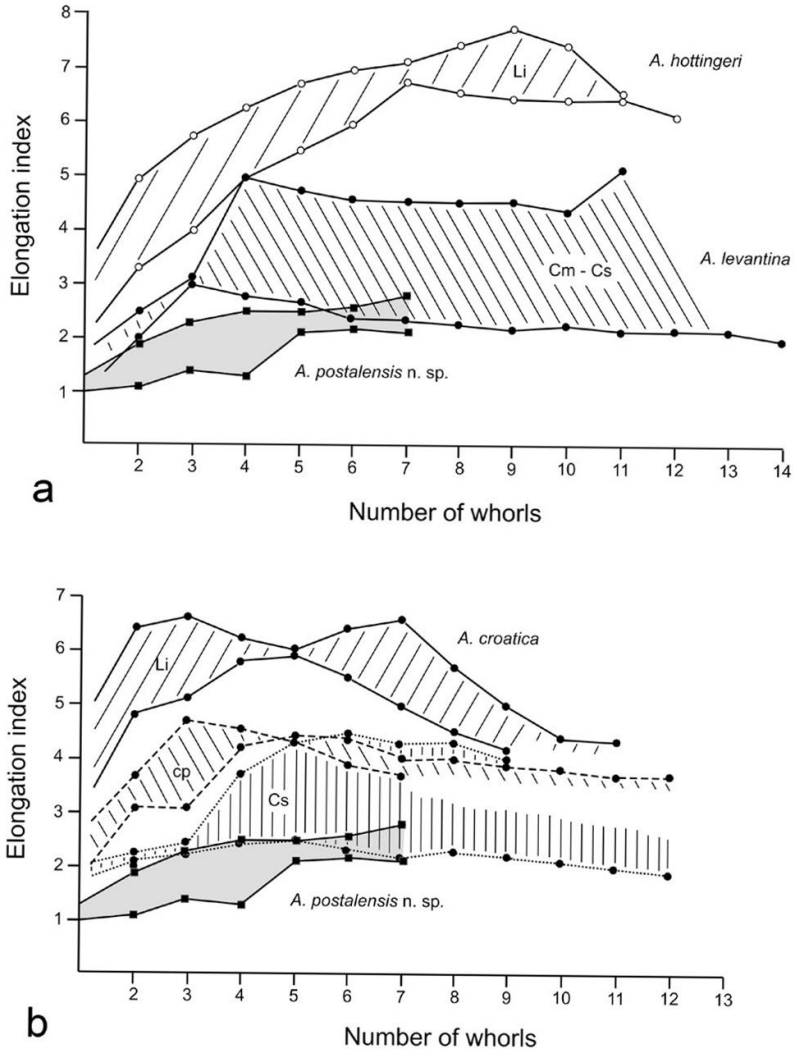

Fig. 38. a) Elongation index in successive whorls in *Alveolina postalensis* Fornaciari, Giusberti and Papazzoni 2019 compared with *A. hottingeri* and *A. levantina*.
b) Elongation index in successive whorls in *A. postalensis* Fornaciari, Giusberti and Papazzoni 2019 compared with *A. croatica*. The specimens are grouped according to their age. Cm=middle Cuisian; Cs=upper Cuisian; cp=transition Cuisian-Lutetian; li=lower Lutetian. From Fornaciari et al. (2019), modified from Drobne (1977).

6.3. DESCRIPTION OF *Alveolina postalensis* Fornaciari, Giusberti and Papazzoni 2019

After having identified the morphology of the new species, measured the main biometric features and assessed its differences in comparison with similar species by means of the above-mentioned analyses, Fornaciari et al. (2019) described the new species named *Alveolina postalensis*.

DISCLAIMER: the description of the new species in the following could not be considered in any way as a formal one or as an emendation to the original description of Fornaciari et al. (2019).

Systematics

The suprageneric classification of the Alveolinidae follows Loeblich & Tappan (1987).
Order Foraminiferida Eichwald, 1830
Suborder Miliolina Delage & Hérouard, 1896
Superfamily Alveolinoidea Ehrenberg, 1839
Family Alveolinidae Ehrenberg, 1839
Genus *Alveolina* d'Orbigny, 1826

Type species

Oryzaria boscii Defrance in Bronn 1825, designated according to the Bulletin of Zoological Nomenclature 1988, vol. 45, part 3, Opinion 1501. The lectotype of *Alveolina boscii* has been recently designated by Tréguier et al. (2019).

***Alveolina postalensis* Fornaciari, Giusberti and Papazzoni, 2019**

p. 1960 *Alveolina levantina* n. sp. - Hottinger, p. 155, pl. 10, fig. 11; non pl. 10, fig. 13.
p. 1966 *Alveolina* (*Alveolina*) aff. *levantina* Hottinger - Scotto di Carlo, p. 72, tav. 58 [10], fig. 1; tav. 59[11], figs 1, 3-4; tav. 60 [12], figs. 1-2; non tav. 58 [10], figs. 2-3; non tav. 59 [11], fig. 2; non tav. 60 [12], fig. 3.
v. 2006 *Alveolina* aff. *croatica* - Papazzoni & Trevisani, p. 30.
v. 2013 *Alveolina* aff. *croatica* - Papazzoni et al., p. 47.
v. 2017b *Alveolina* aff. *croatica* - Papazzoni et al., p. 9-10.
v. 2019 *Alveolina postalensis* – Fornaciari et al., p. 187-199, figs. 3, 5-7, tab. 1-2, appendix.

Etimology: the name derives from Monte Postale section, where most of the specimens come from and which has been elected type locality.

Type level and type locality: *Alveolina* limestones from the upper Ypresian (middle Cuisian) SB11 Zone of Monte Postale (Vicenza Province, northern Italy), coordinates 45°36'06.2"N, 11°13'18.9"E.

Holotype: IPUM 29212, specimen in thin section obtained from the sample MPO0307, located 24 m above the base of the section in Papazzoni et al. (2017b). Repository: "Inventario Paleontologia Università di Modena e Reggio Emilia" (IPUM) at the Dipartimento di Scienze Chimiche e Geologiche, Università di Modena e Reggio Emilia, Italy.

Paratypes: All figured paratypes (seven specimens) are illustrated in **Fig. 40** (b-h). They are IPUM 29174, IPUM 29213, IPUM 29218-29219, IPUM 29226 (Monte Postale section) and IPUM 29165-29166 (Pesciara section). The unfigured paratypes (sixty-six specimens) are listed here below:

- from the Pesciara tuffs: IPUM 29155-29158.
- from the Pesciara section: IPUM 29159-29164.
- from the Pesciara core: IPUM 29167.
- from the Monte Postale section: IPUM 29168- 29173, IPUM 29175-29211, IPUM 29214-29217, IPUM 29220-29225, and IPUM 29227-29228.

Diagnosis: The diagnosis of *Alveolina postalensis* Fornaciari et al. 2019 is referred to megalospheric specimens, as no microspheric ones were found. The megalosphere is large and it has a diameter between 377 and 860 μm. The test is large, fusiform, with ovoidal to fusiform whorls. In the first whorl, the chamberlets are larger and more rounded than in the successive ones, where they are smaller and higher than wide. The whorls are more and more elongated towards the periphery, becoming from ovoidal to fusiform shaped and with rounded poles. The number of the whorl is low, maximum eight (see Table 8).

Description: *Alveolina postalensis* Fornaciari et al. 2019 is characterised by a fusiform test. The proloculus is rounded or slightly oval. The chamberlets of the first whorl are large and subsphaerical and become smaller and less rounded in the two following whorls and grow again becoming ovoidal to almost subrectangular in the most peripheral ones. The whorls are characteristically elongated since the second-third whorl and they have rounded poles at the adult stage. The biometrical features are:

- proloculus diameter: from 377 to 860 μm (mean value: 568 μm);
- mean axial diameter: 3.56 mm;
- mean equatorial diameter: 1.49 mm;
- mean elongation index (EI): 2.28.

For detailed measurements and ranges, see Table 6 and 8.

Stratigraphic and geographic distribution: *Alveolina postalensis* Fornaciari et al. 2019 has been described in the Monte Pesciale and Pesciara sections, both ascribed to the SB11 Zone (Serra-Kiel et al. 1998) by Papazzoni et al. (2017b) and Papazzoni and Trevisani (2006), respectively (**Fig. 39**). *A. postalensis*, according to the synonymy list, is occurring also in Dalmatia (Velusič, lower Lutetian?; Hottinger, 1960) and Gargano, southern Italy (middle Cuisian, SB11; Scotto di Carlo, 1966).

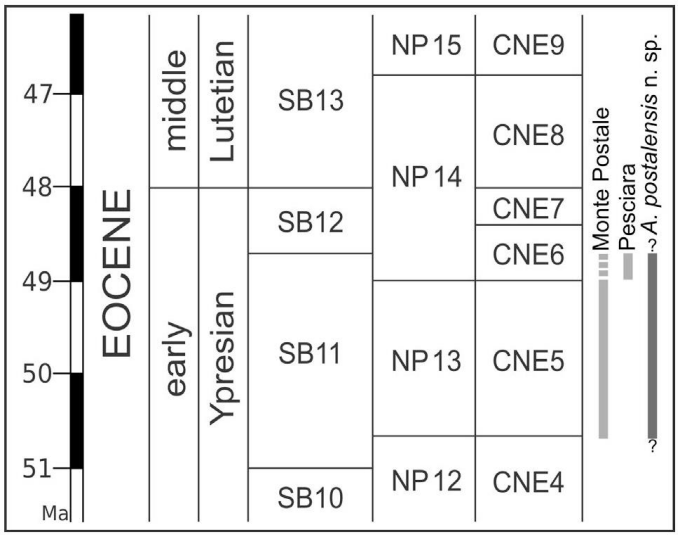

Fig. 39. Biochronostratigraphic framework of the Monte Postale and Pesciara sites, incorporating the SB zones by Serra-Kiel et al. (1998) and calcareous nannoplankton (NP zone by Martini 1971 and CNE by Agnini et al. 2014) zones. Time scale after Vandenberghe et al. (2012). From Fornaciari et al. (2019).

The available data don't allow to exclude the possibility of a biostratigraphic range wider than the SB11. As the Monte Postale and Pesciara sections lack of sediments from the SB10 and the SB12, new sections should be investigated to clear this point.

Nomenclatural remarks: The name *Alveolina Postalensis,* along with *Alveolina Stachei*, *Alveolina Bolcensis*, and *Alveolina Vallecencis*, was originally proposed by Munier-Chalmas (1891, pp. 37, 39, 43, 47, 86) for new species coming from the Monte Postale and Monte Valleco (*sic*) sites (Munier-Chalmas, 1891, p. 39). As the author did not provide any description, reference or indication for these species not complying to the Art. 12 of the ICZN (1999), all these nominal species are *nomina nuda*, hence unavailable names. However, according to the ICZN (1999) Glossary (*nomen nudum*), an unavailable name may be made available later for the same or a different concept. Therefore, Fornaciari et al. (2019) decided to resurrect the name *Alveolina postalensis*, never used for any species after Munier-Chalmas (1891).

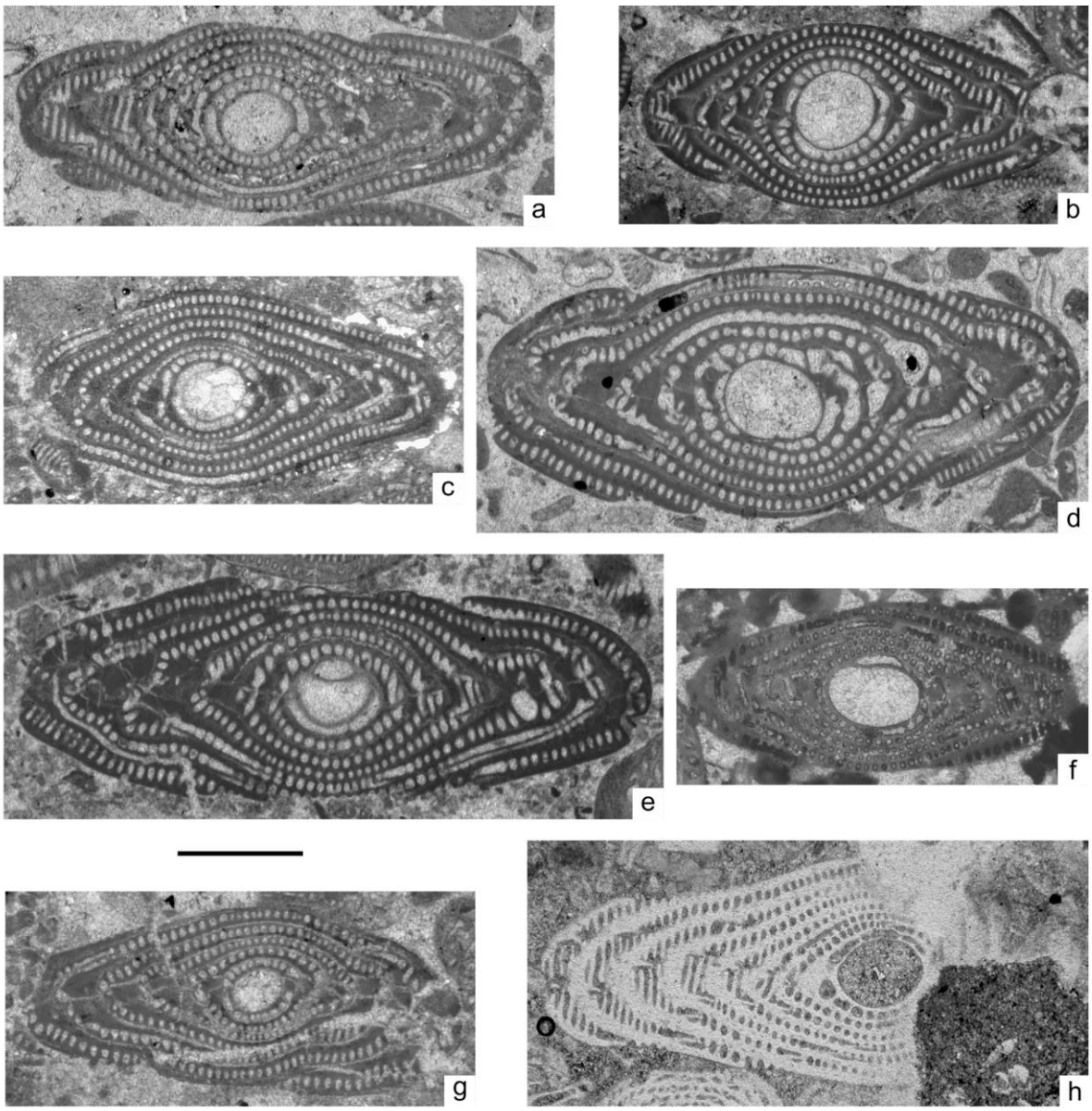

Fig. 40. *Alveolina postalensis* Fornaciari, Giusberti and Papazzoni, 2019. Axial or subaxial sections of megalospheric specimens: a) IPUM 29212 – holotype, Monte Postale sample MPO0307; b) IPUM 29219 – paratype, Monte Postale sample PST 1434; c) IPUM 29218 - paratype, Monte Postale sample MPO0305; d) IPUM 29213 - paratype, Monte Postale sample MPO0307; e) IPUM 29226 - paratype, Monte Postale sample PST1429; f) IPUM 29166 - paratype, Pesciara sample BOL0203; g) IPUM 29174 - paratype, Monte Postale sample PST1315; h) IPUM 29165 - paratype, Pesciara sample BOL0203. All 20x; scale bar = 1 mm. All figured specimens are stored at the Dipartimento di Scienze Chimiche e Geologiche, Università di Modena e Reggio Emilia, Modena, Italy. From Fornaciari et al. (2019).

6.4. COMPARISON WITH RELATED SPECIES

Alveolina postalensis Fornaciari et al. 2019 shares similarities with the species belonging to the *A. levantina* group, composed by *A. levantina, A.* aff. *levantina, A. hottingeri*, and *A. croatica*, according to Hottinger (1960) and Drobne (1977). This group is composed of alveolines with a large size, a large ovoidal proloculus and whorls tightly coiled at the juvenile stage and laxer at the adult one.

According to the considerations exposed in the subchapter 6.2, *Alveolina postalensis* Fornaciari et al. 2019 is definitely distinct from all the other species of the *A. levantina* group.

6.4.1. Comparison with *A. levantina* Hottinger, 1960

Alveolina postalensis and *A. levantina* show similarities in the proloculus size, chamberlets shape and size. Both the species have a large ovoidal proloculus and chamberlets increasing in size and becoming subrectangular in the outermost whorls. However, the chamberlets of the juvenile stage allow to clearly distinguish the two species, as in *A. postalensis* they are larger in the first whorls than in the subsequent ones (with the exception of the outermost ones), whereas in *A. levantina* there is not such trend in the chamberlets size.

Furthermore, *A. levantina* is much more elongated (max EI at the 7th whorl = 4.33; max EI for the entire test = 4.21) than *A. postalensis* n. sp. (max EI at the 7th whorl = 2.69).

6.4.2. Comparison with *A.* aff. *levantina* Hottinger, 1960

Some of the specimens grouped by Scotto di Carlo (1966) under the name of *Alveolina* aff. *levantina*, have been identified as *A. postalensis* by Fornaciari et al. 2019 (see synonymy list). The size of the proloculus (350-650 μm), the axial diameter at the 7th whorl (max 3.86 mm), the equatorial diameter at the 7th whorl (max 1.50 mm) and the EI at the 7th whorl (max 2.57) are consistent with those of *A. postalensis* n. sp. (see Fig. 37). The only difference is in the number of whorls, that in the specimens by Scotto di Carlo (1966) may be higher, up to eleven, instead of eight.

6.4.3. Comparison with the transitional forms between *A. levantina* and *A. hottingeri* (from Drobne 1977)

Drobne (1977, p. 57) reported some slightly elongated specimens from the Ypresian-Lutetian transition of Picán and Boljunsko Polje (Istria) as transitional forms between *A. levantina* and *A. hottingeri*. However, they are both larger and more elongated as compared to *A. postalensis.*

6.4.4. Comparison with *A. hottingeri* Drobne, 1977

Alveolina postalensis and *A. hottingeri* are similar in the proloculus and in the chamberlets. The proloculus, ovoidal for both the species, is 377-860 μm for the first and 400-650 μm for the latter.

The chamberlets show a similar trend in shape and size. However, the two species can be distinguished for their overall size and elongation, comparing the 7th whorl: *A. hottingeri* minimum axial diameter at the 7th whorl is 5.30 mm, whereas *A. postalensis* at the 7th whorl reaches 4.80 mm; also, *Alveolina hottingeri* is much more elongated (EI = 4.93-8.14) than *A. postalensis* (EI = 2.36-2.69) at the 7th whorl. Furthermore, the distance between successive whorls in the polar region is broadening faster in *A. hottingeri* as compared to *A. postalensis.*

6.4.5. Comparison with *A. croatica* Drobne, 1977

As for the comparison with *Alveolina hottingeri, A. postalensis* has a similar trend in the chamberlets shape and size with *A. croatica* as well. In this case, the main difference is in the general size and in the size of the proloculus. *A. postalensis* is much smaller (maximum axial diameter at the 7th whorl of 4.80 mm; see Fig. 5) than *A. croatica* (7.95 mm) and less elongated (maximum EI = 2.69 for *A. postalensis*; 6.09 for *A. croatica*; see Fig. 38b). The proloculus of *A. postalensis* (377-860 μm) is smaller as well (500-1000 μm) than in *A. croatica*. However, *A. croatica* is the more similar species to *A. postalensis* in the morphology.

6.5. PHYLOGENETIC POSITION OF *Alveolina postalensis*

The data collected allowed Fornaciari et al. (2019) to formulate a phylogenetic hypothesis for *Alveolina postalensis*, connected to the *Alveolina levantina* group hypothesis of phylogeny by Drobne (1977).

Drobne (1977) distinguished two parallel lineages in this group. One lineage was represented only by *A. croatica*, and the other one was composed of *A. levantina* and A. *hottingeri*, connected by transitional forms, ranging from the middle Cuisian to the lower Lutetian. This phylogenetic hypothesis was based on the morphologic features. *A. croatica* was distinguished from the phyletic line *A. levantina-A. hottingeri* because of its faster growth, the more irregular spire and the large size of the first whorl's chamberlets. *A levantina* and *A. hottingeri* were connected by transitional forms on the same phyletic line because of their size, smaller for *A. levantina* and progressively larger, and because of their shape, from more pointed poles towards a more pronounced elongation (Drobne 1977)

Alveolina croatica is the species more similar to *A. postalensis*, having a larger proloculus and larger overall size (see subchapter 8.2.5) but they have a different ontogenetic development which can be observed by comparing the upper Cuisian specimens of *A. croatica* with *A. postalensis*. For formulating the phylogenetic hypothesis, Fornaciari et al. (2019) have taken into account the general evolutionary trend observed in larger foraminifera bringing towards forms of larger size and with a larger proloculus, according to the Cope's rule (e.g. Guex, 2003; Benedetti & Pignatti, 2009). This trend has been particularly observed in the alveolinids (e.g., Hottinger, 1960, 1974; Drobne, 1977). On

the basis of this, *A. postalensis* is thought to be the possible ancestor of *A. croatica* (**Fig 41**), because of its morphology and stratigraphic range.

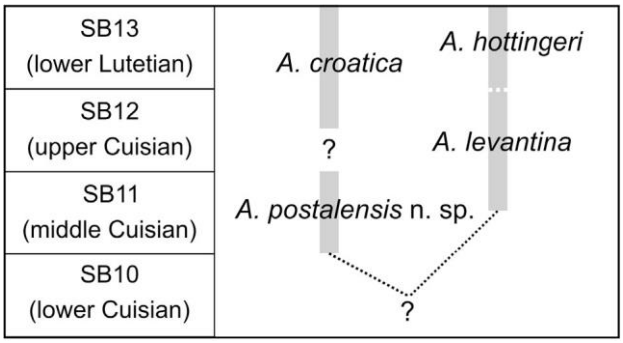

Fig. 41. Phylogenetic scheme proposed for *Alveolina postalensis* Fornaciari, Giusberti and Papazzoni 2019 within the *Alveolina levantina* group. From Fornaciari et al. (2019).

In this evolutionary scenario, inside the *A. levantina* group, there are two parallel phyletic lines. One is composed by *A. postalensis* in the SB11 connected with *A. croatica* in the upper SB12 and SB13 (leaving a short gap in the lower SB12, about which no data are available at present). The other one is composed by *A. levantina* from the upper SB11 and in the SB12, connected to *A. hottingeri* in the SB13. These two phyletic lines possibly share a still unknown common ancestor.

7. CONCLUSIONS

7.1. CONCLUSIONS ON THE THREE PALEOCENE SECTIONS

It should be first remarked that this thesis applies an innovative biostratigraphic approach which allows to overcome the limits of the Oppelzones. As seen, the SB zones are substantially Oppelian-zones, being defined by their assemblages and not by their lower and upper limits. This implies a certain degree of subjectivity in the definition of their boundaries and leaves undefined transition intervals. Despite these features, which make them not suitable for high-resolution stratigraphy, the SB zones have been used for twenty-years as major biostratigraphic tool in shallow-water environments. Recently, some advancements in biostratigraphy have been reached and some additional criteria reducing the subjectivity and improving the precision in the calibration need to be applied to the SB zones (Pignatti and Papazzoni 2017).

This thesis introduces an approach based on an integrated LF and calcareous nannofossils biostratigraphy which correlates the first occurrences (FO) of LF marker species with calcareous nannofossil bio-horizons and with the magnetostratigraphy. This method, if further developed (e.g., with planktonic foraminifera and isotope stratigraphy) and applied, could help in overcoming the undefined transition intervals between the SB zones and achieving a reliable system of biozones.

In particular, the studied sections of Tabiago, Ardo and Monte Giglio, even if lacking homotaxia, offer the chance to directly correlate the larger foraminiferal biozones with the calcareous nannofossil ones. This work set the basis for identifying the most reliable and precise bio-horizons corresponding to the boundaries of the SB zones of the Paleocene. In the investigated sections, the most significant bio-horizons are the following:

- for the SB1: primary bio-horizon: the last appearance of the Cretaceous LF (orbitoidids); additional bio-horizon: *Thalmannita* aff. *madrugaensis* FO;
- for the SB2: primary bio-horizon: *Kayseriella decastroi* FO; additional bio-horizons: *Cuvillierina sireli* FO, *Elazigina dienii* FO, *Ornatononion moorkensii* FO*, Paralockhartia eos* FO and *Slovenites praecursorius* FO, subfamily Miscellaniteinae FO;
- for the SB3: primary bio-horizon: first appearance of the orthophragmines; additional bio-horizons: *Ranikothalia* sp. FO and *Kathina aquitanica* FO;
- for the SB4: *Assilina* sp. FO, *Assilina azilensis* FO and/or *Daviesina salsa* FO.

Further studies are required in the Neothethys to test whether these bio-horizons are synchronous with other sections or not: in case of positive result, the first occurrences recorded in this work could be considered as first appearances and therefore they could be used to erect biochronozones in a standard biochronostratigraphic scale.

From the integrated larger foraminifera and calcareous nannofossils biostratigraphy obtained and correlated with the magnetostratigraphy by Dallanave et al. (2012), it is possible to calibrate the boundaries of the SB zones of the Paleocene as follows:

- boundary SB1/SB2: in the uppermost CNP3 (Agnini et al. 2014), in the upper NP3 (Martini 1971) and in the middle of the Chron C28n;
- boundary SB2/SB3: in the upper CNP7 (Agnini et al. 2014) and in the upper NP5 (Martini 1971);
- boundary SB3/SB4: it approximates the boundaries CNP10/CNP11 (Agnini et al. 2014) and NP8/NP9 (Martini 1971).

The most important outcome of this thesis is a new integrated biostratigraphic scheme for the SB zones of the lower Paleogene of the Western Tethys (Fig. 34). The boundary SB1/SB2 turns out to be about 2 Ma lower than supposed by Serra-Kiel et al. (1998). This suggests that the beginning of the generic diversification of the larger foraminifera after the K/Pg crisis started much earlier than previously thought. The positions of the other boundaries are confirming the former correlation scheme by Serra-Kiel et al. (1998). It should be remarked that the marker species of the SB1 Zone indicated by Serra-Kiel et al (1998) were not retrieved. Furthermore, the new data about the stratigraphic distribution of several species allow us to update the ranges reported by Hottinger (2009, 2014) (Figs. 31, 32).

The approach of the integrated biostratigraphy also allow to better understand the relation between their evolution and paleoenvironmental events. According to our data, for example, the first occurrence of the orthophragminids firmly established at the base of the SB3 is below the base of the *Heliolithus kleinpelli*, which marks the Early Late Paleocene Event. Therefore, the origin of this taxon doesn't seem correlated to it. Further investigations are required to assess the possible link of other larger foraminiferal evolutionary events on paleoenvironmental perturbations in the Paleocene.

Furthermore, in this thesis the graphic method of the Shaw Diagram has been applied to the LF biostratigraphy for the first time. It resulted into an interesting comparison between the Tabiago and the Ardo section, leading to the observation that the recorded bio-horizons are synchronous and allowing to calculate the average sedimentation rate and the ages of the bioevents. The first occurrence of *Kayseriella decastroi* turned out to be at 63.78 (±0.047) Ma, of the orthophragminids at 60.14 (±0.178) Ma and of *Assilina azilensis* at 57.17 Ma. Such detailed dating of the LF events has never been considered possible before.

A final consideration should be added. All the sections (Tabiago, Ardo and Monte Giglio) studied for the biostratigraphy of the Paleocene are hemipelagic ones and the larger foraminifera have been studied in the turbidites. This allowed to perform the direct correlation between the LF and the calcareous nannofossils. However, there are some intrinsic problems. One is the possible gap between the time of the deposition of the LF and the time of the deposition of the turbidites containing them. This implies that the bio-horizons recorded for the LF might be even lower. Another issue is the fact

that the recorded association might not be representative of the real associations due to their transport. Unfortunately such problems cannot be overcome by the present study and further investigations are required to try to solve them.

7.2. CONCLUSIONS ON THE LOWER EOCENE *Alveolina postalensis*

The analyses on a morphotype of *Alveolina* differing from any known species in the assemblages of Monte Postale, Pesciara and the volcanoclastites of the Bolca site allowed to identify and describe a new species, *Alveolina postalensis* Fornaciari, Giusberti and Papazzoni 2019. This species has been described by means of morphologic and biometric features, which have been compared to those of the related species *A. levantina*, *A. hottingeri* and *A. croatica*.

Alveolina postalensis is characterized by a fusiform test whose axial diameter ranges from 2.32 to 5.42 mm, the equatorial diameter from 1.04 to 2.20 mm and the EI from 1.81 to 2.69. The proloculus is rounded or slightly ovoidal, included between 377 and 860 µm. The first whorl around the proloculus has peculiar large chamberlets. The chamberlets' size decrease in the successive whorls but toward the adult stage grow again, becoming large and almost subrectangular in the outermost whorl. The test become elongated from the second or the third whorl. The number of whorls is usually low: specimens with maximum eight whorls have been found.

On the base of the co-occurring LF, *Alveolina postalensis* has been ascribed to the SB11 (middle Cuisian, upper Ypresian, lower Eocene). This species is therefore a good marker for the SB11 but further investigations are requested, on different outcrops, to evaluate its possible presence below and above this biozone.

The identification and the description of a new species in the Monte Postale and Pesciara outcrops, studied for their LF assemblages since the beginning of the last century, demonstrate that there's still a lot of systematic work to do on the LF and that new marker species may be discovered, even in assemblages studied in detail since several years.

REFERENCES

Acar, S., 2019. Selandian benthic foraminiferal assemblages of the Southwestern Burdur (South of Lake Yarişh, Western Turkey) and some taxonomic revisions. Bulletin of the Mineral Research and Exploration **158**, 49-119.

Accordi, G., Carbone, F., Pignatti, J., 1998. Depositional history of a Paleogene carbonate ramp (Western Cephalonia, Ionian Islands, Greece). Geologica Romana **34**, 131– 205.

Agnini, C., Fornaciari, E., Giusberti, L., Backman, J., Capraro, L., Grandesso, P., Luciani, V., Muttoni, G., Rio, D., Tateo, F., 2005. The Early Paleogene of the Valbelluna (Venetian Southern Alps). Fieldtrip Guidebook ODP Leg 208 Post-Cruise Meeeting. Cooperativa Libraria Editrice Università di Padova (CLEUP), Padova. 32 pp.

Agnini, A., Fornaciari, E., Raffi, I., Catanzariti, R., Pälike, H., Backman, J., Rio, D., 2014. Biozonation and biochronology of Paleogene calcareous nannofossils from low and middle latitudes. Newsletter on Stratigraphy **47** (2), 131-181.

Agnini, C., Fornaciari, E., Rio, D., Tateo, F., Backman, J., Giusberti, L., 2007. Responses of calcareous nannofossil assemblages, mineralogy and geochemistry to the environmental perturbations across the Paleocene/Eocene boundary in the Venetian Pre-Alps. Marine Micropaleontology **63**, 19-38.

Agnini, C., Spofforth, D.J.A., Dickens, G.R., Rio, D., Pälike, H., Backman, J., Muttoni, G., Dallanave, E., 2016. Stable isotope and calcareous nannofossil assemblage record of the late Paleocene and early Eocene (Cicogna section). Climate of the Past **12**, 883-909.

Alegret, L. and Thomas, E., 2004. Benthic foraminifera and environmental turnover across the Cretaceous/Paleogene boundary at Black Nose (ODP Hole 1049C, Northwestern Atlantic). Palaeogeography, Palaeoclimatology, Palaeoecology **208** (1-2), 59-83.

Ali, J.R. and Joelley, D.W., 1966. Chronostratigraphic framework for the Thanetian and lower Ypresian deposits of SE England. Geological Society of London Special Publication **101**, 129-144.

Alvarez, L.W., Alvarez, W., Asaro, E., Michel, H.V., 1980. Extraterrestrial cause for the Cretaceous-Tertiary extinction. Science **208**, pp. 1095-1108.

Arenillas, I., Molina, E., Ortiz, E. and Schmitz B., 2008. Foraminiferal and $\delta^{13}C$ isotopic event-stratigraphy across the Danian-Selandian transition at Zumaya (northern Spain): chronostratigraphic implications. Terra Nova **90**, 38-44.

Aubry, M.P., 1984. Handbook of Cenozoic Calcareous Nannoplankton, book 1, Ortholithae (Discoaster). American Museum of Natural History Micropaleontology Press, New York. 263 pp.

Aubry, M.P., 1988. Handbook of Cenozoic Calcareous Nannoplankton, book 2, Ortholithae (Holococcoliths, Ceratoliths, Ortholiths and Other). American Museum of Natural History Micropaleontology Press, New York. 279 pp.

Aubry, M.P., 1989. Handbook of Cenozoic Calcareous Nannoplankton, book 3, Ortholithae (Pentaliths and Other), Heliolithae (Fasciculiths, Sphenoliths and Others). American Museum of Natural History Micropaleontology Press, New York. 279 pp.

Aubry, M.P., 1990. Handbook of Cenozoic Calcareous Nannoplankton, book 4, Heliolithae (Helicoliths, Cribriliths, Lopadoliths and Other). American Museum of Natural History Micropaleontology Press, New York. 381 pp.

Aubry, M.P., 1999. Handbook of Cenozoic Calcareous Nannoplankton, book 5, Heliolithae (Zygoliths and Rhabdoliths). American Museum of Natural History Micropaleontology Press, New York. 368 pp.

Aubry, M.-P., Ouda, K., Dupuis, C., Berggren, W.A., Van Couvering, J.A., the members of theWorking Group on the Paleocene/Eocene Boundary, 2007. The Global standard Stratotype-section and Point (GSSP) for the base of the Eocene series in the Dababiya section (Egypt). Episodes **30**, 271-286.

Baceta, J.I., Pujalte, V., Serra-Kiel, J., Robador, A., Orue-Etxebarria, X., 2004. El Maastrichtiense final, Paleoceno e Ilerdiense inferior de la Cordillera Pirenaica. In: Vera, J.A. (Ed.), Geología de España. Sociedad Geologíca de España-Instituto Geológico y Minero de España, Madrid, 308-313.

Backman, J., Shackleton, N.J., 1983. Quantitative biochronology of Pliocene and early Pleistocene calcareous nannoplankton from the Atlantic, Indian and Pacific Oceans. Marine Micropaleontology **8**, 141–170.

Barbieri, G., De Zanche, V., Medizza, F., Sedea, R., 1982. Considerazioni sul vulcanesimo terziario del Veneto occidentale e del Trentino meridionale. Rendiconti della Società Geologica Italiana **4**, 267-270.

Barbieri, G., De Zanche, V., Sedea, R., 1991. Vulcanismo paleogenico ed evoluzione del semigraben Alpone-Agno (Monti Lessini). Rendiconti della Società Geologica Italiana **14**, 5-12.

Beckmann, J.P., Bolli, H.M., Kleboth, P., Proto Decima, F., 1982. Micropaleontology and biostratigraphy of the Campanian to Paleocene of the Monte Giglio section, Bergamo Province, Italy. Memorie di Scienze Geologiche già Memorie degli Istituti di Geologia e Mineralogia dell'Università di Padova **XXXV**, 91-172.

Benedetti, A., 2015. The new family Ornatorotaliidae (Rotaliacea, Foraminiferida). Micropaleontology **61** (3), 231-236.

Benedetti, A., Di Carlo, M., Pignatti, J., 2011. New Late Ypresian (Cuisian) Rotaliids (Foraminiferida) from Central and Southern Italy and Their Biostratigraphic Potential. Turkish Journal of Earth Sciences **20**, 701-719.

Benedetti, A., Marino, M., Pichezzi, M.R., 2018. Paleocene to lower Eocene larger foraminiferal assemblages from central Italy: new remarks on biostratigraphy. Rivista Italiana di Paleontologia e Stratigrafia **124** (1), 73-90.

Benedetti, A., Pignatti, J., 2009. *Caudammina gutta*, a new species of Hormosinellidae (Foraminiferida) from the Rupelian of Sicily (Italy). Rivista Italiana di Paleontologia e Stratigrafia **115**, 337-348.

Bentham, P. and Burbank, D.W., 1996. Chronology of Eocene foreland basin evolution along the western oblique margin of the South-Central Pyrenees. In: Friend, P.F., Dabrio, C.J. (Eds.). Tertiary Basin of Spain, chapter E, Cambridge University Press **11**, 144-152.

Berggren, W.A., Kent, D.V., Swisher III, C.C., Aubry, M.-P., 1995. A revised Cenozoic geochronology and chronostratigraphy. In: Berggren, W.A., Kent, D.V., Hardenbol, J. (Eds.). Geochronology, Time Scales and Global Stratigraphic Correlations. SEPM Special Publication **54**, 129-212.

Berggren, W.A. and Miller, K.G., 1988. Paleogene tropical planktonic foraminiferal biostratigraphy and magentobiochronology. Micropaleontology 34, 362-380.

Bernaola, G., Baceta, J.I., Orue-Etxebarria, X., Alegret, L., Martin-Rubio, M., Arostegui, J., Dinarès-Turell, J., 2007. Evidence of an abrupt environmental disruption during the mid-Paleocene biotic event (Zumaia section, western Pyrenees). Geological Society of America Bulletin **119**, 785–795.

Bernoulli, D., 1972. North Atlantic and Mediterranean Mesozoic facies: A comparison. In: Hollister C.D., Ewing, J.I. et al., Proceedings of Deep Sea Drilling Project, Initial Reports **11**, 301-871.

Bersezio, R., Fornaciari, M., Gelati, R., Napolitano, A., Valdisturlo, A., 1993. The significance of the Upper Cretaceous to Miocene clastic wedges in the deformation history of the Lombardian southern Alps. Geologie Alpine 1993 **69**, 3-20.

Bertotti, G., Picotti, V., Bernoulli, D., Castellarin, A., 1993. From rifting to drifting: tectonic evolution of the South-Alpine upper crust from the Triassic to the Early Cretaceous. Sedimentary Geology **86**, 53-76.

Bini, A., Bersezio, R., Tucci, G., Scardia, G., Rigamonti, I., Rossi, R., Ferliga, C., Carnati, S., Kovacs, M., Cislaghi, L., Salmineri, R., Redaelli, M., Isgrò, M., Strini, A., 2014. Note illustrative alla Carta Geologica d'Italia alla scala 1:50.000, Foglio 097 Vimercate. Regione Lombardia, 341 pp.

Bini, A., Sciunnach, D., Bersezio, R., Scardia, G., Tomasi, F., Beretta, G. P., Carcano, C., Gelati, R., Miletta, S., Premoli Silva, I., Rogledi, S., Rovida, A., Strini, A., Stucchi, M., Tremolada, F., 2013. Note illustrative della Carta Geologica d'Italia alla scala 1:50.000, Foglio 096 Seregno. Regione Lombardia, 189 pp.

Blow, W.A., 1969. Late Middle Eocene to Recent planktonic foraminiferal biostratigraphy. Proceedings of the 1st International Conference on Planktonic Microfossils, Geneva **1**, 199-422.

Bolli, H.M., Cita, M.B., 1960a. Upper Cretaceous and Lower Tertiary planktonic Foraminifera from the Paderno d'Adda section, Northern Italy. Proceedings of the XXI International Geological Congress **5**, 150-161.

Bolli, H.M., Cita, M.B., 1960b. *Globigerina* and *Globorotalia* del Paleocene di Paderno d'Adda (Italia). Rivista Italiana di Paleontologia e di Stratigrafia **66** (3), 361-408.

Bornemann, A., Schulte, P., Sprong, J., Steurbaut, E., Youssef, M., Speijer, R.P., 2009. Latest Danian carbon isotope anomaly and associated environmental change in the southern Tethys (Nile Basin, Egypt). Journal of Geological Society **166** (6), 1135–1142, doi:10.1144/0016-76492008-104.

Bosellini, A., Carraro F., Corsi, M., De Vecchi, G.P., Gatto, G.O., Malaroda, R., Sturani, C., Ungaro, S., Zanettin, B., 1967. Note Illustrative della Carta Geologica d'Italia scala 1: 100.000, Foglio 49 Verona. Servizio Geologico d'Italia.

Bosellini, A., 1989. Dynamics of Tethyan carbonate platforms. In: Crevello, P.D., Wilson, J.L., Sarg, J.F., Read, J.F. (Eds.), Controls on Carbonate Platform and Basin Platform. S.E.P.M. Special Publication **44**, 3-13.

Bosellini, A., Masetti, D., Sarti, M., 1981. A Jurassic "tongue of the ocean" infilled with oolitic sands: the Belluno Trough, Venetian Alps, Italy. Marine Geology **44**, 59-95.

Boussac, J., 1911. Etudes stratigraphiques et paléontologiques sur le Nummulitique alpin. Essai sur l'évolution des Nummulites. Mémoires pour servir à l'explication de la Carte géologique détaillée de la France. Imprimerie Nationale, Paris.

Bralower, T. J., Premoli Silva, I., Malone, M.J., 2002. New evidence for abrupt climate change in the Cretaceous and Paleogene: An Ocean Drilling Program expedition to Shatsky Rise, northwest Pacific. GSA Today **12**, 4-10.

Bralower, T.J., Premoli Silva, I., Malone, M.J., 2006. Leg 198 synthesis: A remarkable 120 m.y. record of climate and oceanography from Shatsky Rise, northwest Pacific Ocean. In: Bralower, T.J., Premoli Silva, I., Malone, M.J. (Eds.), Proceedings of the Ocean Drilling Program, Scientific Results **198**, 1-47.

Bronn, H.G., 1825. System der urweltlichen Pflanzenthiere, 47 pp. J.C.B. Mohr, Heidelberg.

Bukry, D., 1973. Low-latitude coccolith biostratigraphic zonation. Initial Reports of the Deep Sea Drilling Project **15**, 685–703.

Bukry, D., 1975. Coccolith and silicoflagellate stratigraphy, northwestern Pacific Ocean, Deep Sea Drilling Project Leg 32. Initial Reports of the Deep Sea Drilling Project **32**, 677–701.

Cahuzac, B. and Poignant, A., 1997. Essai de biozonation de l'Oligo-Miocène dans les bassins européens à l'aide des grands foraminifères néritiques. Bulletin de la Société géologique de France **168** (2), 155-169.

Cande, S.C., Kent, D.V., 1995. Revised calibration of the geomagnetic polarity time scale for the Late Cretaceous and the Cenozoic. Journal of Geophysical Research 100, 6093-6096.

Cavelier, C., 1975. Le diachronisme de la zone à *Ericsonia subdisticha* (Nannoplancton) et la position de la limite Éocène-Oligocène en Europe et en Amérique du Nord. Bulletin du Bureau de recherches géologiques et minières **2** (IV) 3, 221-225, 13 tabl.

Cavelier, C. and Pomerol, C., 1986. Stratigraphy of the Paleogene. Bulletin de la Société géologique de France **8** (2), 255-265.

Channell, J.E.T. and Medizza, F., 1981. Upper Cretaceous and Paleogene magnetic stratigraphy and biostratigraphy from the Venetian (Southern) Alps. Earth and Planetary Science Letters **55**, 419-432.

Cita, M.B., Premoli-Silva, I., Toumarkine, M., Bolli, M.H., Luterbacher, H.P., Mohler, H.P., Schaub, H., 1968. Le Paléocene et l'Éocène de Paderno d'Adda (Italie septentrionale). Mémoires du Bureau de Recherches géologiques et minières **58**, 611-627.

Coccioni, R., Catanzariti, R., Frontalini, F., Galbrun, B., Jovane, L., Montanari, A., Savian, J.F., Sideri, M., 2016. Integrated magnetostratigraphy, biostratigraphy, and chronostratigraphy of the Paleogene pelagic succession at Gubbio (central Italy). In: Menichetti, M., Coccioni, R., Montanari, A., (Eds.), The Stratigraphic Record of Gubbio: Integrated Stratigraphy of the Late Cretaceous–Paleogene Umbria-Marche Pelagic Basin. Geological Society of America Special Papers **524**, 139-160.

Coccioni, R., Frontalini, F., Bancalà, G., Fornaciari, E., Jovane, L., Sprovieri, M., 2010. The Dan-C2 hyperthermal event at Gubbio (Italy): Global implications, environmental effects, and cause(s). Earth and Planetary Science Letters **297**, 298-305. doi: 10.1016/j.epsl.2010.06.031

Cohen, K.M., Finney, S.C., Gibbard, P.L., Fan, J.-X., 2013. The ICS International Chronostratigraphic Chart. Episodes **36** (3), 199-204.

Consorti, L., Köroğlu, F., 2019. Maastrichtian-Paleocene larger Foraminifera biostratigraphy and facies of the Şahinkaya Member (NE Sakarya Zone, Turkey): Insights into the Eastern Pontides arc sedimentary cover. Journal of Asian Earth Sciences 183, 103965. doi: 10.1016/j.jseaes.2019.103965

Consorti, L., Rashidi, K, 2018. A new evidence of passing the Maastrichtian-Paleocene boundary by larger benthic foraminifera: The case of *Elazigina* from the Maastrichtian Tarbur Formation of Iran. Acta Paleontologica Polonica **63** (3), 595-605.

Costa, V., Doglioni, C., Grandesso, P., Masetti, D., Pellegrini, G.B., Tracanella, E., 1996. Carta Geologica d'Italia alla scala 1: 50.000, Foglio 063 Belluno. Servizio Geologico d'Italia.

Costa, E., Garcés, M., López-Blanco, M., Serra-Kiel, J., Bernaola, G., Cabrera, L., Beamud, E., 2013. The Bartonian-Priabonian marine record of the eastern South Pyrenean foreland basin (NE Spain): a new calibration of the larger foraminifers and calcareous nannofossil biozonation. Geologica Acta **11**, 177-193.

Cotton, L.J., Zakrevskaya, E.Y., van der Boon, A., Asatryan, G., Hayrapetyan, F., Israyelyan, A., Krijgsman, W., Less, G., Monechi, S., Papazzoni, C.A., Pearson, P.N., Razumovskiy, A., Renema, W., Shcherbinina, E., Wade, B.S., 2016. Integrated stratigraphy of the Priabonian (upper Eocene Urtsadzor section, Armenia. Newsletter on Stratigraphy **50** (3), 269-295 (27). doi: 10.1127/nos/2016/0313

Cramer, B.S., Toggweiler, J.R., Wright, J.D., Katz, M.E., Miller, K.G., 2009. Ocean overturning since the Late Cretaceous: Inferences from a new benthic foraminiferal isotope compilation. Paleoceanography **24**, PA4216. doi: 10.1029/2008PA001683.

D'Archiac, A., 1850. Histoire des progrès de la géologie de 1834 à 1849; première partie **3**, 1-624. Société géologique de France, Paris.

D'Archiac, A., and Haime, J., 1853. Description des animaux fossiles du groupe nummulitique de l'Inde, precede d'un résumé géologique et d'une monographie des Nummulites, 373 pp.

D'Onofrio, R., Luciani, V., Fornaciari, E., Giusberti, L., Boscolo Galazzo, F., Dallanave, E., Westerhold, T., Sprovieri, M., Telch, S., 2016. Environmental perturbations at the early Eocene ETM2, H2, and 11 events as inferred by Tethyan calcareous plankton (Terche section, northeastern Italy). Paleoceanography **31**, 1225-1247.

Dal Degan, D. and Barbieri, S., 2005. Rilievo geologico dell'area di Bolca (Monti Lessini orientali). Bollettino del Museo Civico di Storia Naturale di Verona **27**, 3-10.

Dallanave, E., Agnini, C., Muttoni, G., Rio, D., 2009. Magneto-biostratigraphy of the Cicogna section (Italy): implications for the late Paleocene-Early Eocene time scale. Earth and Planetary Science Letters **285**, 39-51.

Dallanave, E., Agnini, C., Muttoni, G., Rio, D., 2012. Paleocene magneto-biostratigraphy and climate-controlled rock magnetism from the Belluno Basin, Tethys Ocean, Italy. Palaeogeography, Palaeoclimatology, Palaeoecology **337-338**, 130-142.

Dallanave, E., Tauxe, E., Muttoni, G., Rio, D., 2010. Silicate weathering machine at work: rock magnetic data from the late Paleocene-early Eocene Cicogna section, Italy. Geochemistry, Geophysics, Geosystems **11** (7), Q07008.

Dal Piaz, G.V., Bistacchi, A., Massironi, M., 2003. Geological outline of the Alps. Episodes **26** (3).

De Alessandri, G., 1899. Osservazioni geologiche sulla Creta e sull'Eocene della Lombardia. Atti della Società Italiana di Scienze Naturali, Museo Civico di Storia Naturale **38**, 253-320.

De Conto, R.M., Galeotti, S., Pagani, M., Tracy, D., Schaefer, K., Zhang, T., Pollard, D., Beerling, D.J., 2012. Past extreme warming events linked to a massive carbon release form thawing permafrost. Nature **484**, 87-92. doi: 10.1038/nature10929

De Geyter, G., De Man, E., Herman, J., Jacobs, P., Moorkens, T., Steurbaut, E., Vandenberghe, N., 2006. Disused Paleogene regional stages from Belgium: Montian, Heersian, Landenian, Paniselian, Bruxellian, Laekenian, Ledian, Wemmelian and Tongrian. Geologica Belgica **9**, 203-213.

Delage, Y. and Hérouard, E., 1896. Traité de Zoologie Concrète 1, La Cellule et le Protozoaires. 584 pp. Schlecher Frères, Paris.

Desor, F., 1847. Sur le terrain danien, nouvel étage de la Craie. Bulletin de la Société géologique de France **4**, 179-182.

Dewalque, C., 1868. Prodrome d'une description geologique de la Belgique. Librairie Polytechnique De Decq, Bruxelles and Liege, 442.

De Zanche, V. and Conterno, T., 1972. Contributo alla conoscenza geologica dell'orizzonte eocenico di Roncà nel veronese e nel vicentino. Atti e Memorie dell'Accademia Patavina delle Scienze, Lettere ed Arti **84**, 287-295.

Di Carlo, M., Accordi, G., Carbone, F., Pignatti, J., 2010. Biostratigraphic analysis of Paleogene lowstand wedge conglomerates of a tectonically active platform margin (Zakynthos Island, Greece). Journal of Mediterranean Earth Sciences **2**, 31-92.

Di Napoli Alliata, E., Proto Decima, F., Pellegrini, G.B., 1970. Studio geologico, stratigrafico e micropaleontologico dei dintorni di Belluno. Memorie della Società Geologica Italiana **9**, 1-28.

Dinarès-Turell, J., Stoykova, K., Baceta, J.L., Ivanov, M., Pujalte, V., 2010. High-resolution intra- and interbasinal correlation of the Danian-Selandian transition (Early Paleocene): The Bjala section (Bulgaria) and the Selandian GSSP at Zumaia (Spain). Palaeogeography, Palaeoclimatology, Palaeoecology 297, 511-533.

Doglioni, C., Bosellini, A., 1987. Eoalpine and Mesoalpine tectonics in the southern Alps. Geologische Rundschau **76** (3), 735-754. doi: 10.1007/BF01821061.

Dollfus, G.F., 1880. Essai sur l'extension des terrains tertiaires dans le basin anglo-parisien. Bulletin de la Société Géologique de Normandie **6**, 584-605.

Douvillé, H., 1920. Les Foraminiferes de l'Éocene dans la region de Suez. Société géologique de France **4** (XX).

Drobne, K., 1977. Alvéolines paléogènes de la Slovénie et de l'Istrie. Schweizerische Paläontologische Abhandlungen **99**, 1-132.

Drobne, K., Ćosović, V., Moro, A., Bucković, D., 2011. The role of the Paleogene Adriatic Carbonate Platform in the Spatial Distribution of Alveolinids. Turkish Journal of Earth Sciences **20**, 721-751.

Drobne, K., Ogorelec B., Riccamboni, R., 2007. *Bangiana hanseni* n.gen n.sp. (Foraminifera), an index species of Danian age (lower Paleocene) from the Adriatic Carbonate Platform (SW Slovenia, NE Italy, Herzegovina). Razprave IV. Razreda Sazu **XLVIII** (1), 5-71.

Drooger, C.W., 1993. Radial Foraminifera; morphometrics and evolution. Verhandelingen der Koninklijke Nederlandse Akademie van Wetenschappen, Afdeling Natuurkunde **41**, 1-242.

Dumont, A., 1849. Rapport sur la carte géologique de la Belgique. Bulletin de l'Académie royal des Sciences et des Lettres de la Belgique **16**, 351-373.

Dupuis, C., Aubry, M.-P., Steurbaut, E., Berggren, W.A., Ouda K., Magioncalda, R., Cramer, B.S., Kent, D.V., Speijer, R.P., Heilmann-Clausen, C., 2003. The Dababiya Quarry Section: Lithostratigraphy, clay mineralogy, geochemistry and paleontology. Micropaleontology **49**, 41-59.

Ehrenberg, C.G., 1839. Über die Bildung der Kreidefelsen und des Kreidemergels durch unsichtbare Organismen. Physikalische Abhandlungen der Königlichen Akademie der Wissenschaften zu Berlin, 1838 [1840: separate 1839], 59-147.

Eichwald C.E., von, 1830. Zoologia specialis **2**, 323 pp. D.E. Eichwaldus, Vilniae.

Fabiani, R., 1912. Nuove osservazioni sul Terziario fra il Brenta e l'Astico. Atti dell'Accademia delle Scienze Veneta-Trentino-Istriana **5** (1), 7-36.

Fabiani, R., 1914. La serie stratigrafica del Monte Bolca e dei suoi dintorni. Memorie dell'Istituto Geologico della Regia Università di Padova **3**, 223-235.

Fabiani, R., 1915. Il Paleogene del Veneto. Memorie dell'Istituto Geologico della Regia Università di Padova **3**, 1-336.

Floridia, B., 1935. Sul rinvenimento di Orbitoidi non rimaneggiate nel Flysch Lombardo. Bollettino della Società Geologica Italiana **54**, 253-262.

Fornaciari, B., Giusberti, L., Papazzoni, C.A., 2019. *Alveolina postalensis* n. sp. (Foraminiferida, Alveolinidae) from the upper Ypresian of Monte Postale and Pesciara di Bolca (northern Italy). Bollettino della Società Paleontologica Italiana **58** (2), 187-199.

Fornaciari, E., Giusberti, L., Luciani, V., Tateo, F., Agnini, C., Backman, J., Oddone, M., Rio, D., 2007. An expanded Cretaceous-Tertiary transition in a pelagic setting of the Southern Alps (central-western Tethys). Palaeogeography, Palaeoclimatology, Palaeoecology **255**, 98-131.

Gardin, S., Monechi, S., 1998. Palaeoecological change in the middle to low latitude calcareous nannoplankton at the Cretaceous/Tertiary boundary. Bulletin de la Societé Géologique de France **5**, 709-723.

Garzarella, A., Raffi, I., 2018. Taxonomy and evolutionary relationships within the calcareous nannofossil genus *Ericsonia* in the upper Paleocene. Rivista Italiana di Paleontologia e Stratigrafia **124** (1), 105-126.

Giusberti, L., Boscolo Galazzo, F., Thomas, E., 2016. Variability in climate and productivity during the Paleocene-Eocene Thermal Maximum in the western Tethys (Forada section). Climate of the past **12**, 213-240.

Giusberti, L., Capraro, L., Luciani, V., Fornaciari, E., 2019. The Italian record of the Paleocene-Eocene Thermal Maximum. Bollettino della Società Paleontologica Italiana **58** (1), 85-108. doi:10.4435/BSPI.2019.06

Giusberti, L., Kaminski, M.A., Mancin, N., 2018. The bathyal larger lituolid *Neonavarella* n. gen. (Foraminifera) from the Thanetian Scaglia Rossa Formation of northeastern Italy. Micropaleontology **64**, 417-434.Giusberti, L., Rio, D., Agnini, C., Backman, J., Fornaciari, E., Tateo, F., Oddone, M., 2007. Mode and tempo of the Paleocene-Eocene thermal maximum in an expanded section in the Venetian pre-Alps. Geological Society of America Bulletin **119**, 391-412.

Giusberti, L., Rio, D., Agnini, C., Backman, J., Fornaciari, E., Tateo, F., Oddone, M., 2007. Mode and tempo of the Paleocene-Eocene thermal maximum in an expanded section from the Venetian pre- Alps. Geological Society of America Bulletin **119**, 391-412.

Gradstein, F.M., Ogg, J.G., Smith, A., Ogg, G.M., 2012. The Geologic Time Scale 2012. Elsevier, Amsterdam, 1144 pp.

Guex, J., 2003. A generalization of Cope's rule. Bulletin de la Société géologique de France **174**, 449-452.

Hardenbol, J., Thierry, J., Farley, M.B., Jacquin, T., de Graciansky, P.-C., Vail, P.R., 1998. Mesozoic and Cenozoic sequence chronostratigraphic framework of European Basins. In: de Graciansky, P.-C., Hardenbol, J., Jacquin, T., Vail, P.R. (Eds.). Mesozoic and Cenozoic Sequence Stratigraphy of European Basins. SEPM Special Publication **60**, 3-14.

Harland, W.B., Armstrong, R.L., Cox, A.V., Craig L.A., Smith, A.G., Smith, D.G., 1990. A Geological Time Scale 1989. Cambridge University Press, Cambridge, 236 pp.

Harpe, P. de la, 1883. Etudes des Nummulites de la Suisse. Schweizerische Paläontologische Abhandlungen **10**.

Hay, W.W., and Mohler, H.P., Roth, P.H., Schimdt, R.R., Boudreaux, J.E., 1967. Calcareous Nannoplankton Zonation of the Cenozoic of the Gulf Coast and Caribbean-Antillean Area, and Transoceanic Correlation. Transactions of the Gulf Coast Association of Geological Societies **17**, 428-480.

Higgins, J.A., Schrag, D.P., 2006. Beyond methane: towards a theory for the Paleocene-Eocene thermal maximum. Earth and Planetary Science Letters **245** (3-4), 523-537.

Hillebrandt, A. von, 1975. Corrélation entre les biozones de grand foraminifères et de foraminifères planktoniques de l'Ilerdien. Bulletin de la Société géologique de France **7** (17), 162-167.

Hok, T.S., 1932. On the genus Cicloclypeus Carpenter. Part I, and an appendix on the Heterostegines of Tjimanggoe, S. Bantam, Java. Wetenschappelijke Mededeelingen Dienst van der Mijnbouw in Nederlandsch-Indië **19**, 1-194.

Hottinger, L., 1960. Recherches sur les Alvéolines du Paléocene et de l'Eocène. Schweizerische Paläontologische Abhandlungen **75-76** Text (I), 1-243, atlas (II), 18 pls.

Hottinger, L., Lehmann, R. and Schaub, H., 1964. Données actuelles sur la biostratigraphie du Nummulitique méditerranéen. Mémoires du Bureau du Recherches Géologiques et Minières **28**, 611-652.

Hottinger, L., 1974. Alveolinids, Cretaceous-Tertiary Larger Foraminifera. Esso Production Research-European Laboratories, Text (I), 1-84, atlas (II), 106 pls.

Hottinger, L., 2001. Learning from the Past? In: Levi-Montalcini R. (Ed.), Frontiers of Life **4** (2), Discovery and spoliation of the biosphere, 449–477, 18 figs. 2 tab. Academic Press, London & San Diego.

Hottinger, L., 2009. The Paleocene and earliest Eocene foraminiferal Family Miscellaneidae: neither nummulitids nor rotaliids. Carnets de Géologie – Notebooks on Geology, article 2009/06 (CG2009_A06).

Hottinger, L., 2014. Paleogene larger rotaliid foraminifer from the western and central Neotethys. Springer International Publishing, 196 pp.

Hottinger, L. and Schaub, H., 1960. Zur Stufeneinteilung de Palaeocaens un des Eocaens. Einführung der Stufen Ilerdien und Biarritzien. Eclogae Geologicae Helvetica **53**, 453-480.

Inan, N., 1988. Sur la presence de la nouvelle espèce Cuvillierina sireli dans le Thanétien de la Montagne de Tecer (Anatolie centrale, Turquie). Revue de Paléobiologie **7**, 121-127.

Inan, N., 2003. *Cocoarota orali* n. sp. (Foraminifera) from Upper Maastrichtian-Lower Lutetian deposits of Turkey. Micropaleontology **49** (2), 201-204.

Inan, N. and Inan, S., 2008. Selandian (Upper Paleocene) benthic foraminiferal assemblages and their stratigraphic ranges in the northeastern part of Turkey. Yerbilimleri **29** (3), 147-158.

Jenkins, D.G., Luterbacher, H.P., 1992. Paleogene stages and their boundaries: Introductory remarks. Neues Jahrbuch für Geologie und Paläontologie Abhandlungen **186**, 1-5.

Kahsnitz, A., Quinghai, Z., Willems, H., 2016. Stratigraphic distribution of the larger benthic foraminifera *Lockhartia* in South Tibet (China). Journal of Foraminiferal Research **46** (1), 37-47.

Kapellos, C. and Schaub, H., 1973. Zur Korrelation von Biozonierungen mit Grossforaminiferen und Nannoplankton im Paläogen der Pyrenäen. Eclogae Geologicae Helvetica **66**, 687-737.

Kapellos, C. and Schaub, H., 1975. L'Ilerdien dans les Alp es, dans les Pyrénées et en Crimée. Corrélation des zones à grands Foraminifères et à Nannoplancton. Bulletin de la Société géologique de France **7** (17), 148-161.

Kennett, J.P., Stott, L.D., 1991. Abrupt deep sea warming, paleoceanographic changes and benthic extinctions at the end of the Paleocene. Nature **353**, 225–229, doi:10.1038/353225a0.

Kent, D.V., Cramer, B.S., Lanci, L., Wang, D., Wright, J.D., Van der Voo, R., 2003. A case for a comet impact trigger for the Paleocene/Eocene Thermal Maximum and carbon isotope excursion. Earth and Planetary Science Letters **211**, 13-26. doi: 10.1016/S0012-821X(03)00188-2

Kleboth, P., 1982. Stratigraphie und sedimentologie der Hoheren Oberkreide und des Alttertiars der Brianza (Provinz Como, Italien). Memorie di Scienze Geologiche già Memorie degli Istituti di Geologia e Mineralogia dell'Università di Padova **XXXV**, 213-292.

Kuiper, K.F., Deino, A., Hilgen, F.J., Krijgsman, W., Renne, P.R., Wijbrans, J.R., 2008. Synchronizing rock clocks of Earth history. Science **320**, 500-504.

Less, G., 1987. Paleontology and stratigraphy of the European Orthophragminae. Geologica Hungarica, Series Palaeontologica **51**, 1-373.

Less, G., 1998. The zonation of the Mediterranean Upper Paleocene and Eocene by Orthophragminae. Dela, Slovenska akademija znanosti in umetnosti, Opera, Academia Scientiarium et Artium Slovenica **34**, 21-43.

Less, G. and Özcan, E., 2008. The late Eocene evolution of nummulitid foraminifer *Spiroclypeus* in the Western Tethys. Acta Palaeontologica Polonica **53**, 303-316.

Less, G. and Özcan, E., 2012. Bartonian–Priabonian larger benthic foraminiferal events in the Western Tethys. Austrian Journal of Earth Sciences **105**, 129-140.

Less, G., Özcan, E., Báldi-Beke, M., Kollányi, K., 2007. Thanetian and early Ypresian orthophragmines (Foraminifera: Discocyclinidae and Orbitoclypeidae) from the Central Western Tethys (Turkey, Italy and Bulgaria) and their revised taxonomy and biostratigraphy. Rivista Italiana di Paleontologia e Stratigrafia **113** (3), 419-448.

Less, G., Özcan, E., Papazzoni, C.A., Stockar, R., 2008. The middle to late Eocene evolution of nummulitid foraminifer *Heterostegina* in the Western Tethys. Acta Palaeontologica Polonica **53**, 317-350.

Littler, K., Röhl, U., Westerhold, T., Zachos, J.C., 2014. A high-resolution benthic stable-isotope record for the South Atlantic: Implications for orbital-scale changes in Late Paleocene-Early Eocene climate and carbon cycle. Earth and Planetary Science Letters **401**, 18-30.

Loeblich, A.R. Jr. and Tappan H., 1987. Foraminiferal Genera and their Classification. 2 vols. 970 pp. Van Nostrand Reinhold Company, New York.

Luciani, V., 1989. Stratigrafia sequenziale del Terziario nella catena del Monte Baldo (provincie di Verona e Trento). Memorie di Scienze Geologiche dell'Università di Padova **41**, 263-351.

Luciani, V., Dickens, G.R., Backman, J., Fornaciari, E., Giusberti, L., Agnini, C., D'Onofrio, R., 2016. Major perturbations in the global carbon cycle and photosymbiont-bearing planktic foraminifera during the early Eocene. Climate of the Past **12**, 981-1007.

Luciani, V., Giusberti, L., Agnini, A., Backman, J., Fornaciari, E., Rio, D., 2007. The Paleocene-Eocene Thermal Maximum as recorded by Tethyan planktonic foraminifera in the Forada section (northern Italy). Marine Micropaleontology **64**, 189-214.

Luciani, V., Fornaciari, E., Papazzoni, C.A., Dallanave, E., Giusberti, L., Stefani C., Amante, E., in press. Integrated stratigraphy at the Bartonian−Priabonian transition: Correlation between shallow benthic and calcareous plankton zones (Varignano section, northern Italy). Geological Society of America Bulletin.

Malaroda, R., 1954. Il Luteziano di Monte Postale (Lessini medi). Memorie degli Istituti di Geologia e Mineralogia dell'Università di Padova **19** (1955-1956), 3-107.

Malaroda, R., 1967. Calcari di Spilecco. In: Bosellini, A., Carraro, F., Corsi, M., De Vecchi, G.P, Gatto G.O., Malaroda R., Sturani, C., Ungaro, S., Zanettin, B. (Eds.). Note Illustrative della Carta Geologica d'Italia alla scala 1: 100.000, Foglio 49 Verona. Servizio Geologico d'Italia, 21-22.

Marramà, G., Bannikov, A.B., Tyler, J.C., Zorzin, R., Carnevale, G., 2016. Controlled excavations in the Pesciara and Monte Postale sites provide new insights about the palaeoecology and taphonomy of the fish assemblages of the Eocene Bolca *Konservat-Lagerstätte*, Italy. Palaeogeography, Palaeoclimatology, Palaeoecology **454**, 228-245.

Martini, E., 1971. Standard Tertiary and Quaternary calcareous nannoplankton zonation, In: Farinacci, A. (Ed.), Proceeding 2nd International Conference Planktonic Microfossils Roma **2**, 739-785.

Mathur, N.S., Juyal, K.P., Kumar, K., 2009. Larger foraminiferal biostratigraphy of lower Paleogene successions of Zanskar Tethyan and Indus-Tsangpo Suture Zones, Ladakh, India in the light of additional data. Himalayan Geology **30** (1), 45-68.

Medizza, F., 1975. Il nannoplancton calcareo della Pesciara di Bolca (Monti Lessini): Studi e Ricerche sui Giacimenti Terziari di Bolca **2**, 433-444.

Meriç, E., Avşar, N., Nazik, A., Yokeş, M.B., Dinçer, F., 2008. A Review of Benthic Foraminifers and Ostracods of the Antalya Coast. Micropaleontology **54** (3/4), 199-240.

Molina, E., Alegret, L., Arenillas, I., Arz, J.A., Gallala, N., Hardenbol, J., von Salis, K., Steurbaut, E., Vandenberghe, N., Zaghbib-Turki, D., 2006. The Global Boundary Stratotype Section and Point for the base of the Danian Stage (Paleocene, Paleogene, "Tertiary", Cenozoic) at El Kef, Tunesia - Original definition and revision. Episodes **29**, 263-273.

Munier-Chalmas, E., 1891. Étude du Tithonique, du Crétacé et du Tertiaire du Vicentin. These, Paris.

Ogg, J.G., Smith, A.G., 2004. The geomagnetic polarity time scale. In: Gradstein, F.M., Ogg, J.G., Smith, A.G. (Eds.). A Geological Time Scale, 2004. Cambridge University Press, Cambridge, U.K., 589 pp.

Omaña, L., Pons, J. M., Alencaster, G., 2009. Latest Cretaceous foraminifera from the Cárdenas Formation, San Luis Potosì, Mexico: Biostratigraphical, paleoenvironmental and paleobiogeographical significance. Micropaleontology **54** (5), 445-462.

Orbigny, A.D. D', 1826. Tableau méthodique de la classe des Céphalopodes. Annales des Sciences Naturelles **7**, 245-314.

Özcan, E., Scheibner, C. and Boukhalfa, K., 2014. Orthophragminids (foraminifera) across the Paleocene–Eocene transition from North Africa: taxonomy, biostratigraphy, and paleobiogeographic implications. Journal of Foraminiferal Research **44**, 203-229.

Pälike, H., Lyle, M., Nishi, H., Raffi, I., Gamage, K., Klaus, A., the Expedition 320/321 Scientists, 2010. Proceedings of the Integrated Ocean Drilling Program (IODP), 320/321. Integrated Ocean Drilling Program Management International, Tokyo. doi:10.2204/iodp.sd.9.01.2010.

Papazzoni, C.A., Ćosović, V., Briguglio, A., Drobne, K., 2017a. Towards a calibrated larger foraminifera biostratigraphic zonation: celebrating the 18 years of application of Shallow Benthic Zones. Palaios **32**, 1-5.

Papazzoni C.A., Fornaciari E., Giusberti L., Vescogni A. & Fornaciari B., 2017b. Integrating Shallow Benthic and calcareous nannofossil Zones: the lower Eocene of the Monte Postale section (Northern Italy). Palaios **32**, 6-17. doi: 10.2110/palo.2016.014

Papazzoni, C.A., Giusberti L., Trevisani, E., 2014. 10. The Spilecco site. In: Papazzoni, C.A., Giusberti, L., Carnevale, G., Roghi, G., Bassi, D., Zorzin, R. (Eds). The Bolca *Fossil-Lagerstätten*: A window into the Eocene world. Rendiconti della Società Paleontologica Italiana **4**, 1-110.

Papazzoni, C.A., Roghi, G., Zorzin, R., 2013. Analisi delle rocce che circondano la Pesciara. Dati preliminari dalla carota perforata alla base della prima galleria. Studi e Ricerche sui Giacimenti Terziari di Bolca **14** - Miscellanea Paleontologica, **11** [2012], 43-49.

Papazzoni, C.A., Trevisani, E., 2006. Facies analysis, palaeoenvironmental reconstruction, and biostratigraphy of the "Pesciara di Bolca" (Verona, northern Italy): An early Eocene *Fossil-Lagerstätte*. Palaeogeography, Palaeoclimatology, Palaeoecology **242**, 21-35.

Perch-Nielsen, K., 1985. Cenozoic calcareous nannoplancton. In: Bolli, H.M., Saunders, J.B., Perch-Nielsen, K. (Eds.). Plankton Stratigraphy. Cambridge University Press, Cambridge, 427–554.

Petrizzo, M.R., 2005. An early late Paleocene event on Shatsky Rise, northwest Pacific Ocean (ODP Leg 198): evidence form planktonic foraminiferal assemblages. In: Bralower, T.J., Premoli Silva, I., Malone, M.J. (Eds.), Proceedings of the Ocean Drilling Program, Scientific Results **198**, 1-29.

Peybernès, B., Fondecave-Wallez, M.J, Hottinger, L, Eichène, P., Segonzac, G., 2000. Limite Crétacé-Tertiaire et biozonation micropaléontologique du Danien-Sélandien dans le Béarn occidental et la Haute-Soule (Pyrénées Atlantiques). Geobios **33**, 35-48

Pignatti, J., Di Carlo, M., Benedetti, A., Bottino, C., Briguglio, A., Falconi, M., Matteucci, R., Perugini, G., Ragusa, M., 2008. SBZ 2-6 larger foraminiferal assemblages from the Apulian and pre-Apulian domains. Atti del Museo Civico di Storia Naturale di Trieste **53**, 131-146.

Pignatti, J. and Papazzoni, C.A., 2017. Oppelzones and their heritage in current larger foraminiferal biostratigraphy. Lethaia. doi: 10.1111/let.12210

Pfender, J., 1935. A propos de *Siderolites vidali* et de quelques autres. Bulletin de la Société géologique de France **5** (4), 225-236.

Piveteau, J. (Ed.), 1952. Traité de paléontologie **I**, Masson, Paris, 133-301.

Poletti, L., Premoli Silva, I., Masetti, D., Pipan, M., Claps, M., 2004. Orbitally driven fertility cycles in the Palaeocene pelagic sequences of the Southern Alps (Northern Italy). Sedimentary Geology **164**, 35-54. doi:10.1016/j.sedgeo.2003.09.001

Premoli Silva, I., Luterbacher, H.P., 1966. The Cretaceous/Tertiary boundary in the Southern Alps. Rivista Italiana di Paleontologia e Stratigrafia **72**, 1183-1266.

Premoli Silva, I., Tremolada, F., Sciunnach, D., Scardia, G., 2010. Aggiornamenti biocronologici e nuovi interpretazioni ambientali sul Paleocene-Eocene della Brianza (Lombardia). In: Orombelli, G., Cassinis, G., Gaetani, M. (Eds.). Una Nuova Geologia per la Lombardia. Convegno in onore di Maria Blanca Cita. Milano, 6-7 novembre 2008. Istituto Lombardo Accademia di Scienze e Lettere. Incontri di Studio **54**, 592 pp. ISBN 978-88-7916-452-8.

Prever, P.L., 1905. Sulla fauna nummulitica della Scaglia nell'Appennino centrale. Accademia Reale delle Scienze di Torino, **40**.

Quillévéré, F., Norris, R.D., Kroon, D., Wilson, P.A., 2008. Transient ocean warming and shifts in carbon reservoirs during the early Danian. Earth and Planetary Science Letters **265**, 600–615, doi:10.1016/j.epsl.2007.10.040.

Rahaghi, A., 1978. Paleogene biostratigraphy of some parts of Iran. National Iranian Oil Company, Geological Laboratories **7**, 73 pp, 49 pls.

Rahaghi, A., 1983. Stratigraphy and faunal assemblage of Paleocene-Lower Eocene in Iran. National Iranian Oil Company, Geological Laboratories **10**, 73 pp, 49 pls.

Rauzer-Chernousova, D.M. and Fursenko, A.V. (Eds.), 1959. Principles of paleontology. Part I. General part and Protozoa. Academiya Nauk SSSR, Moskow, 482 pp. [in Russian]; English translation: Monson S., 1962. Israel Program for Scientific Translation, Jerusalem, 728 pp.

Renevier, E., 1873. Tableau des terrains sédimentaires fornés pendant les époques de la phase organique du globe terrestre. Bulletin de la Société Vaudoise des Sciences Naturelles, Laussane **12**, 218-252.

Rio, D., Raffi, I., Villa, G., 1990. Pliocene–Pleistocene Calcareous Nannofossil Distribution Patterns in the Western Mediterranean. In: Kasterns, K.A., Mascle, J., et al. (Eds.). Proceedings of the Ocean Drilling Program Scientific results 107, Ocean Drilling Program, College Station **TX**, 513-533.

Robador, A., Orue-Etxebarria, X., Serra-Kiel, J., 1991. The correlation between biozonation of benthonic and planktonic foraminifera. In: Introduction to the Early Paleogene of the South Pyrenean Basin, IGCP 286 "Early Paleogene Benthos". First meeting Jaca (Spain). Instituto Tecnologico Geominerario de España, Madrid, 97-100.

Rodríguez-Pintó, A., Pueyo, E.L., Serra-Kiel, J., Samsó, J.M., Barnolas, A., and Pocoví, A., 2013. The upper Ypresian and Lutetian in San Pelegrín section (Southwestern Pyrenean Basin): magnetostratigraphy and larger foraminifera correlation. Palaeogeography, Palaeoclimatology, Palaeoecology **370**, 13-29.

Rodríguez-Pintó, A., Pueyo, E.L., Serra-Kiel, J., Samsó, J.M., Barnolas, A., and Pocoví, A., 2012. Lutetian magnetostratigraphic calibration of larger foraminifera zonation (SBZ) in the Southern Pyrenees: The Isuela section. Palaeogeography, Palaeoclimatology, Palaeoecology **333-334**, 107-120.

Romein, A.J.T., 1979. Lineages in Early Paleogene calcareous nannoplankton. Utrecht Micropaleontological Bulletins **22,** 231 pp.

Rosenkrantz, A., 1924. De kobenhavnske Gronsandslag og deres Placering i den danske Lagraekke. Med et Skema over det danske Paleocaen. Meddelelser fra Dansk geologisk Forening **6**, 22-39.

Schaub, H., 1981. Nummulites et Assilines de la Tèthys paléogène: taxinomie, phylogénese et biostratigraphie. Schweizerische Palaontologische Abhandlungen **104**, 1-236.

Scheibner, C. and Speijer, R.P., 2009. Recalibration of the Tethyan shallow-benthic zonation across the Paleocene-Eocene boundary: the Egyptian record. Geologica Acta **7** (1-2), 195-214.

Scheibner, C., Speijer, R.P., Marzouk, A.M., 2005. Turnover of larger foraminifera during the Paleocene-Eocene Thermal Maximum and paleoclimatic control on the evolution of platform ecosystems. Geology **33** (6), 493-496.

Schimper, W. P., 1874. Traité de Paléontologie végétale **3**. Paris.

Schlagintweit, F. and Rashidi, K., 2019. Serrakielina chahtorshiana n. gen. et n. sp., and other (larger) benthic Foraminifera from Danian-Selandian carbonates of Mount Chah Torsh (Yazd Block, Central Iran). Micropaleontology **65** (4), 305-338.

Schmitz, B., Alegret, L., Apellaniz, E., Arenillas, I., Aubry, M.-P., Baceta, J.,-U., Berggren, W.A., Bernaola, G., Caballero, F., Clemmensen, A., Dinarès-Turrell, J., Dupuis, C., Heilmann-Clausen, C., Knox, R., Martín-Rubio, M., Molina, E., Monechi, S., Ortiz, S., Orue-Etxebarria, X., Payros, A., Petrizzo, M.R., Pujalte, V., Speijer, R., Sprong, J., Steurbaut, E., Thomsen, E., 2008. Proposed Global Stratotype Sections and Points for the bases of the Selandian and the Thanetian stages (Paleocene series). Report of the International Subcommission on Paleogene Stratigraphy **52**.

Schulte, P., Alegret L., Arenillas, I., Arz, J.A., Barton, P.J., Bown, P.R., Bralower, T.J., Christeson, G.L., Claeys, P., Cockell, C.S., Collins, G.S., Deutsch, A., Goldin, T.J., Goto, K., Grajales-Nishimura, J.M., Grieve, R.A.F., Gulick, S.P.S., Johnson, K.R., Kiessling, W., Koeberl, C., Kring, D.A., MacLeod, K.G., Matsui, T., Melosh, J., Montanari, A., Morgan, J.V., Neal, C.R., Nichols, D.J., Norris, R.D., Pierazzo, E., Ravizza, G., Rebolledo-Vieyra, M., Reimold, W.U., Robin, E., Salge, T., Speijer, R.P., Sweet, A.R., Urrutia-Fucugauchi, J., Vajda, V., Whalen, M.T., Willumsen, P.S, 2010. The Chicxulub Asteroid Impact and Mass Extinction at the Cretaceous-Paleogene Boundary. Science **327**, 1214-1218. doi: 10.1126/science.1177265

Schulte, P., Schwark, L., Stassen, P., Kouwenhoven, T.J., Bornemann, A., Speijer, R.P., 2013. Black shale formation during the Latest Danian Event and the Paleocene-Eocene Thermal Maximum in central Egypt: Two of a kind? Palaeogeography, Palaeoclimatology, Palaeoecology **371**, 9-25.

Schwark, L., Ferretti, A., Papazzoni, C.A., Trevisani, E., 2009. Organic geochemistry and paleoenvironment of the Early Eocene "Pesciara di Bolca" *Konservat-Lagerstätte*, Italy. Palaeogeography, Palaeoclimatology, Palaeoecology **273**, 272-285.

Schwager C., 1883. Die Foraminiferen aus den Eocaenablagerungen der lybischen Wüste und Aegyptens. Palaeontographica (1846-1933) **30** (5-6), 79-54.

Schweighauser, J., 1953. Mikropalaeontologische und stratigraphische Untersuchungen im Paleocaen und Eocaen des Vicentin (Norditalien) mit besonderer Berücksichtigung der Discocyclinen und Asterocyclinen. Schweizerische Paläontologische Abhandlungen **70**, 97 pp.

Scotto di Carlo, B., 1966. Le alveoline del Gargano nord-orientale. Palaeontographia Italica **61**, 65-73.

Serra-Kiel, J., Canudo, J.I., Dinarés, J., Molina, E., Ortiz, N., Pascual, J.O., Samsó, J.M., Tosquella, J., 1994. Cronoestratigrafía de los sedimentos marinos del Terciario inferior de la Cuenca de Graus-Tremp (Zona Central Pirenaica). Revista de la Sociedad Geológica de España **7**, 273-297.

Serra-Kiel, J., Hottinger, L., Caus, E., Drobne, K., Ferrandez, C., Jauhri, A. K., Less, G., Pavlovec, R., Pignatti, J., Samsò, J. M., Schaub, H., Sirel, E., Strougo, A., Tambareau, Y., Tosquella, J., Zakrevskaya, E., 1998. Larger foraminiferal biostratigraphy of the Tethyan Paleocene and Eocene. Bulletin de la Société Géologique de France **169** (2), 281-299.

Serra-Kiel, J., Vicedo, V., Razin, P., Grélaud, C., 2016. Selandian-Thanetian larger foraminifera from the lower Jafnayn Formation in the Sayq area (eastern Oman Mountains). Geologica Acta **14** (3), 315-333.

Shaw, A.B., 1964, Time in Stratigraphy. New York, USA, McGraw-Hill, 365 p.

Sirel, E., 1972. Systematic study of new species of the genera *Fabularia* and *Kathina* from Paleocene. Türkiye Jeoloji Kur Bülteni **15**, 277-249, 8 pls.

Sirel, E., 1999. Four new genera (*Haymanella*, *Kayseriella*, *Elazigella* and *Orduella*) and one new species of Hottingerina from the Paleocene of Turkey. Micropaleontology **45** (2), 113-137.

Sirel, E., 2003. Foraminiferal description and biostratigraphy of the Bartonian, Priabonian and Oligocene shallow-water sediments of the southern and eastern Turkey. Revue de Paléobiologie de Genève **22** (1), 269-339.

Sirel, E., 2009. Reference sections and key localities of the Paleocene stages and their very shallow/shallow-water three new benthic foraminifera in Turkey. Revue de Paléobiologie, Genève **28** (2), 413-435.

Sirel, E., 2012. Seven new larger benthic foraminiferal genera from the Paleocene of Turkey. Revue de Paléobiologie **31** (2), 267-301.

Sirel, E., 2013. Description Of Two New Families, Three New Species and Re-Description Of Four known Genera And One Subfamily From The Larger Benthic Foraminifera Of Paleocene In Turkey. Bulletin of the Mineral Research and Exploration **146**, 27-53.

Sirel, E., 2015. Reference Sections and Key Localities of the Paleogene Stage and Discussion C-T, P-E and E-O Boundaries by the Very Shallow-Shallow Water Foraminifera in Turkey. Ankara üniversitesi yayinlari (Ankara University Press) **461**, 171 pp.

Sirel, E., 2018. Revision of the Paleocene and partly early Eocene larger benthic foraminifera of Turkey. Ankara Üniversitesi Yayınevi Yayın **27**, 260 pp.

Sirel, E. and Deveciler, A., 2018. Description and Some Revision of *Ranikothalia* Caudri, *Nummulites* Lamarck and *Assilina* D'Orbigny Species From Thanetian-Early Chattian of Turkey Ankara. Üniversitesi Yayınevi Yayın 26, 182 pp.

Smout, A.H., 1954. Lower Tertiary foraminifera of the Qatar peninsula. British Museum (Natural History), London, 96 pp., 44 figs., 15 Pls.

Stefani, C. and Grandesso, P., 1991. Studio preliminare di due sezioni del Flysch bellunese. Rendiconti della Società Geologica Italiana **14**, 157-162.

Storey, M., Duncan, R.A., Swisher III, C.A., 2007. Paleocene-Eocene Thermal Maximum and the opening of the northeast Atlantic. Science **316**, 587-589.

Svensen, H., Planke, S., Malthe-Sørenssen, A., Jamtveit, B., Myklebust, R., Rasmussen Eidem, T., Rey, S.S., 2004. Release of methane from a volcanic basin as a mechanism for initial Eocene global warming. Nature **429**, 542-545.

Thierstein, H. R., Geitzenauer, K.R., Molfino, B., Shackleton, N.J., 1977. Global synchroneity of late Quaternary coccolith datum levels: Validation by oxigen isotopes, Geological Society of America **5** (7), 400–404.

Thomas, E. and Shackleton, N.J., 1996. The Paleocene-Eocene benthic foraminiferal extinction and stable isotope anomalies. Geological Society of London Special Publication **101**, 401.

Tosquella, J., Samsó, J.M., Serra-Kiel, J., 1990. Los géneros *Alveolina* y *Nummulites* (macroforaminíferos) del Ilerdiense medio-Cuisiense medio de la Cuenca de Graus, Huesca. Sistemática de *Nummulites*. Boletín geológico y minero **101**, 351-403.

Tréguier, J., Le Coze, F., Benoit, R-A., 2019. Lectotype designation for *Alveolina boscii* and *Fabularia discolites* (Foraminifera) from the rediscovered part of the Defrance collection. Revue de Micropaléontologie **63**, 37-43.

Tremolada, F., Sciunnach, D., Scardia, G, Premoli Silva I., 2008. Maastrichtian to Eocene Calcareous Nannofossil biostratigraphy from the Tabiago section, Brianza area, Northern Italy. Rivista Italiana di Paleontologia e Stratigrafia **114** (1), 29-39.

Trevisani, E., Papazzoni, C.A., Ragazzi, E., Roghi, G., 2005. Early Eocene amber from the "Pesciara di Bolca" (Lessini Mountains, northern Italy). Palaeogeography, Palaeoclimatology, Palaeoecology **223** (3-4), 260-274.

Ungaro, S., 2001. Le biofacies paleoceniche ed eoceniche dei Monti Lessini (Veneto, Italia). Annali dell'Università di Ferrara, Sez. Scienze della Terra **9**, 1-40.

Vandenberghe, N., Hilgen, F.J., Speijer, R.P., 2012. The Paleogene Period. In: Gradstein, F.M., Ogg, J.G., Smith, A.G., Ogg, G.M. (Eds.). The Geological Time Scale 2012, Elsevier, Amsterdam, 855-921.

Venzo, S., 1954. Stratigrafia e tettonica del Flysch (Cretacico-Eocene) del Bergamasco e della Brianza orientale. Memorie descrittive della Carta Geologica d'Italia **31**.

Vescogni, A., Bosellini, F.R., Papazzoni, C.A., Giusberti, L., Roghi, G., Fornaciari, E., Dominici, S., Zorzin, R., 2016. Coralgal buildups associated with the Bolca *Lagerstätten*: new evidences from the Ypresian of Monte Postale (NE Italy). Facies **62**, 1-20.

Vlerk, I.M. van der, 1955. Problems and principles of Tertiary and Quaternary stratigraphy. Quarterly Journal of the Geological Society **115**, 49-63.

Vlerk, I.M. van der, and Umbgrove, J.H.F., 1927. Tertiaire gidsforaminiferen van Nederlandsch-Oost-Indië. Wetenschappelijke Mededeelingen Dienst van der Mijnbouw in Nederlandsch-Indië **6**, 3-35.

Vicedo, V., Robles-Salcedo, R., Serra-Kiel, J., Hidalgo, C., Razin, P., Grélaud, C., 2019. Biostratigraphy and evolution of larger rotaliid foraminifera in the Cretaceous-Paleogene transition of the Southern Oman Mountains. Papers in Palaeontology, 1-26. doi: 10.1002/spp2.1281

Wade, B.S., Pearson, P.N., Berggren, W.A., Pälike, H., 2011. Review and revision of Cenozoic tropical planktonic foraminiferal biostratigraphy and calibration to the geomagnetic polarity and astronomical time scale. Earth-Science Reviews, **104**, 111-142.

Westerhold, T., Röhl, U., Raffi, I., Fornaciari, E., Monechi, S., Reale, V., Bowles, J., Evans, H.F., 2008. Astronomical calibration of the Paleocene time. Palaeogeography, Palaeoclimatology, Palaeoecology **257** (4), 377-403.

Westerhold T., Röhl U., Donner B., McCarren H.K., Zachos J.C., 2011. A complete high-resolution Paleocene benthic stable isotope record for the central Pacific (ODP Site 1209), Paleoceanography **26**. doi:10.1029/2010PA002092

Winterer, E.L., Bosellini, A., 1981. Subsidence and Sedimentation on Jurassic Passive Continental Margin, Southern Alps, Italy. The American Association of Petroleum Geologists Bulletin **65** (3), 394-421.

Zachos, J.C., Pagani, M., Sloan, L., Thomas, E., Billups, K., 2001. Trends, rythms and aberrations in global climate 65 Ma to present. Science **292**, 686-693. doi: 10.1126/science.1059412

Zachos, J.C., McCarren, H., Murphy, B., Röhl, U., Westerhold, T., 2010. Tempo and scale of late Paleocene and early Eocene carbon isotope cycles: implications for the origin of hyperthermals. Earth and Planetary Science Letters **229**, 242-249.

Zhang, Q., Willems, H., Ding, L., 2013. Evolution of the Paleocene-Early Eocene larger benthic foraminifera in the Tethyan Himalaya of Tibet, China. International Journal of Earth Sciences (Geologische Rundschau) **102**, 1427–1445.

Zhang, Q., Willems, H., Ding, L., Xu, X., 2018. Response of larger benthic foraminifera to the Paleocene-Eocene thermal maximum and the position of the Paleocene/Eocene boundary in the Tethyan shallow benthic zones: Evidence from south Tibet. GSA Bulletin **131** (1-2), 84–98.

Zampieri, D., 1995. Tertiary extension in the southern Trento Platform, Southern Alps, Italy. Tectonics **14**, 645-657.

PLATES

INDEX OF THE FIGURED TAXA

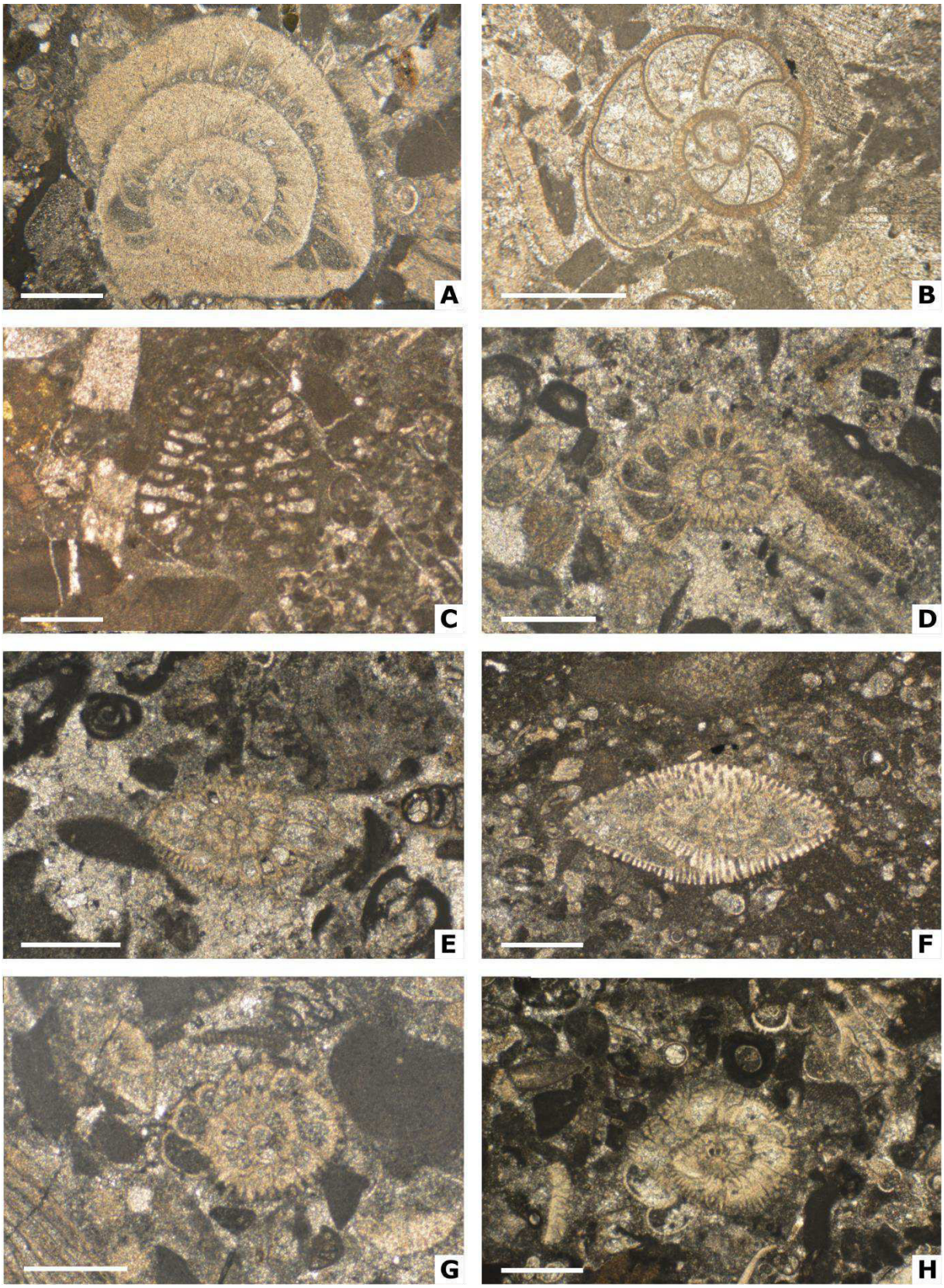

Plate 1.
A *Assilina azilensis*, LEC32 (=FO); **B.** *Cocoarota orali*, LEC21; **C.** *Coskinon* sp., LEC16; **D-E.** *Cuvillierina sireli*, MI15 (=FO); **F.** *C. sireli*, MI18; **G-H.** *C. sireli*, LEC19. **Scale bars:** 0.5 mm.

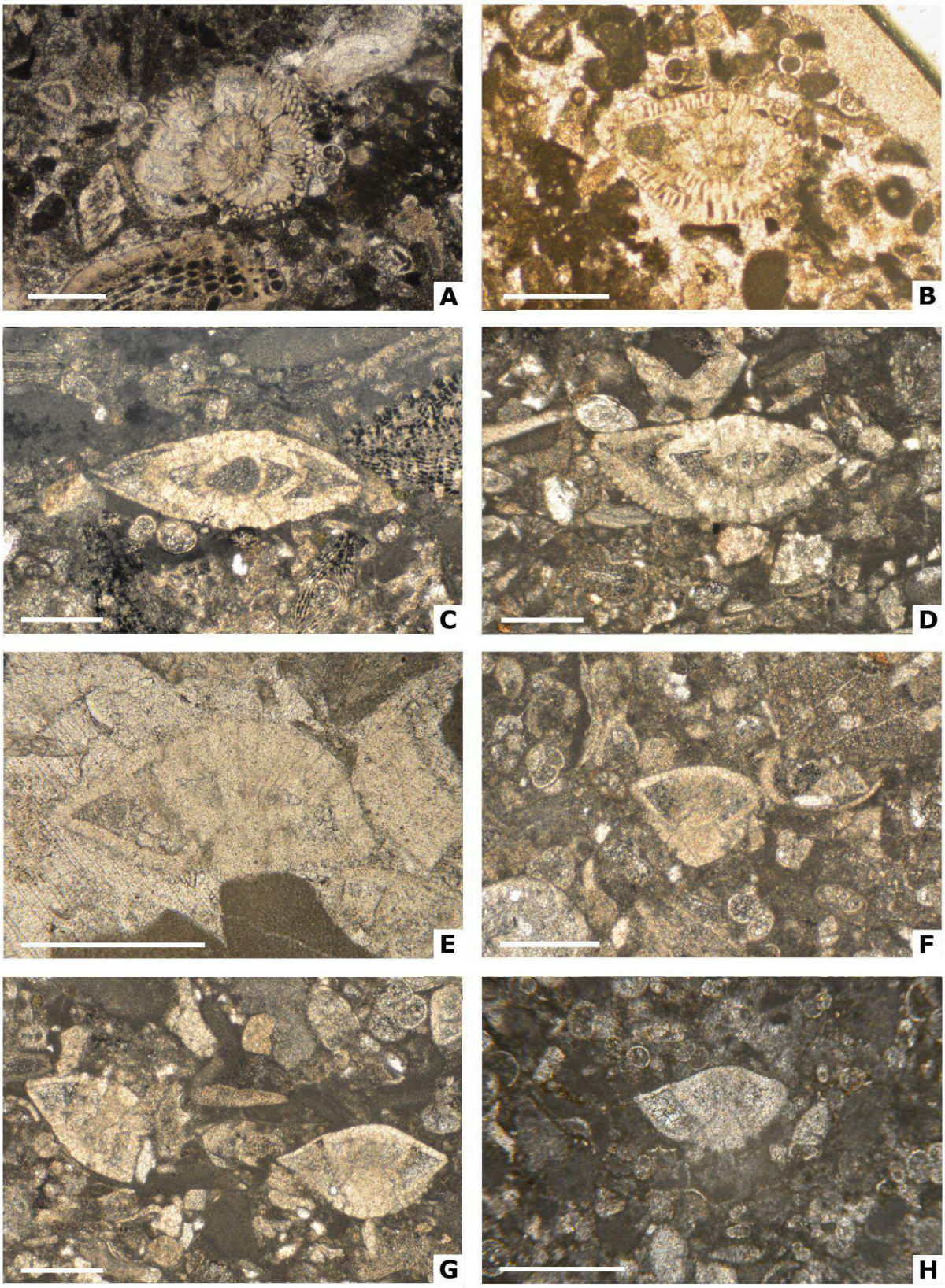

Plate 2.
A. *Cuvillierina sireli*, ARD 20; **B.** *C. sireli*, ARD 22; **C.** *Daviesina intermedia,* LEC7 (=FO); **D.** *D. praegarumnensis,* LEC4 (=FO); **E.** *D. praegarumnensis*, LEC23; **F-G.** *Elazigina dienii*, LEC4 (=FO); **H.** *E. dienii*, ARD12 (=FO). **Scale bars:** 0.5 mm.

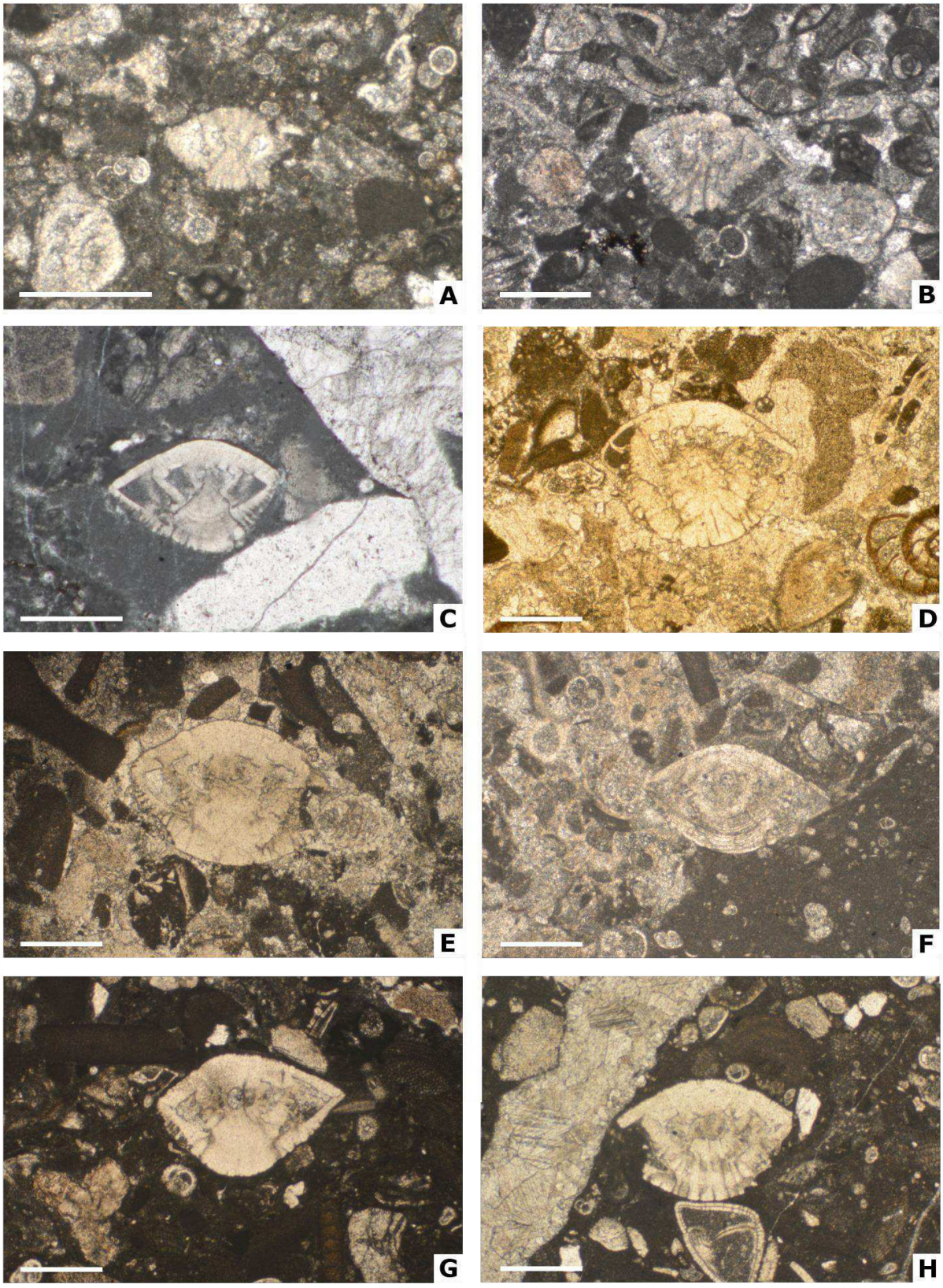

Plate 3.
A. *Elazigina dienii*, ARD 18; **B.** *E. dienii*, ARD 27; **C.** *E. dienii*, CMG734; **D-F.** *E. lenticula*, LEC19; **G-H.** *E. lenticula*, LEC20. **Scale bars:** 0.5 mm.

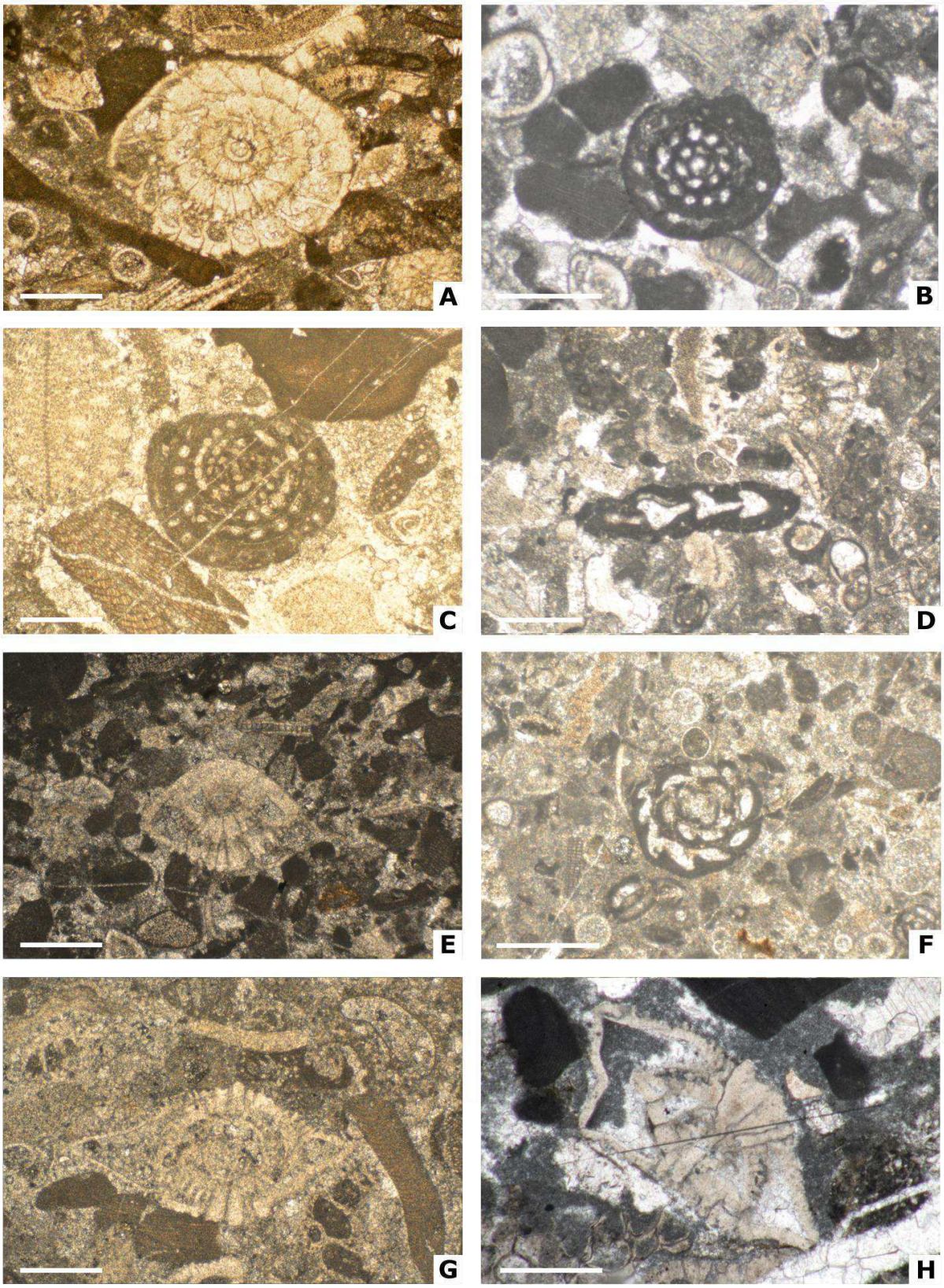

Plate 4.
A. *Elazigina lenticula*, LEC22; **B.** *Globoflarina sp.*, ARD 27 (=FO); **C.** *Glomalveolina* sp., LEC22 (=FO); **D.** *Haymanella paleocenica*, ARD 19 (=FO); **E.** *Kathina aquitanica*, LEC15 (= FO); **F.** *Kayseriella decastroi*, MI9 (= FO), **G.** *Miscellanea juliettae*, LEC23 (= FO), **H.** *M. yvettae,* CMG1625 (= FO). **Scale bars:** 0.5 mm.

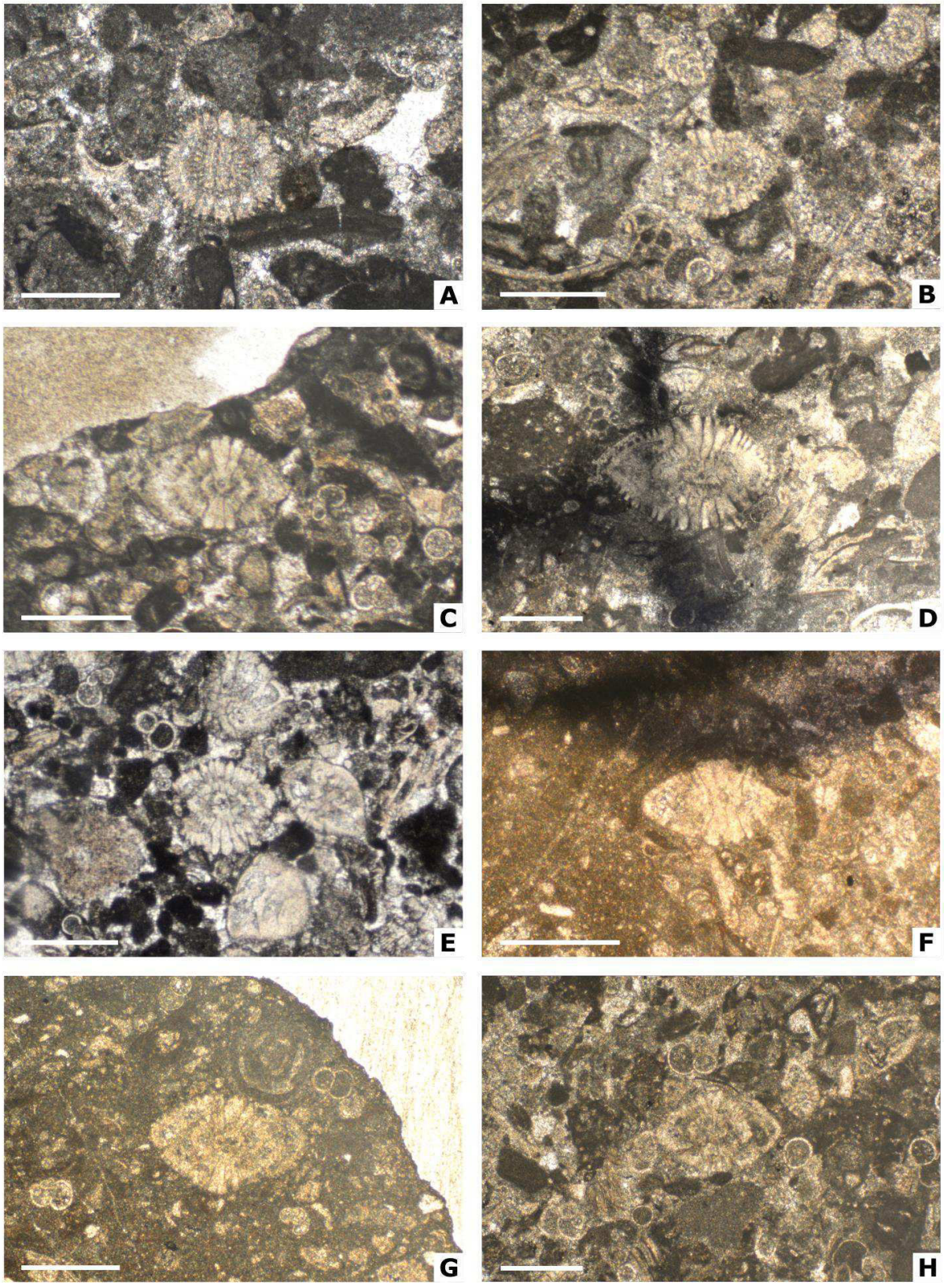

Plate 5.
A. *Miscellanites globularis*, ARD27 (=FO); **B-C.** *M. minutus*, ARD15 (=FO); **D.** *M. minutus*, ARD19; **E.** *M. minutus*, ARD29; **F-H.** *M.* cf. *primitivus*, MI18 (= FO). **Scale bars:** 0.5 mm.

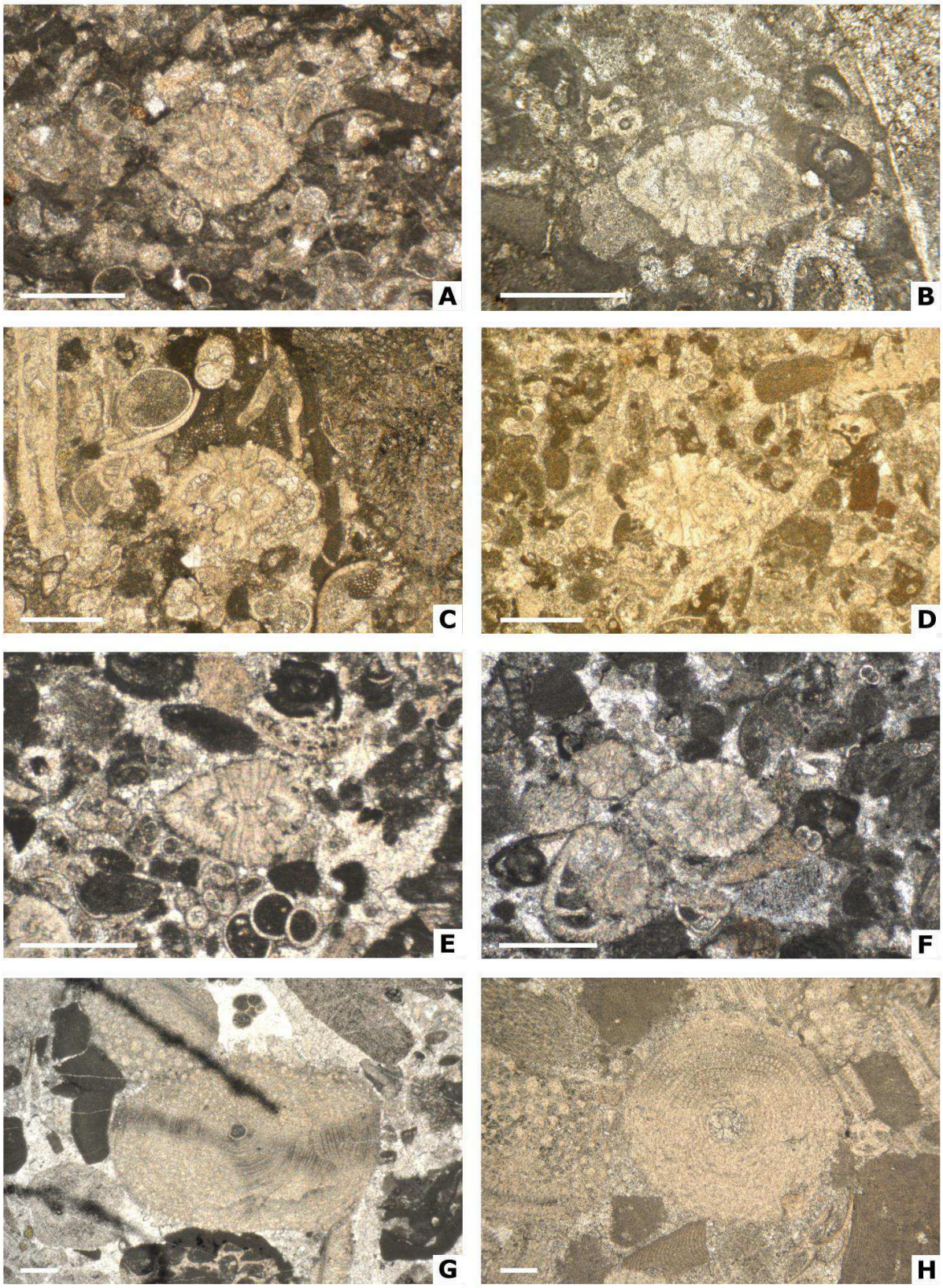

Plate 6.
A. *Miscellanites* cf. *primitivus*, MI20; **B.** *M. primitivus*, LEC14 (=FO); **C.** *M. primitivus*, LEC18; **D.** *M. primitivus*, ARD20bis (=FO); **E.** *M. primitivus*, ARD22; **F.** *M. primitivus*, ARD27; **G.** *Orbitoclypeus* sp., LEC10 (=FO); **H.** *O. multiplicatus haymanaensis,* LEC29 (=FO). **Scale bars:** 0.5 mm.

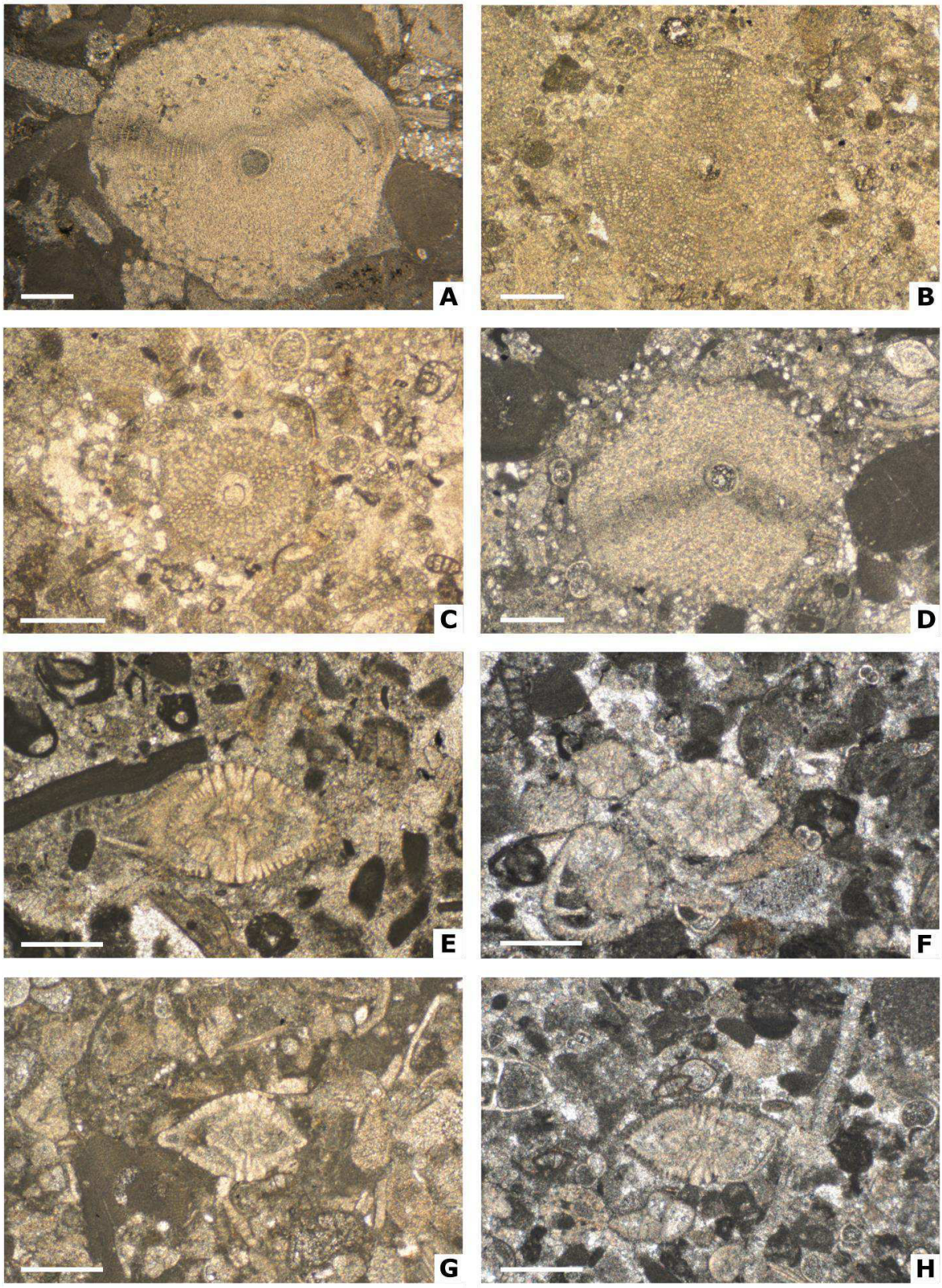

Plate 7.
A. *Orbitoclypeus multiplicatus haymanaensis,* LEC29 (=FO); **B-C.** *O.* cf. *shopeni ramaraoi*, LEC25 (=FO); **D.** *O. shopeni ramaraoi*, LEC32; **E-F.** *Ornatononion moorkensii*, MI15 (=FO); **G.** *O. moorkensii*, LEC29; **H.** *O. moorkensii***,** ARD 27 (= FO). **Scale bars:** 0.5 mm.

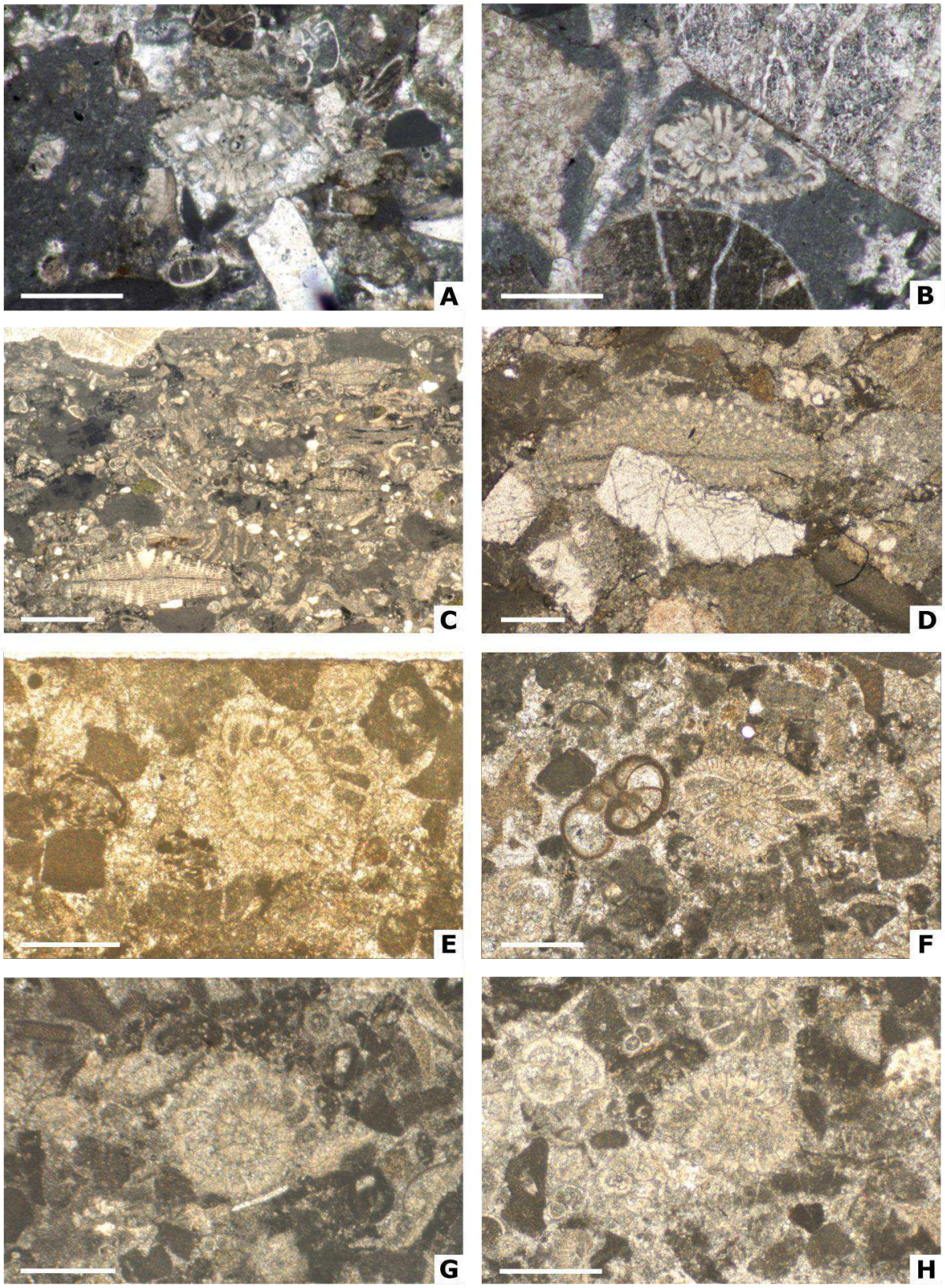

Plate 8.
A-B. *Ornatononion moorkensii*, CMG200 (=FO); **C.** Orthophragminids, LEC7 (= FO); **D.** Orthophragminid, CMG2969 (= FO); **E-G.** *Paralockhartia eos*, MI12 (=FO); **H.** *P. eos*, MI18. **Scale bars:** 0.5 mm.

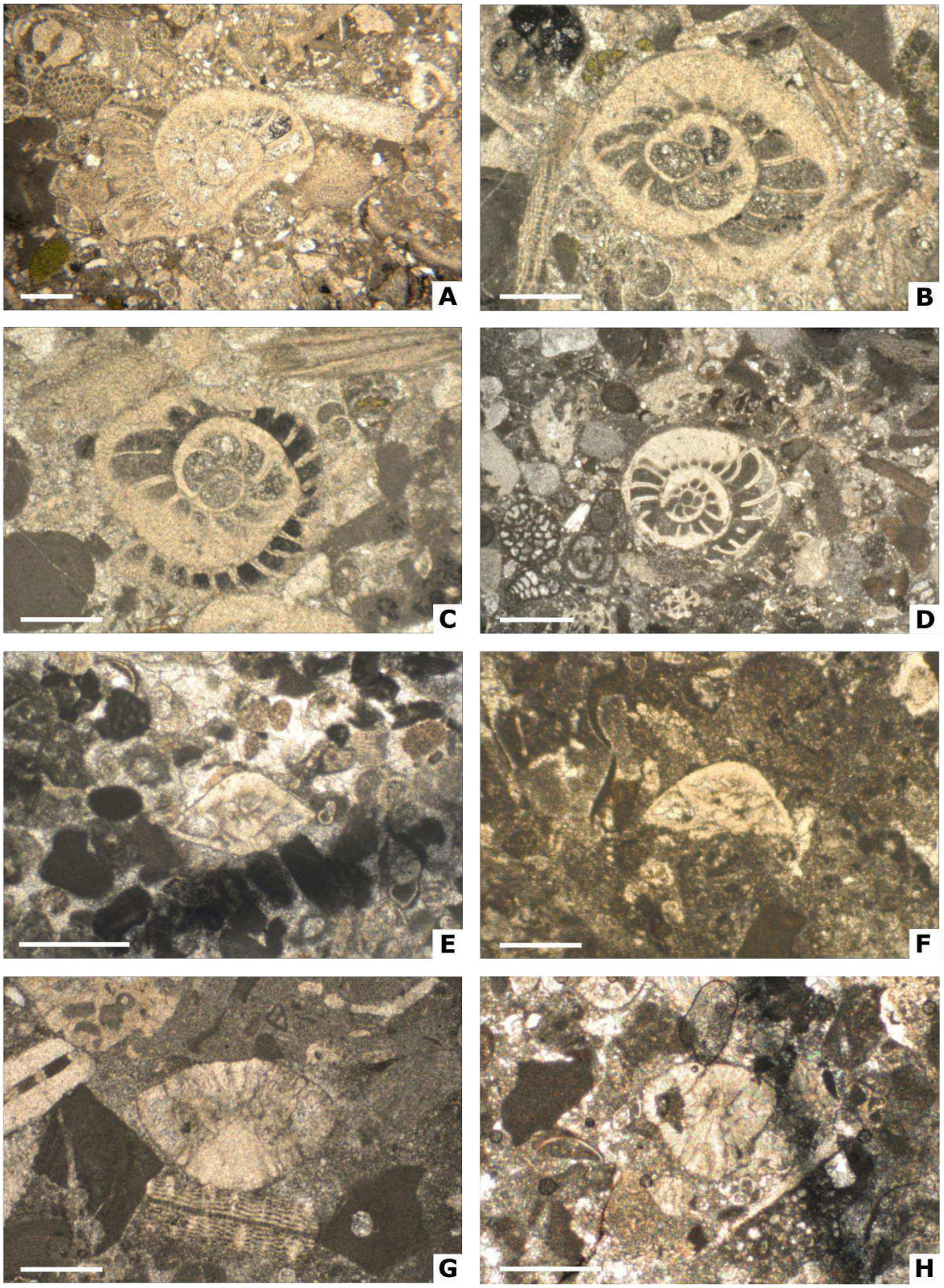

Plate 9.
A. *Ranikothalia* sp., LEC9 (=FO); **B-C.** *Ranikothalia* sp., LEC10; **D.** *Ranikothalia* sp., LEC16; **E.** *Rotorbinella sp.*, ARD 18 (=FO); **F.** *Rotorbinella sp.*, ARD 20; **G.** *Slovenites pembaphis*, LEC16 (=FO); **H.** *Slovenites pembaphis*, ARD27 (=FO). **Scale bars:** 0.5 mm.

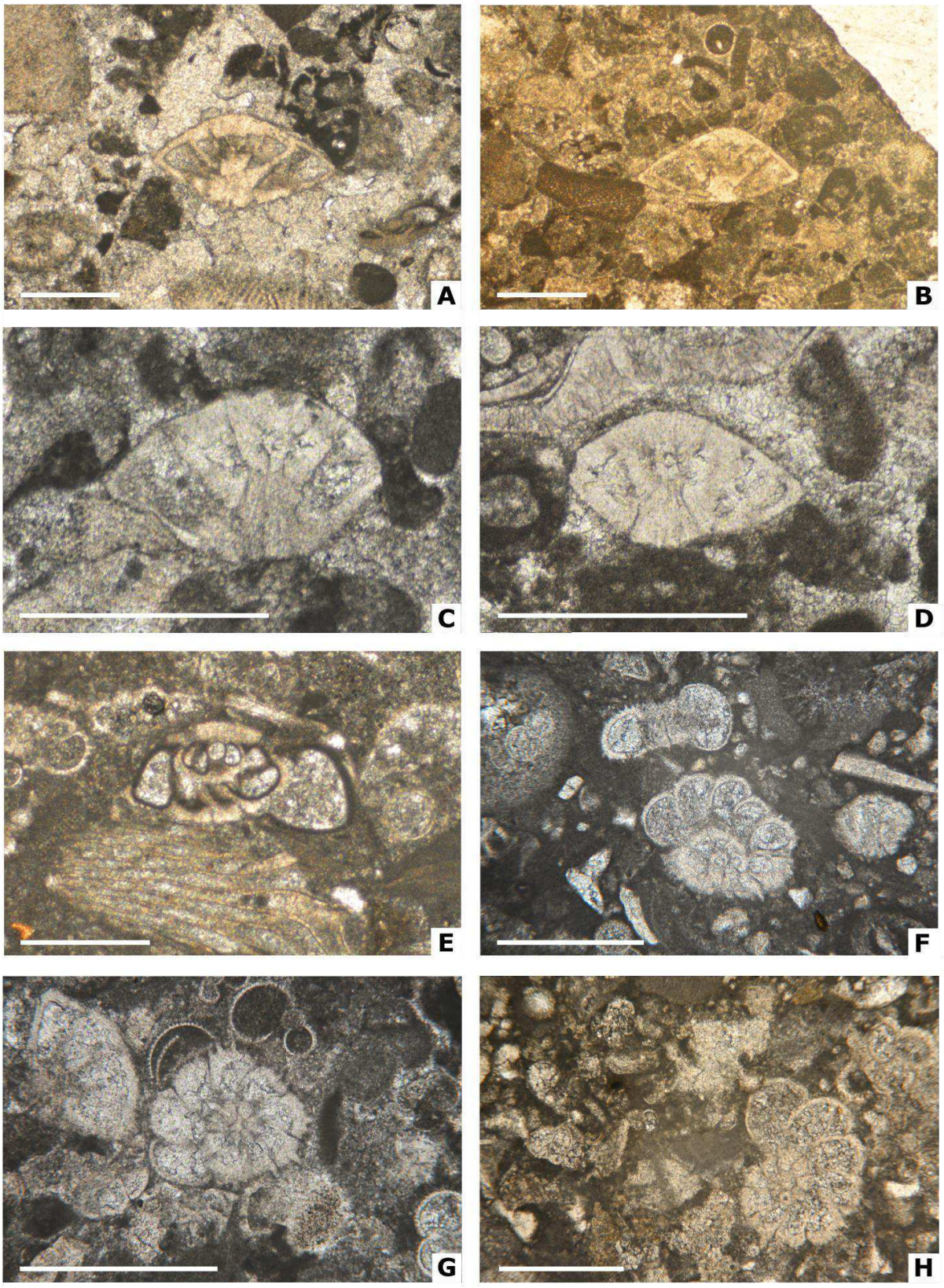

Plate 10.
A-B. *Slovenites praecursorius*, MI15 (= FO); **C-D.** *S. praecursorius*, ARD14; **E.** *Stomatorbina binkhorsti*, MI1; **F.** *Thalmannita* aff. *madrugaensis*, MI1 (=FO); **G.** *T.* aff. *madrugaensis*, ARD6; **H.** *Thalmannita madrugaensis*, LEC4 (=FO). **Scale bars:** 0.5 mm.